UNIVERZITA KARLOVA V PRAZE
FARMACEUTICKÁ FAKULTA V HRADCI KRÁLOVÉ
KATEDRA FARMAKOLOGIE A TOXIKOLOGIE

Studium interakce receptorově specifických radiofarmak s biologickým systémem na buněčné úrovni

Disertační práce

Mgr. Pavel Bárta

Školitel: Prof. PharmDr. Ing Milan Lázníček, CSc.
Konsultant: Doc. PharmDr. František Trejtnar, CSc.
Doktorský studijní program: Farmakologie a toxikologie

Hradec Králové
2012

Prohlašuji, že tato práce je mým původním autorským dílem, které jsem vypracoval samostatně. Veškerá literatura a další zdroje, z nichž jsem při zpracování čerpal, jsou uvedeny v seznamu literatury a v práci řádně citovány.

Pavel Bárta

Poděkování

Na tomto místě bych chtěl poděkovat všem, kteří mě provázeli v průběhu mého doktorského studia a svým odborným vedením mi pomáhali během mé vědecké práce na pracovišti Radiofarmacie při Katedře farmakologie a toxikologie.

Na prvním místě patří mé velké poděkování mému školiteli Prof. PharmDr. Ing. Milanu Lázníčkovi, CSc., který mě přijal do svého vědeckého týmu, poskytnul mi zázemí pro mé studium a realizaci této vědecké práce, a uděloval mi své odborné rady a připomínky, které značnou měrou přispěly k řešení mých úkolů. V neposlední řadě děkuji za jeho vždy vstřícný a přátelský přístup.

Rád bych také poděkoval Doc. Ing. Alici Lázníčkové, CSc. za přípravu radionuklidů pro mé experimenty, a za možnost uskutečnit část mé experimentální práce v rámci projektové podpory programu COST. Také děkuji za její odborné rady a pomoc při řešení problematiky v oblasti radionuklidů, které byly úzce provázány s mým studijním zaměřením.

Některé z úkolů jsem řešil i ve spolupráci se svým konsultantem Doc. PharmDr. Františkem Trejtnarem, CSc., který mi věnoval i mnoho užitečných rad, a proto i jemu patří mé poděkování za jeho vstřícnost a spolupráci, která se promítla do mého studia.

Mnohokrát děkuji i Dr. Karlu Anderssonovi za to, že mi umožnil mou tříměsíční stáž v jeho vědeckém týmu na oddělení Onkologie, radiologie a klinické imunologie na Univerzitě Uppsala ve Švédsku. Pobyt na jeho pracovišti mi umožnil získat cenné zkušenosti při práci s přístrojem LigandTracer a díky vzájemné spolupráci se nám podařilo vydat několik společných odborných publikací, které jsou součástí této disertační práce.

Za společnou spolupráci a velmi přátelské prostředí vděčím i mým kolegům z pracoviště radiofarmak, jmenovitě PharmDr. Ludmile Melicharové, Jarmile Hoderové, Evě Teichmanové, Ivě Filipové, Doc. PharmDr. Petru Pávkovi a mým spolužákům Mgr. Zbyňku Novému a Mgr. Janě Mandíkové.

V neposlední řadě chci poděkovat své rodině, která mi byla po celou dobu mého studia silnou oporou, díky které jsem dosáhl svých dosavadních úspěchů. Mé velké díky pak patří především mým rodičům za jejich obětavost, podporu a pochopení, a proto bych jim rád věnoval tuto svou závěrečnou práci.

Děkuji též za podporu grantu Specifického vysokoškolského výzkumu SVV-265-003.

Použité zkratky

AR42J	pankreatická buněčná nádorová linie
CCK	cholecystokinin – imunoreaktivní peptid podobný gastrinu
CCK2r	„Cholecystokinin-2 receptor“ – receptor pro cholecystokinin typu 2
CML	„myelogenous leukaemia“ – myeloidní leukémie
CRC	„colorectal cancer“- kolorektální karcinom
EDTA	ethylen diamin tetraoctová kyselina
EGF	„epidermal growth factor“ - epidermální růstový faktor
EGFR	„Epidermal growth factor receptor“ – receptor pro epidermální růstový faktor
FDA	„Food and Drug Administration“ – Úřad pro kontrolu potravin a léčiv Spojených států amerických
GISTs	„gastrointestinal stromal tumor“ – gastrointestinální stromální tumor
GLP-1r	„Glucagon-like peptide-1 receptor“ – receptor pro glukagon-like peptid-1
GRPr	„Gastrin-releasing peptide receptor“ – receptor pro gastrin uvolňující peptid
HB-EGF	„heparin-binding EGF-like growth factor“ – heparin vázající EGF růstový faktor
DOTA	1,4,7,10-tetraazacyklododekan-1,4,7,10-tetraoctová kyselina
DTPA	diethylen triamin pentaoctová kyselina
KEX	„kinetic extrapolation“ – kinetická extrapolace
MAb	„Monoclonal antibody“ – monoklonální protilátka
MG11	minigastrin11
NRPC	„number of receptors per cell“ – počet receptorů na buňku
NSCLC	„non-small-cell lung carcinoma“ – nemalobuněčný typ karcinomu plic
OK cells	„opossum kidney cells” – buněčná linie izolovaná z proximálního tubulu ledvin vačice oposum
PRRI	„Peptide receptor radionuclide imaging“ – zobrazování radionuklidem značenými receptorově specifickými peptidy
PRRT	„Peptide receptor radionuclide therapy“ – terapie radionuklidem značenými receptorově specifickými peptidy
RIT	„Radioimmunotherapy“ – radioimunoterapie
RTK	„receptor tyrosine kinase“ – tyrosin kinázový receptor
SCCHN	„squamous cell carcinoma of the head and neck“ – spinocelulární karcinom hlavy a krku
SPPS	„Solid-phase peptide synthesis“ – syntéza peptidů na pevné fázi

SSTrs	„Somatostatin receptors“ – somatostatinové receptory
TK	tyrozinkináza
TGF-α	„transforming growth factor α“ – transformující růstový faktor α

Obsah

1. Úvod

S rostoucím průmyslovým rozvojem současné společnosti a zvyšováním věku dožití dochází ke zhoršování zdravotního stavu lidské populace vlivem vyšší prevalence civilizačních chorob. Ty většinou vyplývají z nezdravého způsobu života jedince a působení nezdravého prostředí, ve kterém jednotlivec vyrůstá. Neustálým ovlivňováním organizmu chemickými látkami často karcinogenními se zvyšuje jeho stresová zátěž a v důsledku toho selhávají přirozené obranné mechanizmy. Imunitní systém je vystavován vyšší zátěži. Nepříznivé působení prostředí, jehož je sám člověk původcem, v kombinaci s přirozenými faktory, jako jsou genetické predispozice jedince nebo působení bakteriálního a virového agens, je tělo oslabováno, a tak s rostoucím věkem a v závislosti na zdravotním stavu člověka vyčerpává organizmus své přirozené obranné mechanizmy. Výsledkem je častý rozvoj různých typů nádorových onemocnění způsobených karcinogeny (chemické látky, viry, atd.). Jejich odhalováním a případnou léčbou se v posledních několika desetiletích věnuje nukleární medicína s nezastupitelnou podporou ze strany radiofarmacie.

Nukleární medicína se kromě funkčního vyšetření orgánů (například srdce, plic nebo kostry), zobrazování fyziologických funkcí (například funkční vyšetření ledvin nebo kumulace jodu ve štítné žláze) či vyšetření akutního zdravotního stavu u mozkové nebo myokardiální ischémie též ve velké míře zabývá diagnostikou a terapií nádorových onemocnění.

Vzhledem k velké rozmanitosti nádorových onemocnění, se kterými se vytrvale zápasí na poli nukleární medicíny, je vhodnější uvést úspěšně aplikované radioterapeutické nebo radiodiagnostické látky dle charakteru jejich molekulové struktury. Přejdeme-li tedy anorganické sloučeniny jako je například technecistan (^{99m}Tc) sodný nebo ^{99m}Tc-DTPA pro statickou scintigrafii mozku nebo jodid (^{131}I) sodný pro scintigrafii štítné žlázy, dostáváme se k intenzivně studovaným biologicky aktivním látkám, jako jsou peptidy a monoklonální protilátky. Tyto biologické sloučeniny vynikají svou specificitou k určitému typu nádoru dle typu receptoru, který ve zvýšené míře exprimují nádorové buňky na svém povrchu.

Mezi radiofarmaky, která jsou odvozena od peptidových hormonů, vyniká v současné době komerčně dostupný [^{111}In-DTPA]octreotide (pod obchodním názvem ^{111}In-OctreoScan®) pro scintigrafii somatostatinových receptorů u neuroendokrinních nádorů (Teunissen et al, 2011). Z radioaktivně značených monoklonálních protilátek, které jsou využívány v terapii nádorových onemocnění, lze zmínit ^{90}Y nebo ^{111}In značený ibritumomab tiuxetan (pod

obchodním názvem Zevalin®; tiuxetan slouží stejně jako DTPA pro chelataci radioisotopů) pro léčbu folikulárního non-Hodgkinova lymfomu (Sharkey et al, 2008).

1.1 Radiofarmaka v onkologii

Rychlý rozvoj radiofarmacie, která je zdrojem látek pro radiodiagnostiku nebo radioterapii, přispěl v posledních letech ke stále rostoucímu uplatnění nukleární medicíny při léčbě nádorových onemocnění spolu s pomocí dalších oborů, jakými jsou imunologie, onkologie nebo radiochemie. Moderní vyvíjené radiofarmaceutické látky, které jsou menší fyziologickou zátěží pro pacienty, mohou vyústit v upřednostnění nukleární medicíny před ostatními technikami léčby nádorových onemocnění, jako je např. chemoterapie (Sharkey et al., 2008; Goldenberg et al., 2006).

Každé radiofarmakum je buď tvořeno samotným radionuklidem, nebo radionuklidem vázaným na transportující ligand. Jako radionuklidy využívanými v diagnostice jsou nejčastěji γ nebo β^+ (emise pozitronů) zářiče. Nejčastějšími zdroji gama záření užívanými v nukleární medicíně jsou izotopy ^{111}In, ^{99m}Tc a ^{123}I, které jsou v oblibě zejména v Evropě. Mezi výše zmíněnými izotopy vyniká izotop technecia pro své vlastnosti, jako je jeho snadná a levná příprava z radionuklidového generátoru, krátká, nicméně dostačující doba poločasu přeměny (6.01 hodin), a nízká, ale pro diagnostiku vyhovující energie záření (0.142 MeV). V kategorii pozitronových zářičů se nejvíce používají izotopy ^{11}C, ^{68}Ga a ^{18}F (Ambrosini et al., 2011).

Nukleární radioterapie se zaměřuje zejména na β zářiče, jejichž významnými představiteli jsou izotopy ^{131}I, ^{90}Y a ^{177}Lu. Vedle nich by se perspektivně mohly uplatnit i α zářiče, a to především izotopy bismutu ^{212}Bi a ^{213}Bi. Nejvíce osvědčeným terapeutickým radionuklidem ze skupiny β zářičů se stal především izotop ytria (^{90}Y) díky svému dalekému dosahu záření (cca 12 mm) a krátkému poločasu přeměny ($t_{1/2}$ = 64 hodin). Podstatou působení radioterapeutických radionuklidů je jejich průnik do cílových nádorových buněk a poškození buněčné DNA, které vede k zániku buňky. Dosah průniku emitovaných částic záření z izotopu mívá za následek nejen terapeutické působení radionuklidu na nádorovou tkáň, ale leckdy i nežádoucí poškozující efekt na tkáň fyziologicky zdravou. Nová radiofarmaka se snaží tento nepříznivý vliv odstranit (Sharkey et al., 2008; Goldenberg, 2003).

Obliba radiofarmak v posledních letech spočívá zejména v jejich terapeutickém využití pro specifický typ nádorového bujení. V tomto případě mluvíme o cílené radionuklidové terapii, pro kterou se nověji vžilo označení molekulární radioterapie. Radiofarmakum užité

v molekulární radioterapii se principielně sestává z radionuklidu, který je zdrojem radioaktivního záření, a transportního ligandu, který je schopen se specificky vázat na cílený extracelulární protein, tedy receptor. Těmito transportními ligandy jsou zejména peptidové analogy odvozené od peptidových hormonů nebo monoklonální protilátky (Loke et al., 2011).

1.2 Monoklonální protilátky

Monoklonální protilátky (MAb) jsou protilátky získané z klonální populace jedné plazmatické buňky. Strukturně se jedná o glykoproteiny, které jsou řazeny do skupiny γ-globulinů. Jejich molekulová hmotnost se pohybuje mezi 150 tisíc až 900 tisíc Da. Struktura protilátek je tvořena čtyřmi peptidovými řetězci, spojenými disulfidickými vazbami, kdy dva a dva řetězce jsou stejné - 2 lehké a 2 těžké (viz obrázek č. 1).

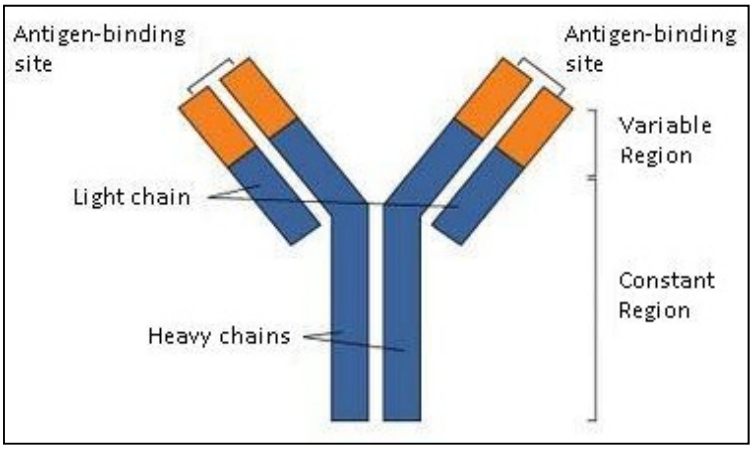

Obrázek č. 1: Základní struktura protilátky (zdroj: Allison, 2009)

Delší části dvou těžkých řetězců spolu vytvářejí krystalizující fragment (Fc) protilátky, který umožňuje vazbu a aktivaci komplementu. Kratší části těžkých řetězců spolu s lehkými řetězci vytváří variabilní (antigen vázající) fragment (Fab) protilátky, který umožňuje specifickou vazbu protilátky na cílovou antigenní strukturu.

1.2.1 Nekonjugované protilátky

Terapie nádorových onemocnění prováděná s pomocí protilátek používá buď přirozených protilátek, takzvaně nekonjugovaných, nebo protilátek konjugovaných.

Nekonjugované protilátky využívají pouze svých biologických vlastností, kterými je stimulace na komplementu závislé cytotoxicity nebo specifické, na buněčných komponentech závislé cytotoxicity. První zmíněný způsob likvidace cizorodých buněk nebo tělu vlastních buněk (například nádorových buněk) spočívá v kaskádě reakcí aktivujících komplementární proteiny, které perforují buněčnou stěnu, a tím způsobují rozvrat prostředí intracelulárního prostoru buňky. Druhý způsob reakce imunitního systému přes specificky se vázající protilátku na cílený antigen je složkou buněčné specifické imunity. V počátcích terapie nádorových onemocnění pomocí protilátek se využívalo jejich přirozených vlastností pro vyvolání buněčné smrti nádorových buněk. K tomuto účelu byly použity především myší protilátky pro léčbu například nádorových onemocnění gastrointestinálního traktu (Sears et al., 1985).

Dalším významným krokem k využití nekonjugovaných protilátek bylo zjištění antiproliferativního vlivu protilátek na buňky rostoucí v médiu bez účasti komplementárního systému nebo efektorových buněk imunitního systému. Tento vliv byl v prvé řadě demonstrován na receptoru pro epidermální růstový faktor (EGFR). Výsledkem pak bylo vytvoření anti-EGFR protilátek (Masui et al., 1984).

Postupem času došlo k přechodu od myších protilátek k protilátkám, které jsou svým původem chimérní (konstantní část protilátky zaměněna za lidský úsek, například cetuximab), humanizované (variabilní část protilátky zaměněna za lidský úsek, například trastuzumab) až k plně lidským protilátkám (například panitumumab), které snižují riziko imunitní reakce pacienta vůči terapeutickým proteinům. Nekonjugované protilátky nemají samy o sobě dostačující schopnost vyléčit nádorová onemocnění u pacienta. Proto jsou často terapie nekonjugovanými monoklonálními protilátkami kombinovány s dalšími možnostmi léčby, nejčastěji s chemoterapií (Coiffier, 2006).

Významnými představiteli nekonjugovaných protilátek jsou cetuximab, nesoucí obchodní název Erbitux® a užívaný například v kombinaci s radioterapií pro léčbu nádoru hlavy a krku, dále rituximab, pod ochodním názvem Rituxan®, užívaným zejména pro terapii non-Hodgkinova lymfomu, a trastuzumab, nesoucí obchodní název Herceptin®, sloužící například pro léčbu karcinomu prsu (Sharkey et al., 2008).

1.2.2 Konjugované protilátky

Konjugované monoklonální protilátky jsou efektivnější při imunoterapii nádorových onemocnění zejména díky terapeuticky aktivní látce, kterou transportují navázanou na své

struktuře. Díky tomu se mnohdy mohou používat v terapii bez spoluúčasti dalších látek. Aktivní látkou navázanou na monoklonální protilátce mohou být cytotoxická léčiva, rostlinné nebo bakteriální toxiny nebo radionuklidy (Goldenberg, 1994; Serengulam et al., 2010).

Výsledek účinku terapie konjugovanou monoklonální protilátkou nesoucí léčivo nebo toxin je závislý na množství aktivní látky dopravené do nádorové buňky, neboť teprve určité nejnižší množství transportované látky je postačující pro vyvolání změn v buňce vedoucích k jejímu zániku. Protilátka tak musí být specifická pro daný typ receptoru, který se ve zvýšené míře exprimuje na povrchu nádorové buňky, nebo je zcela typický pro nádorově transformovanou buňku, a který musí transportovat (internalizovat) protilátku dovnitř buňky po její vazbě na receptorový protein. Optimální je receptor, který se po přenosu navázané protilátky z extracelulárního do intracelulárního prostoru takzvaně recykluje a vrací se zpět napovrch buňky, aby mohl sloužit jako jejich opětovný přenašeč.

V případě protilátek konjugovaných s aktivní látkou, kterou je radionuklid, se jich výše zmíněná problematika nutnosti internalizace tolik nedotýká. Protilátka značená radionuklidem se naváže na specifickou strukturu buňky (nejčastěji receptor) a vlivem emitovaného radioaktivního záření dochází k průniku α- nebo β-částic skrz buněčnou membránu, poškození jejího DNA, a tím k zániku buňky. Limitujícím faktorem zde tedy zůstává dosah radioaktivního záření. Ten se volí zejména s ohledem na zdravou tkáň, která by mohla být zasažena zářením (Argyriou et al., 2009; Sharkey et al., 2008).

Terapie radioaktivně značenými protilátkami v nukleární medicíně nese označení radioimunoterapie (RIT). Úspěšnost léčby není určena pouze uzdravením pacienta, ale je též zajištěna co nejmenší radiační zátěží léčeného. Tento posledně zmiňovaný fakt poukazuje na stále řešenou problematiku radioaktivně značených protilátek, kterou je jejich radiotoxicita. Orgány nejvíce ohroženými radioaktivní zátěži bývají játra, kostní dřeň a ledviny (van Gog et al., 1998).

Po intravenózní aplikaci radioaktivně značených protilátek dochází k významnému nárůstu radioaktivity v krevním řečišti. Krev nesoucí protilátky s navázaným radionuklidem je pročišťována od cizorodých částic a zplodin metabolismu především v játrech. Ty se tak stávají prvním orgánem, kde dochází k významné akumulaci radioaktivity jako důsledek eliminace protilátek z krevního řečiště (Goldenberg et al., 2007).

V závislosti na velikosti molekuly značené protilátky, a tudíž rychlosti její distribuce do cílového místa terapie – nádorové tkáně a též rychlosti degradace protilátky v játrech, se protilátka zadržuje v krvi po určitou dobu. To může vést k nepříznivé kumulaci protilátky v kostní dřeni (van Gog et al., 1998, Goldenberg et al., 2007).

Radionefrotoxicita je pak především záležitostí malých molekul (fragmentů) protilátek, které jsou většinou akumulovány zpětnou tubulární resorpcí v buňkách proximálního tubulu ledvin (Serengulam et al., 2010; Sharkey et al., 2005).

Snaha o co největší eliminaci radiotoxicity doprovázející RIT dosáhla výchozího úspěchu v osmdesátých letech dvacátého století, kdy byla vyvinuta metoda předem cílené radioimunoterapie (anglicky označované Pretargeted RIT), která se do současné doby stále zdokonaluje. Princip metody spočívá v prvotní intravenózní aplikaci monoklonální protilátky specifické pro antigen exprimovaný na cílených nádorových buňkách (viz obrázek č. 2). Tato protilátka, která na sobě nenese radionuklid, je v určitém čase distribuována do místa svého cíle v těle pacienta. Jako antigen se v tomto případě musí zvolit takový receptor, který není transportován s navázanou protilátkou do intracelulárního prostoru. Díky tomu tedy zůstává protilátka stále na povrchu buňky. Zbytek protilátky, která se nenavázala na nádorovou buňku, je organismem, tedy zejména játry, eliminován z krevního řečiště. Nyní nastává druhý krok terapie. Do těla je vpraven nízkomolekulární nosič, který nese terapeutický radionuklid, a který se rychle distribuuje z krevního řečiště do tkáně s předem navázanými protilátkami, na které se nosič specificky naváže. Zbytek nízkomolekulární látky je snadno odstraněn především přes ledviny ven z těla. Celý proces distribuce a eliminace radioaktivně značeného nosiče je velmi rychlý a pacient tak není vystaven přílišné radiologické zátěži, kdy jde především o hematologickou radiotoxocitu (Goldenberg et al., 2006; Govindan et al., 2010; Sharkey et al., 2012).

U tohoto typu terapie se používají protilátky jednak schopné vazby na nádorový antigen a jednak schopné interakce s nosičem radionuklidu. Jako protilátky se volí buď bisfecifické bivalentní protilátky nebo komplex protilátka-streptavidin. V případě bivalentní protilátky je nosičem radionuklidu sloučenina hapten-peptid a pro komplex protilátka-streptavidin je nosičem radioaktivně značený biotin. Pro navázání radionuklidu na strukturu nosiče se používají chelatační látky, jako jsou DOTA nebo EDTA (Knox et al., 2010; Sharkey et al., 2012).

Další nespornou výhodou užití předem cílené RIT je velikost molekul použitých terapeutik. Jelikož protilátka nenese radionuklid a ani případně další chelatační látky umožňující vazbu radioizotopu na strukturu proteinu, je její molekula podstatně menší, lépe se distribuuje v organizmu a nezůstává dlouhou dobu v krevní cirkulaci. To samé platí o molekule nosiče radionuklidu, která je mnohem menší než samotná protilátka, a jak již bylo výše zmíněno, v krevním řečišti zůstává velmi krátkou dobu, rychle se dostává do místa cílové tkáně anebo je snadno glomerulární filtrací odváděna z těla pacienta (Goldenberg et al., 2007).

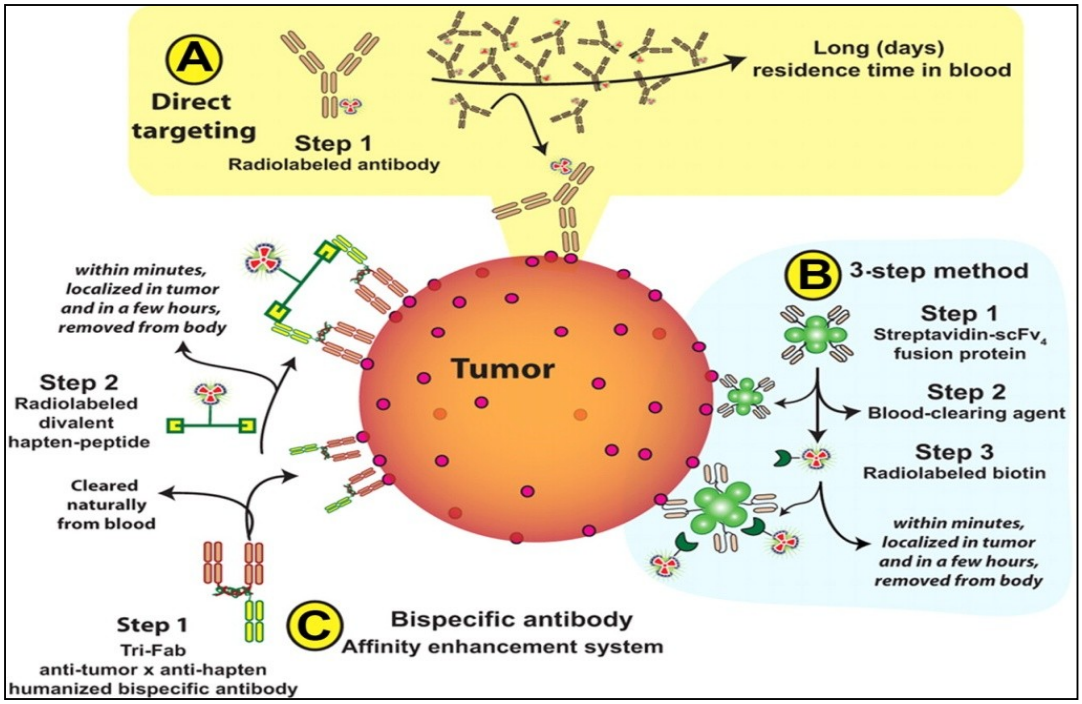

Obrázek č. 2: (A) konvenční způsob RIT, (B) předem cílená RIT pomocí komplexu protilátka-streptavidin, (C) předem cílená RIT pomocí bispecifické trivalentní protilátky (zdroj: Goldenberg, 2009).

1.3 EGFR a jeho ligandy

Receptorové proteiny, jejichž specifickými substráty jsou různé růstové faktory, se řadí do široké skupiny receptorů označovaných jako receptory pro růstové faktory, jejichž funkce je úzce spjata s tyrozinkinázou (TK). Tato skupina receptorů je zodpovědná za zprostředkování přenosu signálů z extracelulárního prostředí do buňky. Struktura receptorů pro růstové faktory je v základu tvořena extracelulární, transmembránovou a intracelulární doménou, kdy posledně zmiňovaná doména je ve spojení s tyrozinkinázovou aktivitou. TK aktivita reguluje řadu buněčných procesů, které mají vliv na funkci tkání a tedy celkový stav organizmu. Ovlivnění buněčných procesů je zejména na úrovni buněčné proliferace, migrace, metabolismu, diferenciace a vzájemné intercelulární komunikace. Tyto základní buněčné pochody pak mají vliv na orgánovou morfogenezi, regeneraci tkání a neovaskularizaci.

Veškeré tyto funkce jsou u zdravých buněk přísně kontrolovány. Vlivem mutací nebo strukturálních změn však může dojít k abnormálnímu využití funkčních vlastností tyrozinkinázových receptorů (RTK) u nádorově transformovaných buněk. Nádorové buňky pak vynikají vysokou mutací, genovým přeuspořádáním a genovou amplifikací, nadměrnou expresí RTK a tím i přílišnou autokrinní, parakrinní a endokrinní stimulací.

Nadměrná exprese RTK vedla k zařazení receptorů pro růstové hormony do skupiny onkoproteinů, které nalezneme u řady nádorových onemocnění jako například karcinomu prsu, gastrointestinálního karcinomu, nádory hlavy a krku nebo nádoru plic (Gschwind et al., 2004; Takeuchi et al., 2011). Skupina RTK extracelulárních receptorů zahrnuje 58 známých členů, kteří se sdružují do 20 receptorových rodin. Významnými představiteli skupiny RTK jsou pak především receptory pro epidermální růstový faktor (EGFR). EGFR rodina zahrnuje čtyři členy – EGFR (ErbB-1), HER2/c-neu (ErbB-2), Her3 (ErbB-3) a Her4 (ErbB-4). Struktura EGF receptoru bez navázaných ligandů (obr. 3) je tvořena extracelulární doménou vázající ligand, transmembránovým regionem a cytoplazmatickou doménou s tyrozinkinázou, která je lemována nekatalyckými regulatorními regiony.

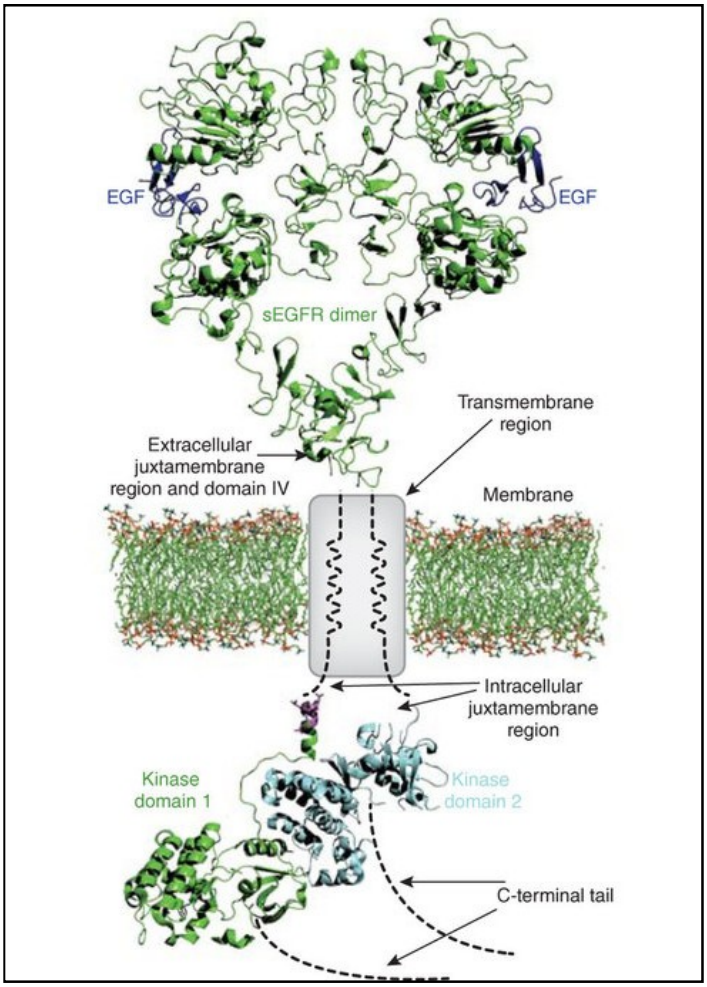

Obrázek č. 3: Struktura dimerizovaného EGFR (zdroj: Bessman et al., 2012).

Po vazbě ligandu na ektodoménu receptorů EGFR, HER3 nebo HER4 dochází k formaci homodimerického nebo heterodimerického tyrozinkináza aktivního komplexu, kdy u posledně zmiňovaného je partnerem tvořícím komplex nejčastěji HER2 receptor.

Výsledkem tvorby dimerů je aktivace kinázové aktivity na intracelulární straně receptoru. Vznikají tak signály, které mají za následek transkripci genů, celulární proliferaci a diferenciaci. Skupinu ligandů aktivujících EGF receptorovou rodinu tvoří EGF, TGF-α, HB-EGF, amphiregulin, betacellulin a epiregulin (Gschwind et al., 2004; Marqués et al., 1999; Moulder et al., 2001).

Zjištění, že některé nádorové buňky v hojné míře exprimují EGF receptory na svém povrchu vedlo k přípravě látek, které inhibují EGF receptory nebo jich využívají pro svůj transport do nádorových buněk, aby v nich působily cytotoxicky. Tyto látky můžeme rozdělit do dvou skupin a to na monoklonální protilátky, které byly již blíže popsány, a nízkomolekulární látky.

Principem působení nízkomolekulárních látek je jejich inhibice tyrozinkinázové aktivity. Jako první popsanou látkou tohoto typu byl chinazolin, po kterém následoval gefitinib (iressa), který byl schválen pro klinické užití při léčbě neoperovatelných karcinomů nemalobuněčného typu karcinomu plic (NSCLC) v USA a Japonsku na počátku 21. století. Dalším úspěšným inhibitorem aktivity EGFR se stal imatinib, který byl povolen FDA pro léčbu pacientů s myeloidní leukémií (CML) a gastrointestinálním stromálním tumorem (GISTs) (Wakeling et al., 1996; Druke ret al., 1996; Joensuu et al., 2001).

Monoklonální protilátky cílené proti EGF receptorům jsou většinou připraveny tak, aby blokovaly bioaktivitu receptorových ligandů, inhibovaly heterodimerizaci receptorů či obsazovaly vazebná místa na receptorech.

První účinnou připravenou protilátkou byl trastuzumab, který je cílený proti HER2 receptoru a svým charakterem je rekombinační humanizovanou MAb. Trastuzumab se váže na receptor na povrchu nádorových buněk, následně se internalizuje do buňky a zde inhibuje buněčnou proliferaci a reparaci DNA, dále spouští apoptosu a imunitní modulaci. Trastuzumab byl schválen pro léčbu metastatického karcinomu prsu (Kalofonos at al., 2006; Gschwind et al., 2004).

Dalšího úspěchu bylo dosaženo s protilátkou cetuximab, což je chimérní MAb cílená proti EGFR. Jejím účinkem je inhibice vazby endogenního ligandu, buněčné motility, buněčné invaze a apoptosy. Cetuximab se s úspěchem používá při léčbě kolorektálního karcinomu (CRC) nebo terapii spinocelulárního karcinomu hlavy a krku (SCCHN) (Gschwind et al., 2004).

Za zmínku jistě stojí i další protilátky, které byly nebo jsou ve stádiu procesu schvalování pro léčbu různých typů nádorových onemocnění charakterizovaných zvýšenou expresí EGF

receptorů. Jsou jimi kupříkladu panitumumab pro léčbu CRC a nebo nimotuzumab pro léčbu SCCHN (Argyriou et al., 2009; Berardi et al., 2010).

1.4 Radioaktivně značené peptidy

Skupina sloučenin s peptidovou strukturou patří do skupiny nízkomolekulárních látek, které jsou se stále vyšší oblibou používány pro radiodiagnostiku (PRRI) a radioterapii (PRRT). Peptidy nebo jejich analogy se dostaly do popředí svého zájmu především díky svým vlastnostem, které se blíží charakteru ideální sloučeniny (vysoká vazebná afinita, specifické vychytávání a zadržování v cílovém místě, rychlá clearance z necílové tkáně, adekvátní kapilární prostupnost, vysoká stabilita, snadná příprava a bezrizikové užití u pacientů díky tomu, že nevyvolávají imunitní reakci organismu) pro diagnostiku a případnou terapii nádorových onemocnění, a které jim dávají výhody oproti některým makromolekulárním látkám a řadě nízkomolekulárních látek (Lee et al., 2010; Laverman et al., 2012).

Peptidické látky jsou v našem organizmu významné v úloze regulátorů řady fyziologických funkcí. Jejich úlohou je především hormonální modulace v řadě tkání, jako je mozek, gastrointestinální trakt a endokrinní, vaskulární nebo lymfoidní systém. Peptidové hormony působí především přes receptory spřažené s G-proteiny. A právě cílení peptidových hormonů na tento typ receptoru je dalším významným kladem v užívání peptidů a jejich analogů v onkologii. Fyziologicky je míra exprese tohoto typu receptoru nízká, ale v případě nádorových buněk je naopak vysoká. Nádorové buňky „lační“ po přílivu transmiterů, které se účastní jejich zvýšeného metabolismu a procesu dělení. Proto karcinogenní buňky exprimují na svém povrchu velké množství receptorů z této rozsáhlé rodiny receptorových proteinů pro peptidové hormony. Tato biologická skutečnost dodává významu studiím a aplikacím řady připravovaných receptorově specifických peptidů v radiodiagnostice nebo radioterapii (Reubi et al, 2008; Trojan a kolektiv, 2003).

Řadu peptidových hormonů – transmiterů v jejich přirozené formě nelze použít pro jejich aplikaci v léčbě a diagnostice nádorových onemocnění. Jejich přirozená forma vede k rychlé degradaci v organismu ze strany regulačních mechanizmů, jako je především enzymové působení. Radioaktivně značené peptidy by se tak ani nedostaly do cílového místa svého působení. V důsledku toho došlo k syntéze takzvaných peptidových analogů, které si ponechávají ve své struktuře aktivní vazebné místo na cílový receptor, ale které záměnou aminokyselin v jejich řetězci nebo modifikací peptidového řetězce unikají rychlému degradačnímu působení zejména v krevním řečišti, potažmo v játrech. Záměna aminokyselin

je většinou za D-formy aminokyselin nebo za nepřirozené aminokyseliny. Modifikace peptidového řetězce se provádí přidáváním postranních řetězců, inkorporací hydrofilních nebo hydrofobních aminokyselin, anebo cyklizací, acetylací či aminací peptidového řetězce. Modifikace peptidového řetězce navíc umožňují rychlejší permeabilitu upravených peptidů do cílové tkáně přes stěny cév a usnadňuje i jejich přípravu, která probíhá nejčastěji metodou syntéza peptidů na pevné fázi (SPPS) (Lee et al., 2010).

Peptidy, potažmo jejich analogy, se pro klinickou aplikaci mohou značit optickými sondami (fluorofory), nanočásticemi (například magnetické oxidy železa, nanočástice zlata) anebo především radionuklidy.

Strategie vývoje radioaktivně značeného peptidového analogu je názorně zobrazena na obr. 4. Na začátku je vytipování nádorového onemocnění s následným molekulárně biologickým prozkoumáním buněčného povrchu nádorově transformované buňky, kde se zkoumá přítomnost receptorů typických pro daný typ nádorových buněk. Receptory jsou vodítkem pro zjištění specifického, na receptor se přirozeně vázajícího peptidu, který se stane předlohou pro připravovaný peptidový analog. Peptidový analog se připravuje synteticky pomocí dvou způsobů. Prvním z nich je využití syntézy peptidů na kapalné fázi (solution-phase peptide synthesis), která je charakterizována komplikovanou přípravou a následnou nezbytností purifikace připraveného peptidu. Oproti tomu vyniká svým rychlým a jednoduchým průběhem syntézy druhý způsob přípravy peptidů označovaný jako syntéza peptidů na pevné fázi (solid-phase peptide synthesis). Posledně zmiňovaný způsob syntézy peptidů většinou vyžaduje minimum čistění finálního produktu. Na připravený peptidový analog se v další fázi přípravy radioaktivně značeného peptidu naváže vhodně zvolené chelatační činidlo, tak aby se neovlivnilo vazebné místo pro interakci s receptorem a stejně tak farmakokinetické vlastnosti peptidu. Se stejnou opatrností se volí vhodný radioizotop (Okarvi, 2004).

Radioizotopy se volí i s ohledem na zamýšlené použití radioaktivně značeného peptidového analogu. Izotopy vhodné pro radiodiagnostiku jsou zejména ^{99m}Tc, ^{123}I, ^{111}In, ^{18}F, ^{64}Cu nebo ^{68}Ga, a pro radioterapeutické užití ^{90}Y a ^{177}Lu. Vazba izotopů na cílový peptid se uskutečňuje buď přímou vazbou radionuklidu na funkční skupinu peptidového řetězce, anebo nejčastěji nepřímou vazbou prostřednictvím chelatačních skupin vázaných kovalentní vazbou na aminokyselinovém řetězci. Nejvíce užívanými chelatačními činidly uplatňovanými v radiochemickém značení jsou diethylen-triamin-pentaoctová kyselina (DTPA) a 1,4,7,10-tetraazacyklododekan-1,4,7,10-tetraoctová kyselina (DOTA). Tato chelatační činidla vytvářejí stabilní komplexy s radioizotopy ^{111}In, ^{64}Cu, ^{68}Ga, ^{90}Y a ^{177}Lu. Pro vazbu ^{18}F na

peptidový řetězec se používá prostetické skupiny N-sukcinimidyl-4-^{18}F-fluorobenzoátu (Lee et al., 2010; Aloj et al., 2004; Laverman et al., 2012).

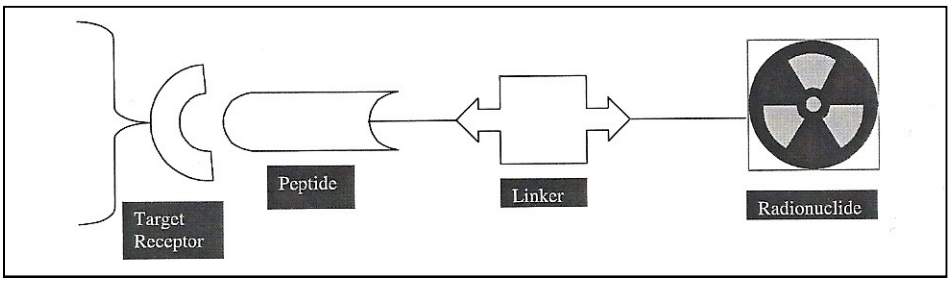

Obrázek č. 4: Ilustrace obecného přístupu k vývoji radioaktivně značených peptidů. (zdroj: Okarvi, 2004)

Proces internalizace radioaktivně značených peptidů do cílových buněk spočívá v jejich navázání na receptorový protein. Vzniklý komplex receptor – peptid je transportován přes cytoplazmatickou membránu buňky ve formě endocytárních částic, které se v prostředí cytoplazmy slučují do větších částic nazývaných endosomy. Endosomy mají kyselé vnitřní prostředí, které vyvolává rychlou disociaci komplexu receptor – peptid. Oddělený receptor je pak většinou externalizován zpět na povrch buňky a tím je takzvaně recyklován. Endosomální částice, ve které zůstal radioaktivně značený peptid, je dále v buněčném prostředí slučována s lysozomem. Působením enzymů uvnitř lysozomů dochází k vyvolání degradace značeného peptidu (viz obrázek č. 5). Samotný radioisotop zůstává v cytoplazmě buňky, kde jím emitované radioaktivní záření v závislosti na své energii vyvolá terapeutický efekt nebo poslouží k diagnostice nádorového procesu (Breeman et al, 2001).

Somatostatinový analog octreotide značený izotopem ^{111}In (D-Phe^{1}-Cys^{2}-Phe^{3}-D-Trp^{4}-Lys^{5}-Thr^{6}-Cys^{7}-Thr^{8}-ol, pod obchodním názvem OctreoScan®) je nejstarším úspěšným radiofarmakem peptidového původu, které se jako první začalo používat pro diagnostické účely v onkologii. Tento cyklický oktapeptid je cílený na nádory neuroendokrinního původu (Laverman et al., 2012; Lee et al., 2011). Svým původem je odvozen od somatostatinu a řadí se tak do skupiny somatostatinových analogů. Somatostatin je regulačním cyklopeptidovým hormonem fungujícím jako neurotransmiter v mozku. Jako regulátor působí inhibičně na tvorbu a sekreci růstového hormonu, insulinu, glukagonu a kalcitoninu přes své receptory spřažené s G-proteinem nesoucích označení somatostatinové receptory (SSTrs), kterých známe 5 druhů dále dělených do podtypů. Z důvodu jeho krátkého biologického poločasu v krvi (cca 3 minuty) se somatostatin nedal použít pro radiodiagnostické účely. Proto byla

připravena celá řada jeho analogů, které postrádají místo pro enzymatické štěpení a jsou tak chráněny před biodegradací (Weckbecker et al., 2003).

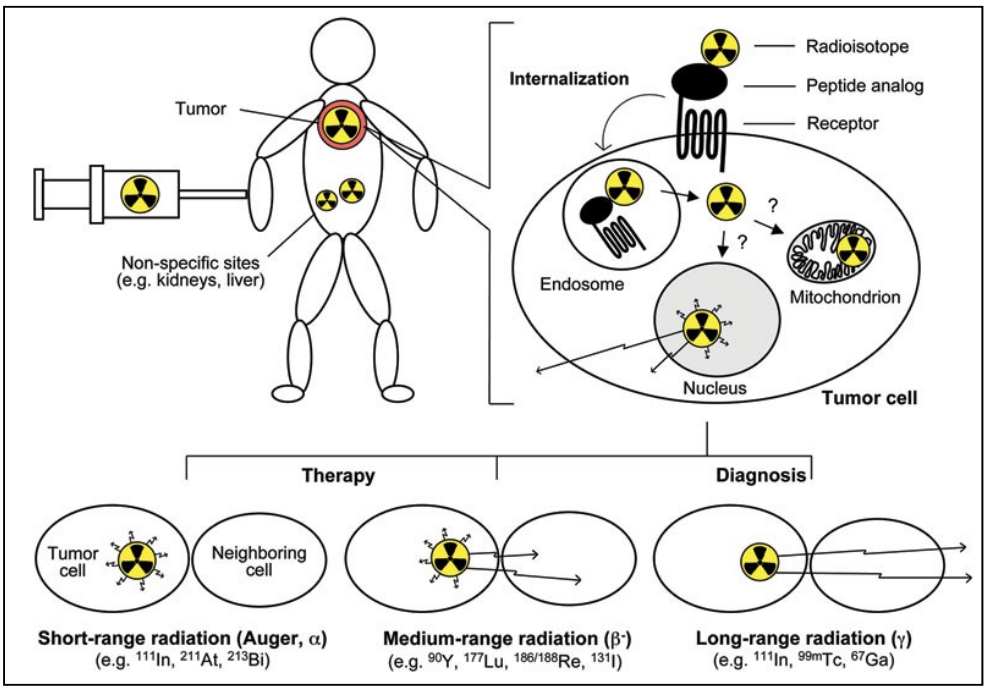

Obrázek č. 5: Základní schéma působení radioaktivně značených peptidových analogů s využitím v terapii nebo diagnostice nádorových onemocnění (zdroj: Eberle et al, 2010).

Skupina radioaktivně značených peptidů není vymezena pouze na somatostatin a jeho analogy. K dnešnímu dni se intenzivně pracuje na řadě receptorově specifických peptidů, které jsou ve stavu vývoje nebo již podstupují různé fáze klinického testování. Jde především o radiopeptidy cílené na cholecystokininový receptor typu 2 (CCK2r) a dále například na gastrinový receptor (GRPr) nebo receptor pro glukagon-like peptid-1 (GLP-1r).

1.5 Cholecystokininové receptory a jejich ligandy

Cholecystokinin (CCK) je gastrinu podobný peptid, který je široce rozšířeným neuropeptidem v centrálním nervovém systému. CCK se skládá z 33 aminokyselin. Vzniká zkracováním prekurzorové molekuly, která má na počátku své degradace ve svém peptidovém řetězci 115 aminokyselin. Z prekurzorové molekuly vznikají formy CCK, které jsou biologicky aktivní. Těmito formami cholecystokininu jsou CCK39, CCK33, CCK8 a CCK4 (Laverman et al., 2012).

Cholecystokinin působí na cílové buňky prostřednictvím specifických receptorů. Do současné doby byly identifikovány tři typy cholecystokininových receptorů na základě jejich afinity k endogenním peptidům CCK a gastrinu. Tyto dva peptidy jsou shodné v té části své struktury, která umožňuje jejich vazbu na CCK receptory. Liší se v sulfataci tyrosinového zbytku na pozici 6 (gastrin) a 7 (CCK).

Prvním typem cholecystokininového receptoru je typ CCK1, který se vyskytuje v pankreatických acinárních buňkách. Druhým typem je receptor CCK2, který se hojně vyskytuje v mozku, žaludku, slinivce a žlučovém měchýři. Třetím typem je CCK2i4sv, který je variantou CCK2 receptoru. Tento typ receptoru byl objeven u lidského kolorektálního karcinomu. CCK1 a CCK2 receptor se liší svou distribucí v organizmu, molekulovou strukturou a afinitou k CCK a gastrinu. CCK1 receptor má mnohem vyšší afinitu (500 až 1000x) k sulfátové formě cholecystokininu něž k nesulfátové formě cholecystokininu. CCK2 receptor vykazuje stejnou afinitu ke gastrinu a cholecystokininu a stejně tak umožňuje vazbu jak sulfátové tak i nesulfátové formy cholecystokininu. CCK2 receptor se proto označuje jako gastrinový receptor a z hlediska nádorových onemocnění ho nalezneme hojně exprimovaný na povrchu nádorových buněk u medulárního tyreoidálního karcinomu, ovariálního karcinomu nebo u gastroenteropankreatických nádorů (Laverman et al., 2012; Koopmans et al., 2009).

Od konce devadesátých let byly provedeny experimenty s různými formami uměle syntetizovaných analogů cholecystokininu nebo gastrinu. To vše se střídavým úspěchem. Připravené analogy mají kratší peptidový řetězec oproti svým přirozeným formám nebo obsahují zaměněné aminokyseliny ve své struktuře. C-terminální část je však u všech stejná. Obsahuje tetrapeptidovou sekvenci -Trp-Met-Asp-Phe-NH_2, která je podstatná pro vazbu peptidu na cílový receptor CCK2. Výchozími strukturami pro CCK/gastrinové analogy se staly CCK8 (Asp-Tyr-Met-Gly-Trp-Met-Asp-Phe-NH_2) a minigastrin (dGlu-Ala-Tyr-Gly-Trp-Met-Asp-Phe-NH_2) (Lee et al., 2010; Roosenburg et al., 2010).

Využití ligandů vázajících se na CCK2 receptor je přednostně zaměřeno na scintigrafické zobrazení a s menším podílem i terapii medulárního tyreoidálního karcinomu. Významného úspěchu v klinickém testování bylo dosaženo u ^{111}In-DTPA-MG0 zejména pak v diagnostických studiích (Behé et al., 2002; Behr et al., 2002). Naopak u radioligandů jako ^{111}In-DOTA-CCK8 a ^{111}In-DOTA-MG11 byla zjištěna nízká scintigrafická citlivost a míra vychytávání, proto se dále nedaly využít pro radioterapii. ^{111}In-DOTA-MG11 navíc vykazoval velmi nízkou stabilitu.

Vedle posledně zmíněných peptidů vykazuje vysokou stabilitu další ligand CCK2 receptoru ^{99m}Tc-demogastrin 2, který se tak stal slibným diagnostickým nástrojem při diagnostice medulárního tyreoidálního karcinomu (Laverman et al., 2012).

2. Cíle předkládané disertační práce

Základním cílem předkládané disertační práce bylo studium interakce vybraných receptorově specifických, radioaktivně značených peptidů a protilátek na cílových buněčných liniích izolovaných z nádorových tkání. Hlavní zaměření práce spočívalo v posouzení nových možností pro hodnocení interakcí ligand-receptor in vitro za použití nově zaváděné techniky. Studium receptorově specifických látek v sobě zahrnovalo i prozkoumání faktorů, které ovlivňují jejich biologické chování v živých systémech.

3. Použité metody

Studium probíhalo jednak pomocí klasických experimentálních metod zkoumání interakce radioligandu na specifickém receptoru v *in vitro* podmínkách, kdy se sledovala míra internalizace radioaktivně značeného ligandu do buněk přes jeho cílový receptor měřená v lyzátu buněk na přístroji detekujícím gama záření. Druhým způsobem bylo opět stanovení míry internalizace do buněk tentokrát měřené v reálném čase. K tomuto účelu byla použita automatická technika s využitím přístroje LigandTracer®, která detekuje množství zachyceného radioligandu v buňkách při jeho zvolené koncentraci v médiu.

Klasická metoda a automatická technika jsou založeny na interakci ligandu a jeho receptoru s dosažením rovnováhy této interakce vyjádřené vztahem pro disociační konstantu reakce K_D, $K_D = \frac{[L][R]}{[LR]}$, kde [L] je koncentrace radioligandu (peptid nebo protilátka), [R] koncentrace volného cílového receptoru a [LR] koncentrace ligand-receptorového komplexu.

Disertační práce je předložena jako soubor šesti publikací, které se týkají jejího tématu studia radioligandů v *in vitro* podmínkách. Uvedené publikace jsou řazeny v kapitolách dle chronologie jejich publikování v odborných časopisech. Odborné publikace v kapitolách I, III, IV a V byly otištěny v odborných časopisech s impakt faktorem, publikace v kapitole II v odborném časopisu bez impakt faktoru a nejnovější publikace uvedená v kapitole VI je ve stavu posouzení o přijetí k opublikování v odborném časopise s impakt faktorem. U publikací uvedených v kapitole I, II, III a VI je předkladatel disertační práce hlavním autorem publikovaných prací.

4. Podíl doktoranda na předkládaných publikacích

V odborné publikaci uvedené v kapitole I autor provedl veškeré buněčné experimenty včetně jejich vyhodnocení a sepsal rukopis publikace včetně souborného zhodnocení výsledků ve spolupráci se spoluautory. Cílem studie bylo provést ohodnocení možnosti využití nové alternativní metody pro kvantifikaci množství buněčných receptorů zvané kinetická extrapolace (KEX). KEX metoda se porovnala s klasickou saturační technikou určování počtu receptorů na buňkách. Výsledkem experimentální studie bylo zjištění, že nová testovaná metoda kvantifikace počtu buněčných receptorů KEX je vhodnou alternativou současně nejčastěji používané saturační techniky, jelikož poskytuje téměř identické údaje o počtu receptorů na jednu buňku a navíc vyžaduje mnohonásobně nižší objem práce a tedy i potřebného času na provedení. Mimo to vykazuje téměř o 2/3 nižší náročnost na množství použitých chemikálií a spotřebního materiálu.

Odborná publikace v kapitole II byla vypracována na základě výsledků měření na buněčných kulturách. Autor provedl experimenty na ledvinných buňkách OK cells a dále sepsal rukopis vědeckého výtisku. Studie byla zaměřena na prozkoumání specifické vazby radioligandů ^{111}In-DOTA-minigastrin11 a ^{177}Lu-DOTA-minigastrin11 na gastrin/cholecystokinový (CCK2R) receptor na povrchu pankreatických nádorových buněk (AR42J) a jejich možnou akumulaci v buňkách proximálního tubulu ledvin (OK cells). Zjištěním práce byla vazba radioligandů na CCK2R a jejich následný transport do nádorových buněk. Tento výsledek poukazuje na to, že struktura peptidu minigastrin11 nebyla narušena radioaktivním značením, které navíc vykazovalo radiochemickou čistotu značení nad 99%. Dalším pozitivním nálezem byla minimální akumulace značeného minigastrinu11 do ledvinných buněk, což naznačuje relativně nízké riziko radionefrotoxicity v případné podání *in vivo*.

Publikace uvedená v kapitole III je společnou prací, do které autor přispěl v podobě buněčných experimentů uskutečněných na použitých buněčných liniích. Autor pracoval se značeným receptorovým substrátem ^{125}I-EGF, který sloužil jako indikátor exprese cílového receptoru při kultivaci buněk v přítomnosti nebo nepřítomnosti gefitinibu. Autor spolupracoval i na úpravách konečné verze rukopisu odborné publikace. V této publikaci jsme se pokusili odhalit možný mechanismus vlivu gefitinibu na interakci mezi epidermálním růstovým faktorem (EGF) a jeho receptorem EGFR. Experimenty probíhaly za použití přístroje LigandTracer® Grey. V reálném čase měřená vazba ligandu na receptory byla dále analyzována pomocí nové matematické metody zvané Interaction Map, která byla schopná

rozpoznat vazbu homogenního ligandu EGF na mnoha heterogenních vazebných místech (receptorech) na povrchu buňky. Výsledkem práce bylo vysvětlení vlivu procesu dimerizace receptorů na rozdílnou afinitu EGF k EGFR pro různé buněčné linie. Gefitinib pak indukuje tvorbu dimerů receptoru EGFR, který v důsledku toho mění charakter své interakce s ^{125}I-EGF.

Podíl autora v odborné publikaci v kapitole IV spočívá především v přípravě ^{131}I-radioligandů a v provedení buněčných experimentů se značenými radioligandy ve spolupráci s Dr. Ludmilou Melicharovou na LigandTracer® Yellow ze strany fakultního pracoviště. Autor se dále podílel na sepsání rukopisu. Cílem odborné publikace bylo vyšetřit, do jaké míry závisí charakter interakce ligand – receptor na volbě buněčné linie. V našem případě se provedly experimenty na buněčných liniích exprimujících receptory z HER-receptorové rodiny. Zjištěné poznatky této studie poukazují na fakt, že hodnota vazebné afinity testovaného proteinu vázajícího se na ten samý typ HER receptoru se může mezi buněčnými liniemi významně lišit. Hodnota afinity testovaného ligandu na jedné buněčné linii tak neodpovídá afinitě u jiné buněčné linie se stejným typem receptoru. Zjištěná hodnota afinity by tak měla být vždy uváděna pro daný typ buněk, které byly využity v hodnocení vazebnosti ligandu.

Do publikace v kapitole V přispěl autor výsledky z buněčných experimentů s ligandy ^{131}I-cetuximab a ^{131}I-panitumumab na buňkách A431 a HepG2, dále spoluúčastí na přípravě použitých ligandů a nastavením podmínek měření. Autor také provedl vyhodnocení měření na přístroji LigandTracer® Yellow a spolupracoval na sepsání rukopisu. Tato publikovaná studie si kladla za cíl opětovné ověření vhodnosti užití metody KEX pro kvantifikaci počtu receptorů na povrchu buněk. KEX metoda se opětovně porovnala s klasickou saturační technikou a navíc se provedlo srovnání i s metodou western blottingu. Výsledky poskytnuté metodou KEX a standardní saturační metodou byly velmi blízké ve svých hodnotách pro všechny použité buněčné linie. Dle počtu EGFR bylo oběma metodami shodně stanoveno následující pořadí buněčných linií: A431>HaCaT>HCT116~HEP-G2. S nalezenými daty radioligandových studií dobře korelovala exprese receptorových proteinů zjištěná pomocí techniky western blottingu.

Poslední autorova práce umístěná v kapitole VI byla sepsána na základě výsledků *in vivo* a *in vitro* měření. *In vitro* měření a jejich vyhodnocení provedl autor samostatně, stejně tak značení protilátky izotopem ^{131}I. Autor spolupracoval na zjištění stability ^{131}I-ligandu pomocí chromatografické analýzy a na sepsání rukopisu. Tato práce analyzovala vliv radioaktivního značení na afinitu protilátky nimotuzumab k EGFR u zvolených buněčných linií a stejně tak

na jeho biodistribuční profil v předklinických *in vivo* experimentech. Výsledky práce ukázaly, že volba radionuklidu a způsob jeho navázání na nimotuzumab měla velmi nízký efekt na afinitu vazby protilátky na cílový receptor EGFR buněčných linií. Oproti tomu volba radionuklidu, způsob jeho vazby na nimotuzumab a postup radioaktivního značení viditelně ovlivnil jeho clearance z krve, vychytávání játry a jeho následnou akumulací v nich.

5. Seznam literatury

Allison M (2009) Bristol-Myers Squibb swallows last of antibody pioneers. Nat Biotechnol 27:781-783.

Aloj L, Morelli G (2004) Design, synthesis and preclinical evaluation of radiolabeled peptides for diagnosis and therapy. Curr Pharm Des 10:3009-3031.

Argyriou AA, Kalofonos HP (2009) Recent advances relating to the clinical application of naked monoclonal antibodies in solid tumors. Mol Med 15:183-191.

Ambrosini V, Fani M, Fanti S, Forrer F, Maecke HR (2011) Radiopeptide imaging and therapy in Europe. J Nucl Med 52:42S-55S.

Behé M, Behr TM (2002) Cholecystokinin-13 (CCK-B)/gastrin receptor targeting peptides for staging and therapy of medullary thyroid cancer and other CCK-B receptor expressing malignancies. Biopolymers 66:399-418.

Behr TM, Behé MP (2002) Cholecystokinin-B/gastrin receptor-targeting peptides for staging and therapy of medullary thyroid cancer and other cholecystokinin-B receptor-expressing malignancies. Semin Nucl Med 32:97-109.

Berardi R, Onofri A, Pistelli M, Maccaroni E, Scartozzi M, Pierantoni C, Cascinu S (2010) Panitumumab: the evidence for its use in the treatment of metastatic colorectal cancer. Core Evid 5:61-76.

Bessman NJ, Lemmon MA (2012) Finding the missing links in EGFR. Nat Struct Mol Biol 19:1-3.

Breeman WAP, Marion de Jong, Kwekkeboom DJ, Valkema R, Bakker WH, Kooij PPM, Visser TJ, Krenning EP (2001) Somatostatin receptor-mediated imaging and therapy: basic science, current knowledge, limitations and future perspectives. Eur J Nucl Med 28:1421-1429.

Coiffier B (2006) Treatment of non-Hodgkin´s lymphoma: a look over the past decade. Clin Lymphoma Myeloma 7:S7-S13.

Druker BJ, Tamura S, Buchdunqer E, Ohno S, Segal GM, Fanning S, Zimmermann J, Lydon NB (1996) Effects of a selective inhibitor of the Abl tyrosine kinase on the growth of Bcr-Abl positive cells. Mature Med 2:561-566.

Eberle AN, Bapst JP, Calame M, Tanner H, Froidevaux S (2010) MSH radipeptides for targeting melanoma metastasis. Adv Exp Med Biol 681:133-142.

Goldenberg DM (1994) Radiolabeled Antibodies. Scientific American Science and Medicine 1:64-73.

Goldenberg DM (2003) Advancing role of radiolabeled antibodies in the therapy of cancer. Cancer Immunol Immunother 52:281-296.

Goldenberg DM, Sharkey RM (2006) Advances in cancer therapy with radiolabeled monoclonal antibodies. Q J Nucl MedMol Imaging 50:248-264.

Goldenberg DM, Sharkey RM, Paganelli G, Barbet J, Chatal JF (2006) Antibody pretargeting advances cancer radioimmunodetection and radioimmunotherapy. J Clin Oncol 24:823-834.

Goldenberg DM, Sharkey RM (2007) Novel radiolabeled antibody conjugates. Oncogene 26:3734-3744.

Goldenberg DM (2009) Some like it hot: lymphoma radioimmunotherapy. Blood 113:4903-4913.

Govindan SV, Goldenberg DM (2010) New antibody conjugates in cancer therapy. ScientificWorldJournal 10:2070-2089.

Gschwind A, Fischer OM, Ullrich A (2004) The discovery of receptor tyrosine kinases: targets for cancer therapy. Nat Rev Cancer 4:361-370.

Joensuu H, Roberts PJ, Sarlomo-Rikala M, Andersson LC, Tervahartiala P, Tuveson D, Silberman S, Capdeville R, Dimitrijevic S, Druker B, Demetri GD (2001) Effect of the tyrosine kinase inhibitor STI571 in a patient with a metastatic gastrointestinal stromal tumor. N Engl J Med 344:1052-1056.

Kalofonos HP, Grivas PD (2006) Monoclonal antibodies in the management of solid tumors. Curr Top Med Chem 6:1687-1705.

Knox SJ, Goris ML, Tempero M, Weiden PL, Gentner L, Breitz H, Adams GP, Axworthy D, Gaffigan S, Bryan K, Fisher DR, Colcher D, Horak ID, Weiner LM (2010) Phase II trial of yttrium-90-DOTA-biotin pretargeted by NR-LU-10 antibody/streptavidin patients with metastatic colon cancer. Clin Cancer Res 6:406-414.

Koopmans KP, Neels ON, Kema IP, Elsingra PH, Links TP, de Vries EG, Jager PL (2009) Molecular imaging in neuroendocrine tumors: Molecular uptake mechanisms and clinical results. Crit Rev Oncol Hematol.

Laverman P, Sosabowski JK, Boerman OC, Oyen WJG (2012) Radiolabeled peptides for oncological diagnosis. Eur J Nucl Med Mol Imagin 39:S8-S92.

Lee S, Xie J, Chen X (2010) Peptide-based probes for targeted molecular imaging. Biochemistry 49:1364-1376.

Loke KS, Padhy AK, Ng DC, Goh AS, Divgi C (2011) Dosimetric consideration in radioimmunotherapy and systemic radionuclide therapies: A review. World J Nucl Med 10:122-138.

Marqués MM, Martínez N, Rodríguez-García I, Alonso A (1999) EGFR family-mediated signal transduction in the human keratinocyte cell line HaCaT. Exp Cell Res 252:432-438.

Moulder SL, Yakes FM, Muthuswamy SK, Bianco R, Simpson JF, Arteaga CL (2001) Epidermal growth factor receptor (HER1) tyrosine kinase inhibitor ZD1839 (Iressa) inhibits HER2/neu (erbB2)-overexpressing breast cancer cells *in vitro* and *in vivo*. Cancer Research 61:8887-8895.

Masui H, Kawamoto T, Sato JD, Wolf B, Sato G, Mendelsohn J (1984) Growth inhibition of human tumor cells in athymic mice by anti-epidermal growth factor receptor monoclonal antibodies. Cancer Res 44:1002-1007.

Okarvi SM (2004) Peptide-based radiopharamaceuticals: future tools for diagnostic imaging of cancers and other diseases. Med Res Rev 24:357-397.

Reubi JC, Maecke HR (2008) Peptide-based probes for cancer imaging. J Nucl Med 49:1735-1738.

Roosenburg S, Laverman P, van Delft FL, Boerman OC (2010) Radiolabeled CCK/gastrin peptides for imaging of CCK2 receptor-expressing tumors. Amino Acids 41:1049-1058.

Sears HF, Herlyn D, Steplewski Z, Koprowski H (1985) Phase II clinical trial of a murine monoclonal antibody cytotoxic for gastrointestinal adenocarcinoma. Cancer Res 45:5910-5913.

Sharkey RM, Goldenberg DM (2005) Perspectives on cancer therapy with radiolabeled monoclonal antibodies. J Ncl Med 46:115-127.

Sharkey RM, Goldenberg DM (2008) Use of antibodies and immunoconjugates for the therapy of more accessible cancers. Adv Drug Deriv Rev 60:1407-1420.

Sharkey RM, Goldenberg DM (2012) Cancer radioimmunotherapy. Immunotherapy 3:349-370.

Serengulam VG, Goldenberg DM (2010) New antibody conjugates in cancer therapy. ScientificWorldJournal 10:2070-2089.

Takeuchi K, Ito M (2011) Target therapy for cancer: anti-cancer drugs targeting growth-factor signalling molecules. Biol Pharm Bull 34:1774-1780.

Teunissen JJM, Kwekkeboom DJ, Valkema R, Krenning EP (2011) Nuclear medicine techniques for the imaging and treatment of neuroendocrine tumours. Endocr Relat Cancer 1:S27-51.

Trojan S a kolektiv (2003) Lékařská fyziologie. GRADA Publishing ISBN 80-247-0512-5, strana 44-52.

Van Gog, Brakenhoff RH, Stigter-van Walsum M, Snow GB, van Dongen GA (1998) Perspectives of combined radioimmunotherapy and anti-EGFR antibody therapy for the treatment of residual head and neck cancer. Int J Cancer 77:13-8.

Wakeling AE, Barker AJ, Davies DH, Brown DS, Green LR, Cartlidge SA, Woodburn JR (1996) Specific inhibition of epidermal growth factor receptor tyrosine kinase by 4-anilinoquinazolines. Breast Cancer Res Treat 38:67-73.

Weckbecker G, Lewis Lewis I, Albert R, Schmid HA, Hoyer D, Bruns C (2003) Opportunities in somatostatin research: biological, chemical and therapeutic aspects. Nat Rev Drug Disc 2:999-1017.

6. Seznam odborných publikací

I. CIRCUMVENTING THE REQUIREMENT OF BINDING SATURATION FOR RECEPTOR QUANTIFICATION USING INTERACTION KINETIC EXTRAPOLATION

Barta P, Björkelund H, Andersson K: Circumventing the requirement of binding saturation for receptor quantification using interaction kinetic extrapolation. Nucl Med Commun. 2011 Sep; 32(9):863-867.

Technical note

Nuclear Medicine Communications

Circumventing the requirement of binding saturation for receptor quantification using interaction kinetic extrapolation

Pavel Barta[a,c], Hanna Björkelund[a,b] and Karl Andersson[a,b]

Quantification of the number of receptors per cell (NRPC) is important when assessing whether a tumor surface biomarker is suitable for medical imaging. One common method for NPRC quantification is to use a binding saturation assay, which is time consuming and requires large amounts of reagents. The aim of this study was to evaluate an alternative method based on kinetic extrapolation (KEX) and compare it with the classical manual saturation technique with regard to accuracy as well as time and reagent consumption. Epidermal growth factor receptor (EGFR) and HER2 receptor surface expression were quantified on five tumor cell lines using three ^{125}I-labeled and ^{131}I-labeled ligands (cetuximab and EGF for EGFR, trastuzumab for HER2 receptor) for both techniques. The KEX method involved interaction measurements in the LigandTracer, followed by KEX through computerized real-time interaction analysis to correct for nonsaturation on cells. Variability and NRPC estimates of the EGFR and HER2 receptor levels using the KEX method were comparable with the results from the classical saturation technique. However, the ligand consumption for the KEX method was 26–46% of the classical saturation technique. Furthermore, the KEX method reduced the workload radically. From the observations described in this study, we believe that the KEX method enables fast, credible, and easy NRPC quantification with a reduction in reagent consumption. *Nucl Med Commun* 32:863–867 © 2011 Wolters Kluwer Health | Lippincott Williams & Wilkins.

Nuclear Medicine Communications 2011, **32**:863–867

Keywords: kinetics, ligand–receptor interaction, receptor quantification

[a]Department of Radiology, Oncology and Radiation Sciences, Uppsala University, [b]Ridgeview Instruments AB, Uppsala, Sweden and [c]Department of Pharmacology and Toxicology, Faculty of Pharmacy in Hradec Kralove, Charles University in Prague, Czech Republic

Correspondence to Dr Karl Andersson, Ridgeview Instruments AB, Ulleråkersvägen 62, SE75643 Uppsala, Sweden
Tel: +46 733 689 717
e-mail: karl@ridgeviewinstruments.com

Received 21 December 2010 **Revised** 28 February 2011
Accepted 27 April 2011

Introduction

The quantification of the number of receptors expressed on the surface of a cell is an important measurement task conducted in many fields of biological sciences [1], including when assessing the suitability of a tumor surface biomarker as target for medical imaging. The number of receptors per cell (NRPC) indicates to what extent a particular gene is expressed, transcribed, and translated. Furthermore, a variety of detection technologies requires knowledge on NRPC for obtaining reliable results.

The quantification of NRPC is commonly conducted with a labeled ligand, which is allowed to interact with the intended receptor at a concentration sufficiently high to saturate the receptor population on the cells. After being washed, the cells are counted and the signal from the labeled ligand is measured. The NRPC can then be calculated from the information on specific activity or label efficiency [2]. Such saturation measurements are the gold standard of NRPC quantification, but other methods exist such as a flow cytometric method [3] and western blot analysis [4].

In this study, we describe an alternative method for obtaining NRPC using the real-time detection device LigandTracer (Ridgeview Instruments AB, Uppsala, Sweden). Ligand–receptor interaction is measured and interaction kinetic modeling is applied to correct for nonsaturation on the cell surface receptors. In this way, the saturation requirement can be circumvented, leading to a significant reduction in reagent and work-time consumption. We denote the method as kinetic extrapolation (KEX). On the basis of the quantification of the epidermal growth factor receptor (EGFR) and the HER2 receptor on five cell lines using three labeled ligands [EGF and cetuximab (Erbitux) for EGFR; trastuzumab (Herceptin) for HER2], we estimated the performance of the KEX method in comparison with the classical saturation technique.

Materials and methods

Cell cultures

The human squamous carcinoma cell line A431 (CLR 1555; ATCC, Rocksville, Maryland, USA), the human ovarian carcinoma cell line SKOV3 (HTB-77, ATCC, Rocksville), the human glioma cell line U343MGaCl2:6 (denoted U343), the human adenocarcinoma cell line SKBR3 (HTB-30; ATCC, Rocksville), and the human keratinocyte cell line HaCaT (DKFZ, Heidelberg, Germany) were used for cell receptor quantification in this study. The cells were seeded in a small local area in a Petri dish (Nuclon, dish size 100 × 20; NUNC A/S,

DOI: 10.1097/MNM.0b013e3283483e1c

Roskilde, Denmark) for the KEX method as described previously [5] and in a 24-well plate for the manual saturation technique (Nuclon, 24-wells plate; NUNC A/S). Ham's F10 cell culture medium (Biochrom AG, Berlin, Germany) for SKOV3 and U343 cells, Dulbecco's modified Eagle medium cell culture medium (Biochrom AG, Berlin, Germany) for A431 cells, and Dulbecco's modified Eagle medium cell culture medium (Sigma-Aldrich, St. Louis, Missouri, USA) for HaCaT cells were used, supplemented with 10% fetal calf serum (Sigma, St. Louis, Missouri, USA), penicillin 100 IU/ml and streptomycin 100 μg/ml, (Biochrom AG, Berlin, Germany), and L-glutamine [2 nmol/l, for Ham's F10 and DMEM (Sigma-Aldrich) culture medium only]. The cells were grown at 37°C in an incubator with humidified atmosphere and 5% CO_2 until experimental day.

Radiolabeling

A total of 2.5 μg of human EGF (Chemicon International, USA) and 80 μg of the monoclonal antibodies trastuzumab (purified from Herceptin; Roche AB, Stockholm, Sweden) and cetuximab (purified from Erbitux; Merck KGaA, Darmstadt, Germany) were labeled with 5–10 MBq ^{125}I (Perkin-Elmer, Wellesley, Massachusetts, USA) or 10 MBq ^{131}I (Institute of Isotopes Co., Ltd. Budapest, Hungary) according to the chloramine-T protocol [6]. The labeling reactions were performed with chloramine-T (Sigma, St. Louis, Missouri, USA) and sodium metabisulfite (Aldrich, Stockholm, Sweden). The desired radiolabeled protein was purified on a NAP-5 column (GE Healthcare, Waukesha, Wisconsin, USA) equilibrated with PBS (10 mmol/l, pH 7.4, 140 mmol/l NaCl).

Estimating the number of receptors per cell using the kinetic extrapolation method

The ^{125}I-ligand and ^{131}I-ligand binding on appropriate cell receptors was measured in real time at room temperature using LigandTracer Grey and LigandTracer Yellow, respectively. The three-step addition of radiolabeled protein in full culture medium (3 ml for LigandTracer Grey and 5 ml for LigandTracer Yellow) was performed after a short baseline run (10 min) without the ligand. In the majority of assays 3, 15, and 30 nmol/l of protein were used, but other ranges starting at 0.1–4.2 nmol/l and ending at 10–90 nmol/l were tested as well. The incubation times were chosen adequately for each ligand concentration to accomplish clear curvature and to approach equilibrium. When the assay was finished, cells were washed twice with PBS + 0.1% BSA and once with PBS, followed by trypsination and resuspension in complete culture medium. Aliquots of 0.5 ml were taken for cell counting and radioactivity measurement (automatic γ counter 1480 WIZARD 3″, Perkin-Elmer). Each cell line and ligand combination was tested two to nine times for receptor quantification. Binding traces from the three-step incubation were fitted to a kinetic model (1 : 1 for EGF, bivalent interaction for cetuximab and trastuzumab) in a TraceDrawer 1.2 (Ridgeview Instruments AB, Uppsala, Sweden). In the case of 1 : 1 binding, the binding traces were fitted to:

$$\text{Signal} = B_{\max} \times (C/(C + k_d/k_a)) \times (1 - \exp(-(k_a \times C + k_d) \times t))$$

where $B_{\max}$ is the signal corresponding to completely saturated cell surfaces, C is the concentration, k_d is the dissociation rate constant, k_a is the association rate constant, and t is the time [7]. Thus, it is possible to estimate $B_{\max}$ from a single nonsaturated binding trace. The bivalent model is similar but cannot be expressed analytically and hence requires numerical integration. The ratio between $B_{\max}$ and the highest measured signal was used to correct for incomplete saturation.

Estimating the number of receptors per cell using the classical manual technique

Cells were seeded in triplicate in 24-well plates for the classical saturation technique. ^{125}I-ligand in complete medium was added to cells in six concentrations (0.5, 1.5, 5, 15, 50, and 150 nmol/l; 0.5 ml/well). Plates were kept on ice the whole time. After 4 h of incubation (approximately 4°C), cells were washed six times with serum-free medium and trypsinated. Resuspended cells were then counted and the radioactivity was measured to evaluate cell receptor levels. For ^{125}I-trastuzumab and the cell lines SKBR3, as well as for ^{131}I-cetuximab at the cell lines A431 and HaCaT, only the highest concentration of ligand was used to assess the NRPC.

Results and discussion

The KEX method was developed in a two-step manner. In the first step, a focused correlation study with the manual saturation technique was conducted using three cell lines (A431, SKOV3, and U343), three ligands labeled with ^{125}I, and two receptors. Thereafter, KEX and a simplified version of the manual technique (highest concentration only) were conducted in parallel to gather further data on the accuracy of KEX. The second step was conducted using three cell lines, with both ^{125}I and ^{131}I in two different laboratories (Uppsala, Sweden, and Hradec Kralove, Czech Republic).

The results obtained from the correlation study (first step) of the KEX method and the classical manual saturation technique are summarized in Fig. 1. The cells covered a wide range in receptor quantity: from 3×10^4 per cell (HER2 on U343) to 6×10^6 per cell (HER2 on SKOV3). The results from the KEX method and the manual saturation technique agreed, and the variability of the two methods were similar, potentially with a slight advantage for the manual technique. The KEX method often produces slightly higher NRPC values than the manual saturation technique. This is probably due to the combination of (i) an overestimation of $B_{\max}$ by the

Fig. 1

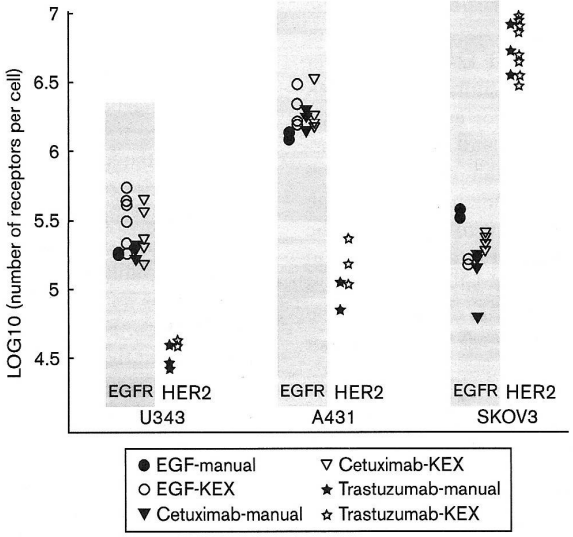

Results from the kinetic extrapolation (KEX) method and the classical manual saturation technique summarized in one graph. Open symbols represent the KEX method and filled symbols represent the classical manual technique. EGF, epidermal growth factor; EGFR, epidermal growth factor receptor.

Fig. 2

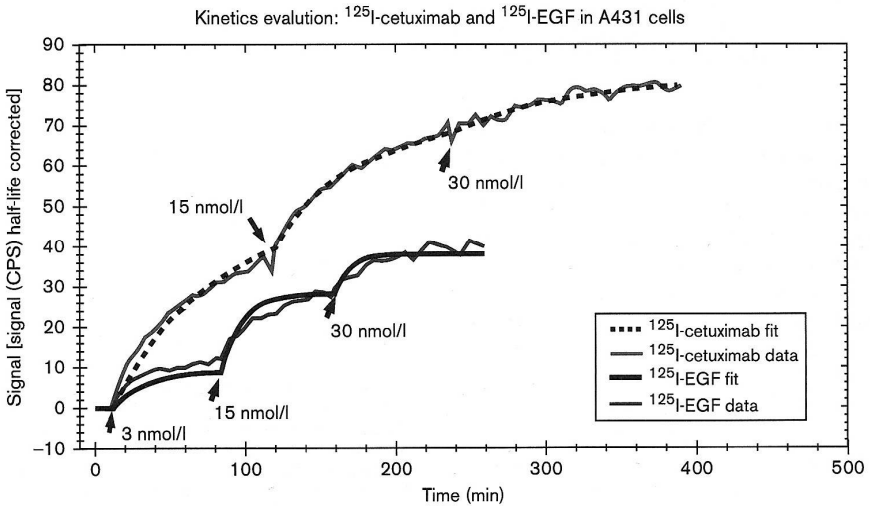

Example of the kinetic evaluation used in the kinetic extrapolation (KEX) method. LigandTracer Grey analysis curves are solid curves with noise, blue (upper) for ^{125}I-cetuximab and red (lower) for ^{125}I-epidermal growth factor (EGF). The smooth black curves represent binding kinetic fits from TraceDrawer 1.2 for ^{125}I-cetuximab (dotted) and ^{125}I-EGF (solid) binding to EGF receptor (EGFR) in A431 cells. The highest signal was approximately 38 CPS and 80 CPS for EGF and cetuximab, respectively. B_{max} as derived from the kinetic fit, which corresponded to full cell EGFR saturation, was approximately 58 and 84 CPS for EGF and cetuximab, respectively (not seen).

kinetic extrapolation, and (ii) an underestimation of signal values in the manual technique, which underestimates B_{max}. The correction for lack of saturation in the KEX method varied between 1 and 2, that is, from no correction to 50% saturation. In Fig. 2, two typical binding traces with accompanying kinetic fits are shown: 1 : 1 binding for ^{125}I-EGF and bivalent binding for ^{125}I-cetuximab to A431 cells. The signal at the highest

concentration was 38 counts per seconds (CPS) and 80 CPS, respectively, and the kinetic model estimated B_{max} to 58 and 84, respectively. In this particular case, the calculated NRPC at harvest should be adjusted by a factor of 1.53 (= 58/38) for labeled EGF and 1.05 (= 84/80) for labeled cetuximab due to incomplete saturation. The KEX method applied to the HER2 receptor at SKOV3 using herceptin was repeated nine times, and allowed assessment of correlation among the batch of trastuzumab labeling (three batches, three measurements of each), the highest concentration (ranging from 10 to 90 nmol/l), the highest signal level (ranging from 24 CPS to 131 CPS), and the estimated NRPC. One batch of labeling produced slightly lower NRPC results than the other two. The highest concentration and highest signal level were not correlated with NRPC.

The summary of the average NRPC for cells divided according to the technique type is shown in Table 1. The values of EGFR per cell and HER2 receptor per cell for the given cell lines are in agreement with published data, where available [8]. The average standard deviation was 19% of NRPC for the KEX method (three cell lines, three receptors, each repeated two to nine times) and 17% of NRPC for the classical manual saturation technique (two or three replicates per cell line–label combination).

In the second step, NRPC estimates have been conducted for HER2 on SKBR3 cells by use of ^{125}I-trastuzumab, and for EGFR on A431 and HaCaT cells by use of ^{131}I-cetuximab, as presented in Table 1. All collected NRPC data are shown in Fig. 3. The agreement of the methods is clear with only one exception (^{125}I-EGF on SKOV3 cells).

It was noted that in the classical manual technique saturation was not always reached, even for the highest ligand concentration (150 nmol/l), mainly for labeled trastuzumab added to SKOV3 cells. The time required to reach equilibrium for high-affinity interaction can be 10 or even 100 h [9] and this will result in underestimation of the true NRPC when using the classical manual technique. The KEX method regularly did not reach saturation, but there was no problem due to the correction for B_{max} by use of kinetic fits: the NRPC assessment became accurate even when low ligand concentrations were used and the receptor saturation was not reached. This is the main advantage of the KEX method for NRPC evaluation compared with the manual saturation technique. The limitation of the KEX method is that it requires a binding trace with visible curvature, and this may be difficult to obtain when the NRPC is approximately 10^4 or smaller (e.g. U343 cells with HER2 receptor).

Verification of specificity and correction for nonspecific binding, as commonly assessed by addition of excess of unlabeled ligand (blocking), were not included in this study due to the cost. The cells and ligands used in this report are standard material handled in our laboratory, and the specificity of the ligands has been proved repeatedly by such blocking experiments (see e.g. [2,10]). The fact that the results in this study are in agreement with previously published reports indicates that the blocking procedure is not critical for obtaining accurate NRPC for these ligands. Furthermore, the highest concentration in the KEX method is often at a low level in which the nonspecific interactions are less common.

The reagent consumption and workload of the two methods were also compared. The KEX method consumed approximately 9.1 pmole of labeled ligand per run in comparison with 20 or 35 pmole of cetuximab/trastuzumab and EGF, respectively, per experiment for the

Fig. 3

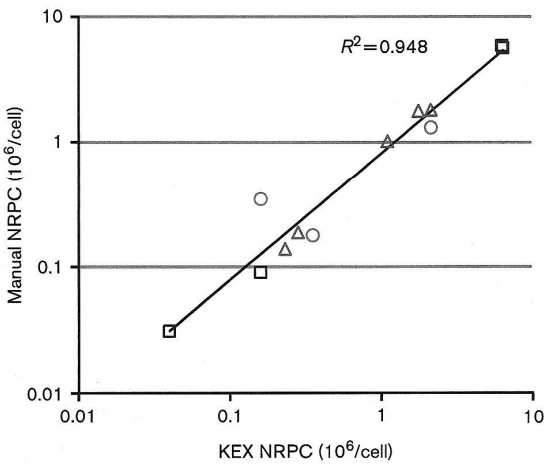

Correlation plot of number of receptors per cell (NRPC) values obtained with the two different methods. Data from five cell lines (A431, SKOV3, U343, SKBR3, and HaCaT) expressing various levels of epidermal growth factor (EGF) receptor and HER2 receptor are shown in the graph. Trastuzumab (squares), cetuximab (triangles), and EGF (circles) were used to assess NRPC. KEX, kinetic extrapolation.

Table 1 Summary of the results obtained for the KEX method and the classical manual saturation technique

	A431		SKOV3		U343		SKBR3		HaCaT	
Number of receptors per cell (x 10^6)	KEX	Manual	KEX	Manual	KEX	Manual	KEX	Manual	KEX	Manual
^{125}I- [^{131}I-] cetuximab (EGFR)	2.1 (1.7)	1.8 (1.7)	0.23	0.14	0.28	0.19	MD	MD	(1.1)	(1.0)
^{125}I-EGF (EGFR)	2.1	1.3	0.16	0.35	0.35	0.18	MD	MD	MD	MD
^{125}I-trastuzumab (HER2)	0.16	0.091	6.3	5.6	0.040	0.031	6.2	5.8	MD	MD

EGFR, epidermal growth factor receptor; KEX, kinetic extrapolation; MD, missing data.

manual technique. If blocking experiments are included, the KEX method will save even more reagent. The time spent on laboratory work and the use of disposable cell culture dishes and media by the KEX method were reduced by approximately 60 and 90% respectively compared with the classical saturation technique.

In conclusion, we described an improved NRPC assay, which uses the ability to accurately extrapolate the level of saturation by kinetic fitting. The novel KEX method will be particularly useful for laboratory experiments with expensive ligands.

Acknowledgements

The authors thank Associate Professor Lars Gedda for constructive comments on the study. This study was in part funded by Rector's Mobility Fund of Charles University in Prague, Czech Republic.

Conflicts of interest

H.B. and K.A. are employees of Ridgeview Instruments AB. K.A. is a shareholder of Ridgeview Instruments AB.

References

1 Hulme EC, Trevethick MA. Ligand binding assays at equilibrium: validation and interpretation. *Br J Pharmacology* 2010; **161**:1219–1237. doi: 10.1111/j.1476-5381.2009.00604.x.
2 Nestor M. Effect of cetuximab treatment in squamous cell carcinomas. *Tumor Biol* 2010; **31**:141–147. doi 10.1007/s13277-010-0018-8.
3 Brotherick I, Lennard TWJ, Wilkinson SE, Cook S, Angus B, Shenton BK. Flow cytometric method for the measurement of epidermal growth factor receptor and comparison with the radio-ligand binding assay. *Cytometry* 1994; **16**:262–269.
4 Hanna W. Testing for HER2 status. *Oncology* 2001; **61**:22–30.
5 Björke H, Andersson K. Measuring the affinity of a radioligand with its receptor using a rotating cell dish with in situ reference area. *Applied Radiat Isotopes* 2005; **64**:32–37.
6 Greenwood FC, Hunter WM, Glover JS. The preparation of 131I-labelled human growth hormone of high specific radioactivity. *Biochem J* 1963; **89**:114.
7 Björkelund H, Gedda L, Andersson K. Avoiding false negative results in specificity analysis of protein-protein interactions. *J Mol Recognit* 2011; **24**:81–89. doi:10.1002/jmr.1026.
8 Adamson ED, Rees AR. Epidermal growth factor receptors. *Mol Cellular Biochem* 1981; **34**:129–152.
9 Andersson K, Björkelund H, Malmqvist M. Antibody-antigen interactions: what is the required time to equilibrium? Available from Nature Procedings *<http://hdl.handle.net/10101/npre.2010.5218.1>*. 2010.
10 Persson MI, Gedda L, Jensen HJ, Lundqvist H, Malmström PU, Tolmachev V. Astatinated trastuzumab, a putative agent for radionuclide immunotherapy of ErbB2-expressing tumours. *Oncol Rep* 2006; **15**:673–680.

II. CELLULAR UPTAKE OF 111IN – AND 177LU-RADIOLABELLED DOTA-MINIGASTRIN11 ON PROXIMAL KIDNEY CELLS AND TUMOR CCK2 RECEPTOR BEARING CELL LINE

Bárta P, Melicharová L, Lázníčková A, Lázníček M: Cellular uptake of ^{111}In- and ^{177}Lu-radiolabelled DOTA-minigastrin11 on proximal kidney cells and tumor CCK2 receptor bearing cell line. Folia Pharm. Univ. Carol. 2011 XXXIX, ISBN 978-80-246-1912-5:7-16.

CELLULAR UPTAKE OF ^{111}IN- AND ^{177}LU-RADIOLABELED DOTA-MINIGASTRIN11 ON PROXIMAL KIDNEY CELLS AND TUMOR CCK2 RECEPTOR BEARING CELL LINE

PAVEL BÁRTA, LUDMILA MELICHAROVÁ,
ALICE LÁZNÍČKOVÁ, MILAN LÁZNÍČEK

Department of Pharmacology and Toxicology, Faculty of Pharmacy in Hradec Králové,
Charles University in Prague, Czech Republic
e-mail: pavel.barta@faf.cuni.cz

ABSTRACT

The gastrin/cholecystokinin receptor (CCK2R) has been discovered as the possible cell tumor target for peptide receptor radionuclide imaging and therapy (PRRT). Gastrin is the physiological ligand of CCK2R in human body. Several synthesized gastrin analogues bind to CCK2R with different affinity. Minigastrin11 is one of them. The aim of this study was to investigate the specific binding of radiolabeled minigastrin11 on CCK2 receptors using the rat exocrine pancreatic tumor cell line (AR42J) and its cellular accumulation in *in vitro* condition using opossum kidney cell line (OK cells).

Cells were incubated in the internalization medium containing either ^{111}In-DOTA-MG11 or ^{177}Lu-DOTA-MG11 for the selected time. At the end of incubation, cells were disintegrated and cell accumulated radioactivity was determined.

The cellular uptake of ^{111}In- and ^{177}Lu-labeled peptides was almost equal in AR42J cells. The cell-bound radioactivity was between 1.5 to 2% of the whole activity in the experiment. The peptide accumulation study made on OK cells has shown that the cellular uptake of radiolabeled minigastrin11 was very low. The cell-bound portion was between 0.05 and 0.08% of the whole activity in the system.

The results showed that minigastrin11 labeled with ^{111}In and ^{177}Lu was significantly bound to CCK2R receptors on AR42J cells and radioactivity was consequently transported into these tumor cells. Negligible accumulation of ^{111}In-DOTA-MG11 and ^{177}Lu-DOTA-MG11 in the kidney cells means that radiolabeled MG11 does not represent a risk of radionephrotoxicity for the patients treated with the agent.

Keywords: Gastrin – Minigastrin – AR42J cells – OK cells – PRRT

INTRODUCTION

The discovery of somatostatin receptors on various kinds of tumors has triggered the development of radiolabeled somatostatin analogs to be used in tumor diagnosis and peptide receptor radionuclide therapy (PRRT) in the last decades. Somatostatin analogues

have started to be common tumor markers in nuclear medicine. However, other radiolabeled peptides have also enormous value as biological vehicles to deliver radioactivity to tumor cells for a cancer visualization and treatment. Now a day, radiolabeled peptide-based agents are originated from the peptide hormones and neurotransmitters such as somatostatin, cholecystokinin (CCK), gastrin, bombesin, substance P, vasoactive intestinal peptide (VIP), and neuropeptide (NP)-Y[1,2]. The action of mentioned peptides is mediated through specific membrane-bound receptors which mostly belong to G protein-coupled receptors. Peptides act via their specific receptors as regulatory ligands influencing cell proliferation, migration, differentiation or apoptosis[3]. The overexpression of peptide receptors is usually accompanied with tumor progression; this characterization of the peptide led to their investigation in the cancer therapy and diagnosis.

It is more than a century since the gastric hormone (gastrin) has been discovered[4]. The rise of research in the peptide receptor radionuclide therapy at the end of 20th century, has demonstrated an interesting possibility of gastrin/cholecystokinin-2 receptor as the target for imaging and therapy of some tumors[4,5].

Gastrin is gastrointestinal peptide, which has become the promising implement in PRRT. This peptide is physiologically targeted against gastrin/cholecystokinin-2 (CCK2) receptor. CCK2 receptor, with high affinity for gastrin, is increasingly expressed in several tumor types, including small cell lung cancers, medullary thyroid carcinomas, neuroendocrine gastroenteropancreatic tumors, and others[1,5].

Human gastrin peptide chain is assembled of 34 or 17 amino acids. The two type of gastrin are called classical gastrins, which are included gastrin-34 and gastrin-17 (cleaved from gastrin-34)[4]. They can also exist in several C-terminal truncated forms such as minigastrin, a 13-residue peptide[5]. Human gastrin is synthesized in G-cells, which are localized in the glands of the pyloric antral part of the stomach[4]. The stimulation of gastrin release occurs in response to gastric luminal amino acids, peptides, and neuronal stimulation, while its secretion is inhibited by gastric acid via paracrine mediator somatostatin which is secreted from D-cells located in corpus epithelium[4,6]. Gastrin synthesis starts in endoplasmatic reticulum where the preprogastrin, gastrin precursor, is translated and then cleaved to progastrin. Progastrin passes through Golgi complex into secretary vesicles. Its molecule is cleaved to G34-Gly, which can be either shortened to G17-Gly or converted to amidated gastrin G34 and the latter into G17. Progastrins, G34-Gly and G17-Gly are so called non-classical gastrins, which are able to influence cell proliferation in colon. G34 and G17 belong to the group of classical gastrins, responsible for proliferation and differentiation in stomach and acid secretion[4,6,7]. The actions of gastrins are mediated through CCK2 receptors having high affinity for them. Besides all effects of gastrins mentioned above, new actions at CCK2 receptor were recently described. These effects include stimulation of migration, invasion, tubulogenesis, and inhibitions of apoptosis[8–11]. These amidated-gastrin properties are the principle for their oncogenic effects.

The first very intensively studied human tumor expressing CCK2 receptor was medullary thyroid cancer (MTC). It was found out that this kind of human cancer lacked somatostatin receptors in advanced and clinically aggressive forms, but not the CCK2 receptors[12–15]. This fact led to the development of gastrin analogues for diagnosis and therapy. Gastrin analogues investigation has been triggered for the purpose of CCK2 receptor tumors diagnostic imaging and radionuclide therapy in several laboratories.

Behr et al. showed promising results for the diagnostic and therapeutic application of ^{131}I-radioiodinated human gastrin-I[2,16]. Reubi et al. came with series of nonsulfated cholecystokinin (CCK) analogues coupled at the N-terminus to diethylenetriaminepentaacetic acid (DTPA) and 1,4,7,10-tetraazacyclododecane-1,4,7,10-tetraacetic acid (DOTA) for radiometal binding[2,5,17]. Derivatives of gastrin followed the radiolabeling example of its close relative peptide CCK. Nonsulfated gastrin then has been shown to be more suitable for tumor targeting due to its stability, CCK-2 receptor selectivity, high affinity, and promising in vivo profile. Behr et al. developed (^{111}In-DTPA^{0})minigastrin, which had high uptake in stomach and tumor lesions in metastatic MTC patients[2,18].

Many other gastrin analogues have been prepared, but unfortunately some of them may have unadvisable side effects. Their uptake at receptor-positive tissues can be followed with extremely high uptake in to the kidney[5,16,19]. This radioimmunotherapy limitation is quite common and has already been discovered during preclinical and clinical experiments with radiolabeled somatostatin analogue such as 90Y-DOTA-Tyr^{3}-octreotide (DOTATOC)[20]. It generally refers to radiolabeled low-molecular-weight biomolecules such as peptides and monoclonal antibody fragments, which are transported into proximal tubular kidney cells. It is supposed that the responsible agents for kidney uptake are megalin and cubilin which are the endocytic receptors. These two proteins on epithelial cells in proximal renal tubules are responsible for the uptake of many substances such as peptides, peptide hormones, protein-bound vitamins, and proteins from primary urine back to bloodstream[21,22]. Their uptake can be facilitated with peptide analogues such as the presence of positively charged amino acids[20]. Thus, the kidneys are the main dose-limiting organs during peptide-based radiotherapy of cancer patients using high doses of therapeutic radionuclides[21,22].

AIM OF STUDY

The aim of this study was to investigate the binding affinity and uptake of ^{111}In- and ^{177}Lu-labeled minigastrin analogue in *in vitro* conditions. ^{111}In- and ^{177}Lu-DOTA-dGlu-Ala-Tyr-Gly-Trp-Met-Asp-Phe-NH_2 (^{111}In-DOTA-MG11 and ^{177}Lu-DOTA-MG11) were prepared and then tested for their specific binding to CCK2 receptor at cell line AR42J (Rat exocrine pancreatic tumor) and for their uptake and retention to renal proximal tubular cell line OK cells (Opossum kidney cells).

MATERIALS AND METHODS

Chemicals

RPMI 1640 medium and fetal calf serum were purchased from PAA Cell Culture Company. Minimal essential medium (MEM), L-glutamine, nonessential amino acids (NEAA), ethylenediaminetetraacetic acid (EDTA)/trypsin, 3(morpholino) propanesulphonic acid (MOPS), *N*-(2-hydroxyethyl)-piperazine-*N'*-(2-ethanesulphonic acid) (HEPES), Triton X-100, chemicals used for radiolabeling, and high performance liquid chromatography (HPLC) analysis were purchased from Sigma-Aldrich, Czech Republic. DOTA-mini-

gastrin11 was purchased from Pichem, Graz, Austria. The isotope ^{111}In was purchased from Amersham and ^{177}Lu from PerkinElmer. Bicinchoninic acid assay (BCA) kit was purchased from (Pierce, Rockford, USA). Ringer solution was prepared in our department in composition of (mM): NaCl 122.5, KCl 5.4, $CaCl_2$ 1.2, $MgCl_2$ 0.8, Na_2HPO_4 0.8, NaH_2PO_4 0.2, glucose 5, and HEPES 10 (titrated to pH 7.4 by NaOH at 37 °C). Phosphate buffered saline (PBS) was prepared in our department in composition of (mM): NaCl 137, KCl 2.7, Na_2HPO_4 0.01 and NaH_2PO_4 0.01 (titrated to pH 7.4). Acid wash buffer was prepared in our department in composion of 50 mM glycine buffer pH 2.8, and 0.1 M NaCl.

Cell Line

Opossum kidney cell line (OK cells) and Rat pancreatic tumor cell line AR42J were purchased from European Collection of Cell Cultures.

Peptide Radiolabeling and Radiochemical Analysis

Minigastrin11 was labeled with isotopes according to this protocol. Two hundred of 0.4 M acetate buffer solution (pH 5) was mixed with 10 µl of peptide (1 µg/1 µl) and 0.1 ml of ^{111}In (1 mCi/0.1 ml of 0.04 M HCl) or 1 µl of ^{177}Lu (1 mCi/0.8 – 1 µl of 0.05 M HCl). The solution was heated for twenty minutes at 92 °C and then left to cool down. Gradient RP-HPLC analysis of radiolabeled peptide was made for the determination of radiochemical purity. HPLC machine (System Agilent 1100 Series, Agilent Technologies Inc., Santa Clara, CA, USA) with the column 125 × 4 mm and 10 µm (Merck) and with UV and radiometric detection (Polon, Polatom) were used. The mobile phase was A: 0.1% trifluoracetic acid and B: CH_3CN.

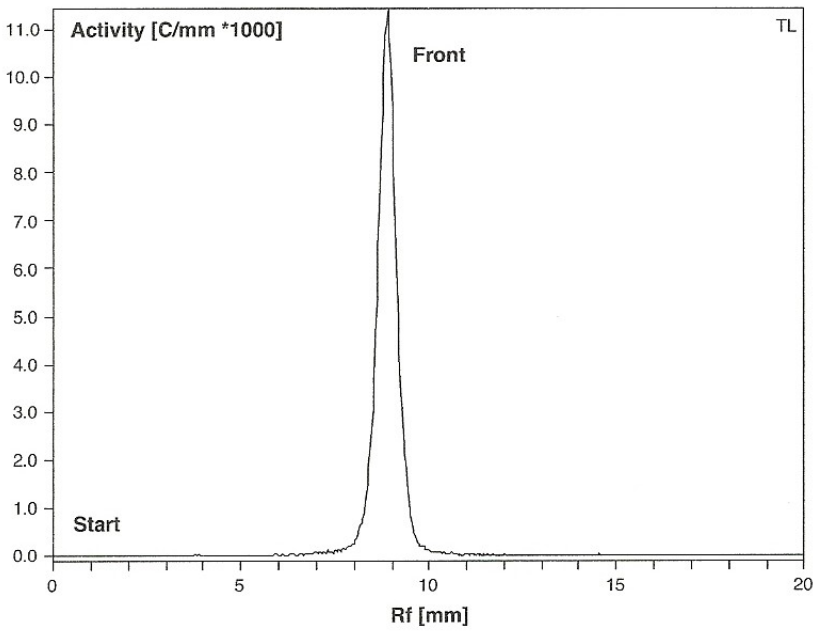

Fig. 1. An example of ITLC SG radioactivity profile (^{111}In-DOTA-MG11)

Cell Culturing

Renal OK cells were seeded in Minimum Essential Medium Eagle (MEM) supplemented with 2 mM L-glutamine, 1% NEAA and 10% FCS in 5% CO_2 atmosphere at 37 °C. Confluent monolayers were split 1:4 twice a week using (EDTA)/trypsin solution.

Pancreatic tumor cells line AR42J were seeded in RPMI-1640 supplemented with 2 mM L-glutamine and 10% FCS in 5% CO_2 atmosphere at 37 °C. Subculturing was performed employing (EDTA)/trypsin solution.

Accumulation Study

For experiments, OK cells of passage number 17–24 were used. They were left to grow to confluency on Petri dish (6 cm diameter). The experiments were initiated with cell wash of PBS (2×). The addition of 3 ml Ringer solution with radiolabeled minigastrin (10 nM) followed. The cells were incubated for indicated intervals (0, 20, 40, 60, 80, 100, 120, 140, 160 and 180 minutes) in 5% CO_2 atmosphere at 37 °C. When the incubation was over then the uptake buffer was aspirated, and the dishes with cell monolayers were rapidly rinsed with ice-cold PBS (6×). The cells were disintegrated by Triton X-100 (0.1% v/v) in 10 mM MOPS. To elicit the measuring error caused by nonspecific sorption to the cells and Petri dishes, the radioactivity uptake at time 0 was used as a blank value where the internalization medium was discarded immediately after addition. The intracellular radioactivity was normalized to the cell protein content by the BCA method[23].

For accumulation studies, AR42J cells (passage number 41–44) were treated with (EDTA)/trypsin solution and concentrated to 1×10^6 cells per ml of internalization medium (RPMI 1640 supplemented with 2 mM L-glutamine and 1% FCS) per microcentrifuge tube. Incubation was started by the addition of 1 ng of radiolabeled peptide per tube (0.71 nM). Cells were incubated at 37 °C in triplicates for both minigastrins for the indicated interval time periods (0, 5, 15, 30, 60, 90 and 120 minutes). Cellular uptake was stopped by removal of the internalization medium and twice washing of the cells with ice-cold PBS. Thereafter, the cells were incubated twice at ambient temperature in acid wash buffer for 5 minutes. The supernatant was removed and cells were lysed by treatment of 1 M NaOH and cell radioactivity collected (accumulated radioligand fraction).

Measurement of ^{111}In and ^{177}Lu Activity

Radionuclides activity was measured by a gamma spectrometer 1480 Wizard™ 3'' (Wallac, Finland). Radioactivity of all samples was compared with analyzed standard sample activity.

Data Analysis

All values are the results of two independent experiments with triplicates in each experiment. The evaluation of obtained experimental data was made in GraphPad Prism.

RESULTS

OK cells, Radioligand Uptake

Graphs depicted in Figures 2 and 3 show the process of ^{111}In-DOTA-MG11 and ^{177}Lu-DOTA-MG11 accumulation in *in vitro* conditions. The amount of cumulated peptides

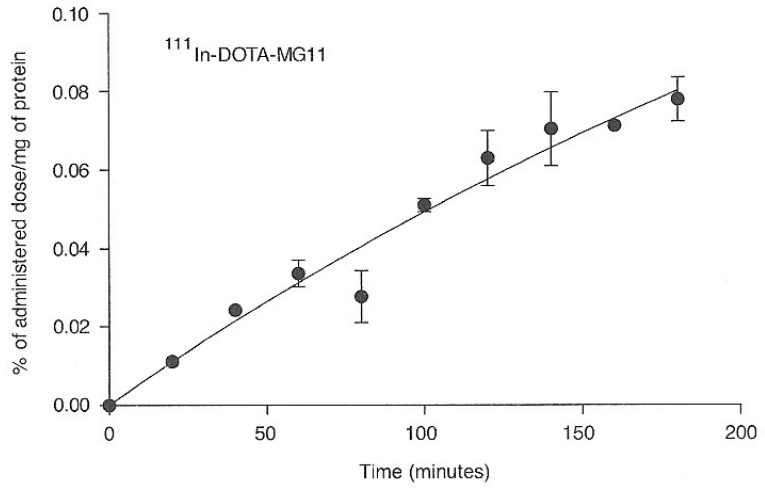

Fig. 2. Internalization of ^{111}In-DOTA-MG11 in OK cells. Data expressed as mean ± SD

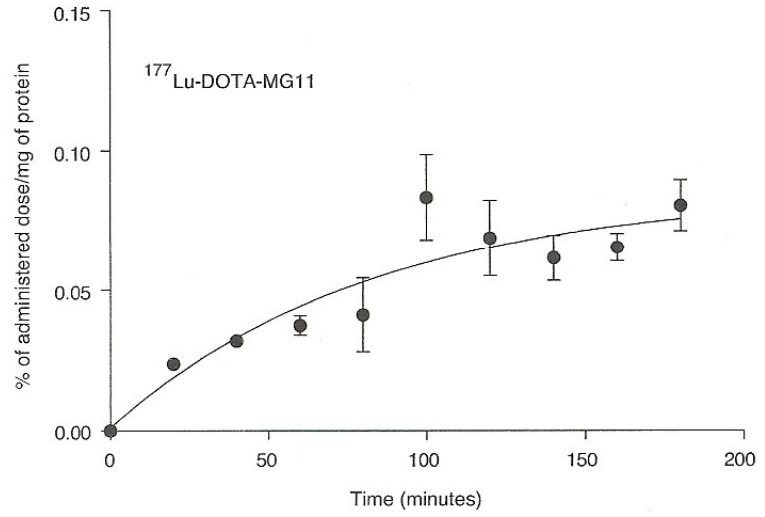

Fig. 3. Internalization of ^{177}Lu-DOTA-MG11 in OK cells. Data expressed as mean ± SD

was relatively low. The internalized fraction was only about 0.01% of the whole peptide radioactivity added to cells. This activity was similar for the both radionuclides used for peptide labeling. It can be seen that slightly higher amount of ^{177}Lu-DOTA-MG11 was internalized into kidney cells than that of ^{111}In-labeled minigastrin.

AR42J cells, Radioligand Uptake

Rat exocrine pancreatic tumor cell line AR42J expressing CCK2 receptors exhibited higher accumulation of the both peptides than that of the kidney cells (Figures 4 and 5). The equilibrium of peptide uptake in the cells was reached between 30 and 60 minutes for ^{177}Lu labeled minigastrin. On the other hand, the uptake equilibrium for ^{111}In-labeled minigastrin was not reached even after 120 minutes of experiments.

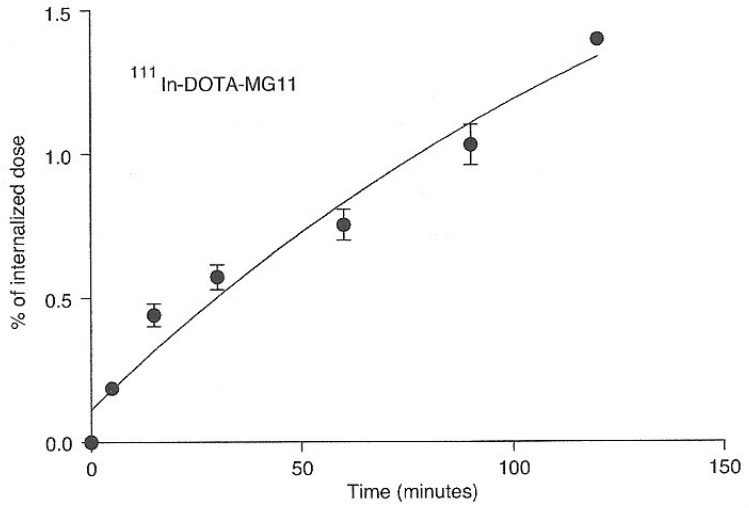

Fig. 4. Internalization of ^{111}In-DOTA-MG11 in AR42J cells. Data expressed as mean ± SD

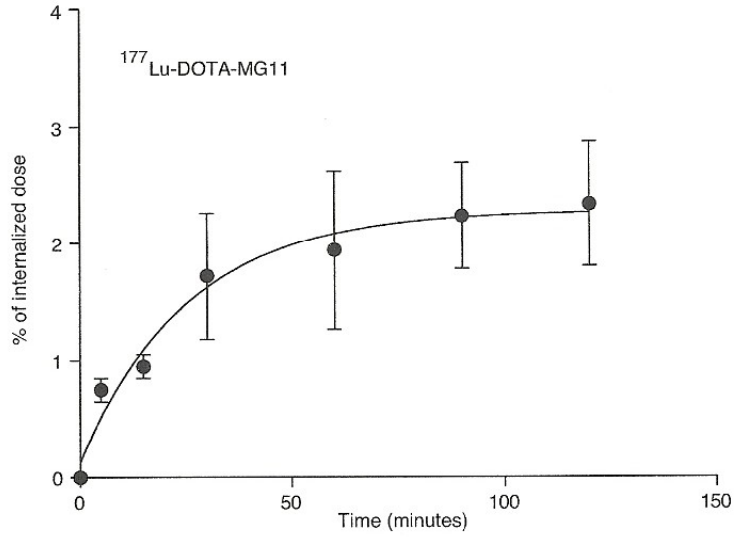

Fig. 5. Internalization of ^{177}Lu-DOTA-MG11 in AR42J cells. Data expressed as mean ± SD

DISCUSSION

A lot of gastrin analogues with similar properties to gastrin, mainly the ability of specific receptor binding, were prepared up to now. They are called minigastrins, and they have been investigated for tumor peptide receptor radiotherapy and diagnosis. Medullar thyroid carcinoma carrying gastrin/cholecystokinin receptors was the first evidence for radiolabeled minigastrin development, as somatostatin analogues had not been able to bind effectively on these tumor cells due to low somatostatin receptor density[2,16,18].

Minigastrin11 is one of the promising gastrin analogues. The uptake of this peptide was tested in *in vitro* conditions in our study. The two cell lines, pancreatic tumor cell line

and kidney cells, were chosen for this study. The first one was AR42J cells, which carry specific CCK2 receptors. This cell line has been used in *in vitro* or *in vivo* (injected nude mice) study[24]. These cells were employed as reference cell line, by which the internalization of labeled minigastrin mediated by the CCK2 receptor system was supposed[2,25].

OK cells are derived from proximal tubule and they are thought to have megalin-cubilin complex. This complex is responsible for radiolabeled peptide accumulation in the kidneys[21,22]. Kidney cells were used for the study of radiolabeled peptide uptake to evaluate the possible risk of radionephrotoxicity[26].

In this study, ^{111}In and ^{177}Lu were used for radiolabeling of minigastrin11. ^{111}In is frequently used for diagnostic purposes whereas ^{177}Lu is used for radiotherapy in nuclear medicine. These two radioisotopes were attached to the peptide via DOTA chelate. Radiochemical purity of ^{111}In-DOTA-MG11 was over 99% (Figure 5).

^{111}In and ^{177}Lu labeled minigastrins were tested for their ability to bind on gastrin-specific receptors (AR42J cells) and for their possible uptake via megalin/cubilin complex into kidney cells (OK cells).

The analysis of ^{111}In-DOTA-MG11 and ^{177}Lu-DOTA-MG11 uptake in AR42J cells showed slightly different results. The both peptides were bound to CCK2 receptors on AR42J cells and consequently internalized into the cells. The internalized fraction of ^{177}Lu-DOTA-MG11 initially increased with incubation time and the internalization curve reached its plateau approximately in one hour after dosing. In the case of ^{111}In-labeled minigastrin, the plateau was not reached even after 180 minutes of incubation. Moreover, the amount of internalized ^{111}In-DOTA-MG11 was lower than that for ^{177}Lu-DOTA-MG11. Nevertheless, both radiolabeled peptides under study were able to bind on gastrin receptors on AR42J cells and consequently internalized into the cells.

The accumulation study of radiolabeled minigastrin11 in the kidney was carried out on proximal tubule cells. The peptide uptake was very low compared with results obtained in exocrine pancreatic cells. ^{111}In-DOTA-MG11 and ^{177}Lu-DOTA-MG11 uptake was below 0.1% of administered dose per mg of proteins which means that radiolabeled minigastrin 11 did not significantly internalize into proximal tubule cells. The two labeled peptides under study would not cause a risk of radionephrotoxicity in their possible clinical application.

CONCLUSION

The structure of the both tested peptides ^{111}In-DOTA-MG11 and ^{177}Lu-DOTA-MG11 was not changed by radiolabeling. This was approved on tumor cell line with gastrin specific receptor CCK2. Moreover, the process of radiolabeling was applied with an excellent quality, where the radiochemical purity was over 99%.

The next pursued task of this study was the possible radionephrotoxic influence of employed peptides. Fortunately, very low accumulation of radiolabeled minigastrin11 was observed on the model kidney cell line, for the both radionuclides.

The results of this study showed, the ^{111}In and ^{177}Lu labeled peptides can be used as the suitable diagnostic and therapeutic markers in nuclear medicine. However, *in vitro* results are the first step in a long way study of minigastrin utilization in medicine. However

further investigation in the field of in vivo study must be done to confirm our finding in this study.

ACKNOWLEDGEMENTS

We gratefully acknowledge and thank for financial support of this study from Grant Agency of Czech Republic No. 305/07/0535. Authors wish to thank Davoud Ahmadimoghaddam for his technical assistance.

REFERENCES

1. Reubi, J. C.: Peptide receptors as molecular targets for cancer diagnosis and therapy. Endocr. Rev., 24, 2003, 389–427.
2. Nock, B. A. et al.: CCK-2/gastrin receptor-targeted tumor imaging with (99m)Tc-labeled minigastrin analogs. J. Nucl. Med., 46, 2005, 1727–1736.
3. Krenning, E. P. et al.: Peptide receptor radionuclide therapy. Ann. N. Y. Acad. Sci., 1014, 2004, 234–245.
4. Dockray, G. J.: Topical review. Gastrin and gastric epithelial physiology. J. Physiol., 518 (Pt 2), 1999, 315–324.
5. Mather, S. J. et al.: Selection of radiolabeled gastrin analogs for peptide receptor-targeted radionuclide therapy. J. Nucl. Med., 48, 2007, 615–622.
6. Dockray, G., Dimaline, R. & Varro, A.: Gastrin: old hormone, new functions. Pflügers. Arch., 449, 2005, 344–355.
7. Caplin, M. et al.: Expression and processing of gastrin in pancreatic adenocarcinoma. Br. J. Surg., 87, 2000, 1035–1040.
8. Pagliocca, A. et al.: Stimulation of the gastrin-cholecystokinin(B) receptor promotes branching morphogenesis in gastric AGS cells. Am. J. Physiol. Gastrointest. Liver Physiol., 283, 2002, G292–299.
9. Noble, P. J. et al.: Stimulation of gastrin-CCKB receptor promotes migration of gastric AGS cells via multiple paracrine pathways. Am. J. Physiol. Gastrointest. Liver Physiol., 284, 2003, G5–84.
10. Todisco, A. et al.: Molecular mechanisms for the antiapoptotic action of gastrin. Am. J. Physiol. Gastrointest. Liver Physiol., 280, 2001, G298–307.
11. Wroblewski, L. E., Pritchard, D. M., Carter, S. & Varro, A.: Gastrin-stimulated gastric epithelial cell invasion: the role and mechanism of increased matrix metalloproteinase 9 expression. Biochem. J., 365, 2002, 873–879.
12. Reubi, J. C. & Waser, B.: Unexpected high incidence of cholecystokinin-B/gastrin receptors in human medullary thyroid carcinomas. Int. J. Cancer, 67, 1996, 644–647.
13. Reubi, J. C. et al.: Somatostatin receptors and somatostatin content in medullary thyroid carcinomas. Lab. Invest., 64, 1991, 567–573.
14. Behe, M. & Behr, T. M.: Cholecystokinin-B (CCK-B)/gastrin receptor targeting peptides for staging and therapy of medullary thyroid cancer and other CCK-B receptor expressing malignancies. Biopolymers, 66, 2002, 399–418.
15. Froberg, A. C. et al.: Comparison of three radiolabelled peptide analogues for CCK-2 receptor scintigraphy in medullary thyroid carcinoma. Eur. J. Nucl. Med. Mol. Imaging, 36, 2009, 1265–1272.
16. Behr, T. M. et al.: Targeting of cholecystokinin-B/gastrin receptors *in vivo*: preclinical and initial clinical evaluation of the diagnostic and therapeutic potential of radiolabelled gastrin. Eur. J. Nucl. Med., 25, 1998, 424–430.
17. Reubi, J. C. et al.: Unsulfated DTPA- and DOTA-CCK analogs as specific high-affinity ligands for CCK-B receptor-expressing human and rat tissues in vitro and in vivo. Eur. J. Nucl. Med., 25, 1998, 481–490.
18. Behr, T. M. et al.: Radiolabeled peptides for targeting cholecystokinin-B/gastrin receptor-expressing tumors. J. Nucl. Med., 40, 1999, 1029–1044.

19. Behr, T. M. et al.: Cholecystokinin-B/gastrin receptor binding peptides: preclinical development and evaluation of their diagnostic and therapeutic potential. Clin. Cancer. Res., 5, 1999, 3124–3138.
20. Bodei, L. et al.: Receptor-mediated radionuclide therapy with 90Y-DOTATOC in association with amino acid infusion: a phase I study. Eur. J. Nucl. Med. Mol. Imaging, 30, 2003, 207–216.
21. Melis, M. et al.: Renal uptake and retention of radiolabeled somatostatin, bombesin, neurotensin, minigastrin and CCK analogues: species and gender differences. Nucl. Med. Biol., 34, 2007, 633–641.
22. Christensen, E. I. & Verroust, P. J.: Megalin and cubilin, role in proximal tubule function and during development. Pediatr. Nephrol., 17, 2002, 993–999.
23. Noble, J. E. & Bailey, M. J.: Quantitation of protein. Methods Enzymol., 463, 2009, 73–95.
24. Dufresne, M., Seva, C. & Fourmy, D.: Cholecystokinin and gastrin receptors. Physiol. Rev., 86, 2006, 805–847.
25. Svoboda, M., Dupuche, M. H., Lambert, M., Bui, D. & Christophe, J.: Internalization-sequestration and degradation of cholecystokinin (CCK) in tumoral rat pancreatic AR 4-2 J cells. Biochim. Biophys. Acta, 1055, 1990, 207–216.
26. Schwegler, J. S., Heppelmann, B., Mildenberger, S. & Silbernagl, S.: Receptor-mediated endocytosis of albumin in cultured opossum kidney cells: a model for proximal tubular protein reabsorption. Pflügers Arch., 418, 1991, 383–392.

III. GEFITINIB INDUCES EPIDERMAL GROWTH FACTOR RECEPTOR DIMERS WHICH ALTERS THE INTERACTION CHARACTERISTICS WITH 125I-EGF

Björkelund H, Gedda L, **Barta P**, Malmqvist M, Andersson K: Gefitinib induces epidermal growth factor receptor dimmers which alters the interaction characteristics with ^{125}I-EGF. PLoS One. 2011 Sep; 6(9):e24739.

OPEN ACCESS Freely available online

PLoS one

Gefitinib Induces Epidermal Growth Factor Receptor Dimers Which Alters the Interaction Characteristics with ^{125}I-EGF

Hanna Björkelund[1,2]*, Lars Gedda[1], Pavel Barta[3], Magnus Malmqvist[1,2,4], Karl Andersson[1,2]

1 Biomedical Radiation Sciences, Department of Radiology, Oncology and Radiation Science, Uppsala University, Uppsala, Sweden, **2** Ridgeview Instruments AB, Uppsala, Sweden, **3** Department of Pharmacology and Toxicology, Faculty of Pharmacy in Hradec Kralove, Charles University in Prague, Prague, Czech Republic, **4** Bioventia AB, Uppsala, Sweden

Abstract

The tyrosine kinase inhibitor gefitinib inhibits growth in some tumor types by targeting the epidermal growth factor receptor (EGFR). Previous studies show that the affinity of the EGF-EGFR interaction varies between hosting cell line, and that gefitinib increases the affinity for some cell lines. In this paper, we investigate possible mechanisms behind these observations. Real-time interaction analysis in LigandTracer® Grey revealed that the HER2 dimerization preventing antibody pertuzumab clearly modified the binding of ^{125}I-EGF to EGFR on HER2 overexpressing SKOV3 cells in the presence of gefitinib. Pertuzumab did not affect the binding on A431 cells, which express low levels of HER2. Cross-linking measurements showed that gefitinib increased the amount of EGFR dimers 3.0–3.8 times in A431 cells in the absence of EGF. In EGF stimulated SKOV3 cells the amount of EGFR dimers increased 1.8–2.2 times by gefitinib, but this effect was cancelled by pertuzumab. Gefitinib treatment did not alter the number of EGFR or HER2 expressed in tumor cell lines A431, U343, SKOV3 and SKBR3. Real-time binding traces were further analyzed in a novel tool, Interaction Map, which deciphered the different components of the measured interaction and supports EGF binding to multiple binding sites. EGFR and HER2 expression affect the levels of EGFR monomers, homodimers and heterodimers and EGF binds to the various monomeric/dimeric forms of EGFR with unique binding properties. Taken together, we conclude that dimerization explains the varying affinity of EGF – EGFR in different cells, and we propose that gefitinib induces EGFR dimmers, which alters the interaction characteristics with ^{125}I-EGF.

Citation: Björkelund H, Gedda L, Barta P, Malmqvist M, Andersson K (2011) Gefitinib Induces Epidermal Growth Factor Receptor Dimers Which Alters the Interaction Characteristics with ^{125}I-EGF. PLoS ONE 6(9): e24739. doi:10.1371/journal.pone.0024739

Editor: Laszlo Buday, Hungarian Academy of Sciences, Hungary

Received June 22, 2011; **Accepted** August 16, 2011; **Published** September 12, 2011

Funding: This project was jointly funded by Uppsala University and Ridgeview Instruments AB (RIAB). Hanna Björkelund, Magnus Malmqvist, and Karl Andersson participated in the study on the same conditions as university employees, i.e., without any restrictions on study design and what data to include in the publication. Uppsala University had no role in study design, data collection and analysis, decision to publish, or preparation of the manuscript. The role of RIAB was solely to provide access to LigandTracer devices and to pay the salaries of Hanna Björkelund, Magnus Malmqvist, and Karl Andersson.

Competing Interests: The authors have read the journal's policy and have the following conflicts: Ridgeview Instruments AB (RIAB) develops and sells the device LigandTracer, which is described in the manuscript. RIAB and Bioventia AB has a financial interest in the development of the Interaction Map analysis tool. The interaction map analysis tool is protected by a patent (see the reference list, ref. 25) but the patent does not cover the use of interaction maps for displaying heterogeneous interactions as in the current manuscript. The interaction map analysis tool may become a product in the future. Hanna Björkelund, Magnus Malmqvist, and Karl Andersson are employed by RIAB. Magnus Malmqvist and Karl Andersson are shareholders of RIAB. RIAB acknowledges the adherence to all PLoS ONE policies on sharing data and materials. All equipment described in the report is commercially available, and no patents restrict the use of the described assays.

* E-mail: hanna@ridgeviewinstruments.com

Introduction

The extracellular binding of EGF to EGFR (also denoted ErbB1) triggers signals that are transduced through the cells and causes cell proliferation. Atypical activity and over-expression of EGFR is associated with a number of tumors, making it a common target for cancer research. Although well studied, many questions still remain unanswered about the interaction of EGF with EGFR, the resulting signaling and its involvement in cancer.

Apart from EGFR, the epidermal growth factor receptor family consists of the HER2, HER3 and HER4 receptors. The four receptors are known to dimerize, as homodimers or as heterodimers with other members of the family. The presence of EGFR dimers in EGF unstimulated cells have been discussed for many years, where some groups claim that EGFR dimers exist without stimulation [1,2] while the more common belief is that EGFR dimerization requires a conformation change caused by the binding of EGF to monomeric EGFR [3,4,5]. Upon receptor dimerization, the cytoplasmic tyrosine kinase domain is activated through phosporylation [6]. HER2 is consecutively and ligand independently activated and is the preferred binding partner of EGFR [7]. HER2 dimerization with EGFR enhances and prolongs the downstream signaling caused by EGF binding [8], possibly due to the endocytosis deficiency of HER2, which in turn negatively affects the EGFR downregulation [9].

The EGF – EGFR interaction is known to be complex. Scatchard plots depict the presence of both low affinity and high affinity receptor populations, the latter less abundant [10,11]. More recent studies presents a difference in affinity to EGF between the monomeric and homodimeric form of EGFR [12], where homodimers bind EGF more strongly. Furthermore, the high affinity population has been pointed out as the primary

mediators of the EGFR signaling [13]. This vaguely suggests that EGFR dimers correspond to the high affinity population observed in the past.

The use of tyrosine kinase inhibitors (TKI) is a mean of disrupting the proliferation and anti-apoptotic downstream signaling [14]. One example is gefitinib (IRESSA^{TM}) which is directed towards EGFR and used as therapy against non-small cell lung cancer [15]. The aim is to inhibit tumor growth, but the response varies to a large extent between patients [16]. The reason behind this variation has been extensively investigated and discussed during the last decade, without much success. Lapatinib is another TKI targeted towards EGFR and HER2 for HER2 overexpressing mammary tumors [17]. It binds the inactive forms of EGFR as opposed to gefitinib that stabilize the active conformation [18,19,20,21]. Gefitinib, but not lapatanib, have previously been shown to promote dimerization of EGFR. These dimers are considered non-active and conformationally different from ligand triggered dimer forms [21].

We have previously investigated the kinetic properties and the affinity of the ^{125}I-EGF – EGFR interaction in different cell lines exposed to various treatments (complete or serum free medium, in the presence or absence of gefitinib) [22]. No effect of gefitinib was observed in U343 and SKBR3 cells, but it clearly affected the binding of ^{125}I-EGF in A431 and SKOV3 cells. The overall affinity increased in both cell lines, but the kinetics properties (association and dissociation rate) were differently affected between the two. In addition, the shape of the real-time binding curves produced in LigandTracer Grey displayed evidence of more than one EGF binding interaction taking place simultaneously. The overall affinity was quantified and it was found to vary as much as 40 times between cell lines (from 0.2 nM in SKBR3 to 8 nM in A431).

The aim of this work was to investigate the biological mechanism behind the effect of gefitinib on the ^{125}I-EGF – EGFR interaction and the differences in affinity between hosting cell lines. We present a detailed interaction analysis study of how the binding of ^{125}I-EGF to EGFR is affected by tyrosine kinase inhibitors and the HER2 dimerization preventing antibody pertuzumab. Real-time binding traces of the interaction together with cross-linking assays show a connection between the effect of gefitinib and EGFR dimer levels. We also introduce a novel tool for binding trace analysis of complex interactions: the Interaction Map. Having previously been applied to molecular interaction analysis by SPR [23], this tool shows promise for resolving the complex results of protein-cell interactions.

Results

Gefitinib and serum free medium does not alter the EGFR or HER2 expression in A431, U343, SKOV3 or SKBR3 cells

The EGFR and HER2 expression level under different culturing conditions (complete medium or serum free medium, with or without gefitinib) was quantified either manually or with the kinetic extrapolation (KEX) method [24] using LigandTracer (Table 1). No clear differences were observed between treatments in any of the four cell lines. The apparent affinity to ^{125}I-EGF varied greatly between the cell lines, as described previously [22] and presented in Table 1. For this set of cell lines, there seems to be some correlation between HER2 and EGFR expression and the overall affinity, with a higher affinity in cells expressing a large number of HER2 receptors and fewer EGFR.

Pertuzumab affects the binding of ^{125}I-EGF to SKOV3 cells but not to A431 or U343 cells

The dimerization preventing antibody pertuzumab binding to HER2 was added to investigate the role of EGFR-HER2 heterodimerization to the measured ^{125}I-EGF interaction, producing binding traces presented as representative curves in Figure 1. Little or no differences were observed for U343 cells and A431 cells (data not shown). The addition of pertuzumab to SKOV3 cells modified the binding of ^{125}I-EGF, observed as differences in curvature, when simultaneously treated with gefitinib. The increase in affinity caused by gefitinib, observed as a higher saturation of receptors with the first concentration and a slower dissociation (Fig. 1C and D, black curves), was essentially canceled by pertuzumab (Fig. 1C and D, red curves).

The effects of EGF, gefitinib and pertuzumab on EGFR dimerization in A431 and SKOV3 cells

The amount of dimerized EGFR receptors in A431 and SKOV3 cells was studied by immunoblots using the reagent BS^3 as a receptorcross-linking agent. The cells were incubated with or without EGF, fetal calf serum (FCS), gefitinib and pertuzumab before lysis, as presented in Figure 2 (representative data from one of four experiments). A presence of EGFR dimers without stimulation of EGF is seen in both cell lines, although to a higher extent in SKOV3 where the differences between stimulated and unstimulated cells are small (Fig. 2A–D, lane 1 and 2). No differences were observed between cells stimulated with complete or serum free medium in the presence of gefitinib (Fig. 2A–D, lane 3–4 and 6–7). Detection of β-actin was used as a loading control.

Table 1. The EGFR and HER2 expression of A431, U343, SKOV3 and SKBR3 cells in four culturing conditions.

	A431			U343			SKOV3			SKBR3		
	EGFR	HER2	$K_{D,\ app}$	EGFR	HER2	$K_{D,\ app}$	EGFR	HER2	$K_{D,\ app}$	EGFR	HER2	$K_{D,\ app}$
Complete medium	2.1±0.4E6	1.5±0.1E5	8 nM	6.4±0.5E5	3.1±0.6E4	1.4 nM	3.4±0.6E5	2.0±0.3E7	0.9 nM	4.1±0.3E5	5.8±0.5E6	0.2 nM
Serum free medium	2.2±0.5E6	1.7±0.2E5		6.7±0.6E5	3.5±0.4E4		1.9±0.2E5	2.1±0.05E7		3.5±0.5E5	7.2±0.6E6	
Gefitinib +complete medium	2.2±0.3E6	2.6±0.5E5		6.9±1.0E5	2.2±0.3E4		3.2±0.6E5	2.3±0.1E7		4.6±0.6E5	6.4±2.6E6	
Gefitinib +serum free medium	1.3±0.2E6	2.0±0.5E5		5.3±0.1E5	2.7±0.3E4		2.18E+05E5	3.0±0.4E6		5.7±0.3E5	6.5±0.3E6	

Estimation of EGFR and HER2 receptors were conducted either manually or by the KEX method using LigandTracer. Estimations of the affinities have been described previously [22]. Data are presented as mean±S.E (n = 2–6). No clear effects of the treatments on the EGFR and HER2 expression is observed in either of the cell lines.
doi:10.1371/journal.pone.0024739.t001

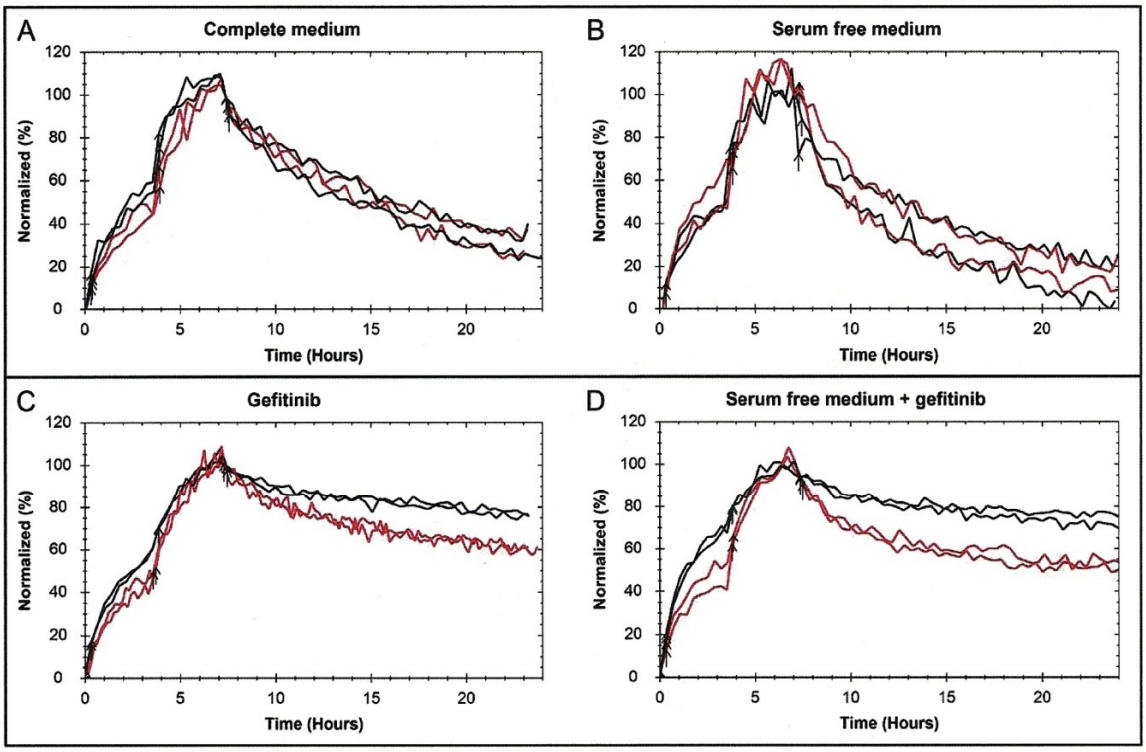

Figure 1. The effect of pertuzumab on the ^{125}I-EGF – SKOV3 interaction. The binding of ^{125}I-EGF to cultured SKOV3 cells in LigandTracer Grey, in the presence (red) or absence (black) of the HER2 dimerization disrupting antibody pertuzumab. The cells were cultured in A) complete medium, B) serum-free medium, C) complete medium containing 1 μM gefitinib or D) serum free medium with 1 μM gefitinib. The ^{125}I-EGF – SKOV3 interaction is affected by pertuzumab, most evidently in gefitinib treated cells where the shape of the binding traces is clearly altered. The curves are representative data from triplicates or quadruplicates and have been normalized to the equilibration level of the second concentration for better comparison.
doi:10.1371/journal.pone.0024739.g001

However, the absolute number of EGFR seemed to vary between treatments.

The intensities of the EGFR monomer and dimer bands were quantified using ImageJ to study the effect of X (where X was EGF, gefitinib or pertuzumab) on dimerization. The effect was calculated as

$$EffectValue^{X} = \frac{Dimerization^{X}}{Dimerization^{NoX}} = \frac{\frac{Dimer^{X}}{Monomer^{X}}}{\frac{Dimer^{NoX}}{Monomer^{NoX}}}$$

where an EffectValue significantly different from 1 signifies an impact of X on the EGFR dimerization. Another lysate within the same gel treated identically apart from the exposure of X was used as the reference (Tables 2 and 3).

Exposure of EGF increased dimerization in A431 cells 3.9 times. No effect of EGF on EGFR dimerization was observed in SKOV3 cells.

EGFR dimerization in EGF unexposed A431 cells increased 3.0–3.8 times upon gefitinib tratement (Table 2). Gefitinib increased EGFR dimerization in most of the EGF exposed A431 cells as well, but to a lesser extent (1.4–1.9 times). A significant effect of gefitinib was observed in EGF treated SKOV3 cells ($p<0.1$), with an increase of 1.8–2.2 times. No effect of gefitinib on EGFR dimerization was detected in EGF untreated SKOV3 cells.

No effect of pertuzumab on the EGFR dimerization in A431 cells was observed (Table 3). In SKOV3 cells, a significant ($p<0.1$) disruption of in average 40–60% of the EGFR dimerization was detected upon pertuzumab treatment.

Lapatinib effects the binding of ^{125}I-EGF to A431 cells in a different manner than gefitinib

Exposure of lapatinib modified the kinetics of the ^{125}I-EGF–A431 interaction (Fig. 3A). A fast on–fast off interaction was observed in all treatments, but the contribution of it increased when the cells were treated with lapatinib (Fig. 3A, green and black curves). This resulted in an overall faster interaction during both association and dissociation. The difference between the signal height of the first and second concentrations, as indicated by an arrow, is slightly less when treated with serum free medium (Fig. 3A, black curves). These alterations were different from the effects of gefitinib in A431 cells, where the overall affinity increased upon exposure and the dissociation rate varied between complete and serum free medium (Fig. 3B, green and black curves).

The heterogeneity of the binding of ^{125}I-EGF can be visualized by Interaction Maps

Interaction Map is a mathematical method to decipher a heterogeneous interaction into its underlying components. It is based on the main assumption that the binding of a ligand to a

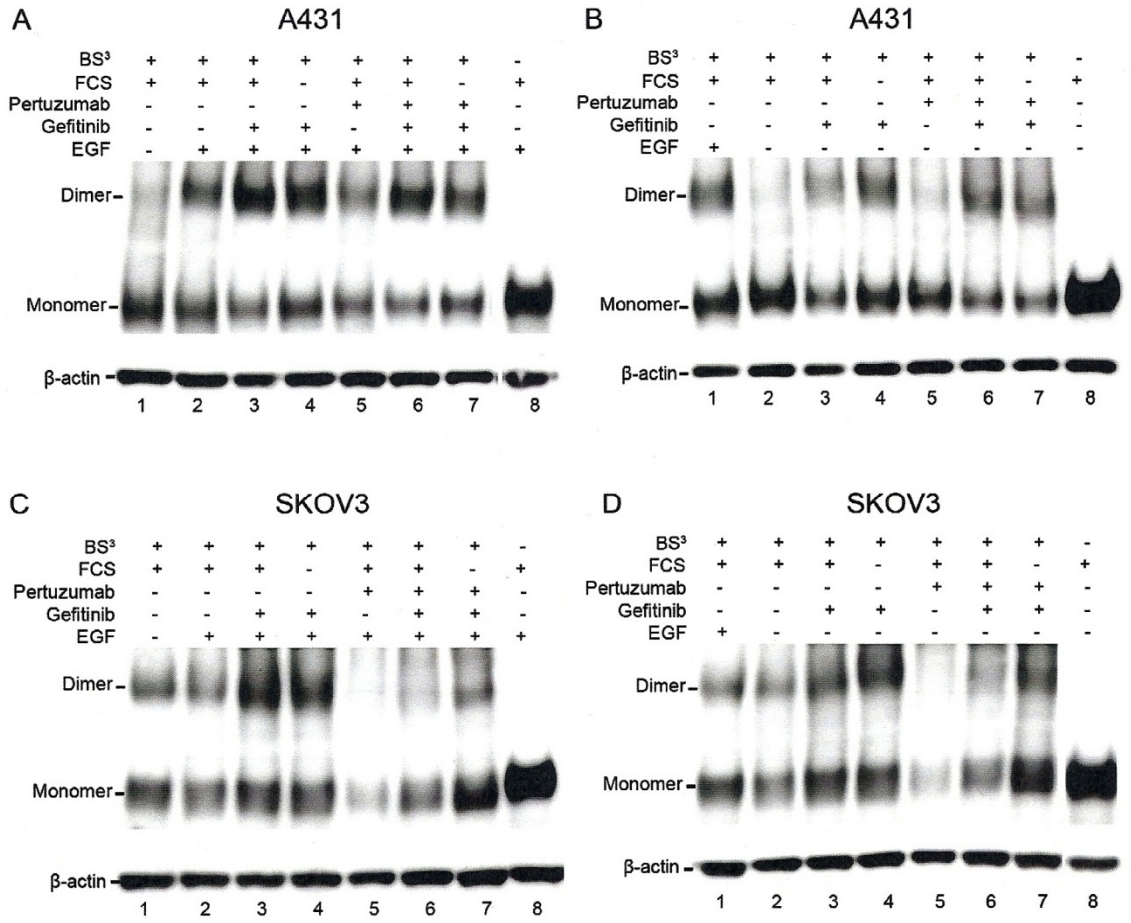

Figure 2. EGFR dimerization effects of EGF, gefitinib and pertuzumab observed in cross-linking analysis. EGFR targeting antibodies were used to depict EGFR monomers and dimers on A431 (A and B) and SKOV3 (C and D) lysates. The cells were treated with or without gefitinib and pertuzumab in complete (+FCS) or serum free medium. The difference between A and B as well as C and D is the stimulation of EGF. EGFR dimers exist without stimulation of EGF (A–D, lane 1–2), particularly in SKOV3 cells. Gefitinib increases the dimer levels in both cell lines, regardless of other treatment (A–D, lane 3–4 and 6–7). Pertuzumab does not affect the overall dimer levels of EGFR in A431 cells much (A and B, lane 5–7), but clearly disrupts EGFR dimerization in SKOV3 (C and D, lane 5–7). The BS^3 free lysates were used as negative controls for the cross-linking assay and the β-actin band was used as a loading control. This is a representative of one of four experiments.
doi:10.1371/journal.pone.0024739.g002

heterogeneous mixture of targets can be expressed as a sum of interactions [23,25] where each interaction is represented in an on-off map by its specific pair of recognition ($\log(k_a)$) and stability ($\log(k_d)$) coordinates and a color corresponding to the calculated contribution (warm colors–large contribution).

Interaction Maps were first calculated on simulated data representing known interaction properties similar to the ones shown to exist in the EGF-EGFR interaction (Fig. 4), which verified that the algorithm could accurately resolve a multitude of different simultaneous interactions. When applied on real interaction data, the Interaction Maps displayed up to three different simultaneous interactions in A431 cells (Fig. 5A–C). The Interaction Map of the binding of ^{125}I-EGF to A431 in complete medium depicted two interactions: one fast on–fast off, A1, [4.79, −3.25] with a K_D of 9 nM and one slow on–slow off, A2 [3.98,−4.94], with a K_D of 1 nM (Fig. 5A). These two interactions contributed approximately equally to the measured binding curve. When exposed to gefitinib in serum free medium (Fig. 5B), the recognition of the more stable interaction increased slightly from $\log(k_a)$: 3.98 (A2) to $\log(k_a)$: 4.37 (B2), while as the weaker interaction (A1) remained in position (B1). Furthermore, a fast on–slow off high affinity interaction (B3) appeared at position [6.11,−5.28], corresponding to a K_D of 41 pM. Pertuzumab did not alter the positions and contributions of the peaks (Fig. 5C, peaks C1, C2, C3).

The Interaction Maps of SKOV3 cells presented interaction patterns different to A431 cells. In complete medium two contributing ^{125}I-EGF–SKOV3 interactions occurred simultaneously with approximately the same recognition but different stability (D1 [5.07,−3.48] and D2 [4.85,−4.59] (Fig. 5D)). The more stable interaction D2, with a K_D of about 0.4 nM, contributed to approximately 65% of the measured binding curve. Upon gefitinib treatment in serum free medium, D2 shifted to a higher stability (E2 [4.89,−5.82]) corresponding to a K_D of 20 pM

Table 2. The effect of gefitinib on EGFR dimerization in A431 and SKOV3 cells.

A431				
	Without pertuzumab		**With pertuzumab**	
Effect of:	**Without EGF**	**With EGF**	**Without EGF**	**With EGF**
Gefitinib+complete medium	3.6±1.0*	1.9±0.1*	3.8±0.9*	1.6±0.2*
Gefitinib+serum free medium	3.6±0.8*	1.4±0.1*	3.0±0.6*	1.4±0.2
SKOV3				
	Without pertuzumab		**With pertuzumab**	
Effect of:	**Without EGF**	**With EGF**	**Without EGF**	**With EGF**
Gefitinib+complete medium	1.2±0.1*	2.0±0.1*	1.1±0.2	2.1±0.4*
Gefitinib+serum free medium	1.5±0.1*	1.8±0.1*	1.2±0.2	2.2±0.4*

The intensity of the monomer and dimer Western blot bands were analyzed and compared within gels. The table presents EffectValues, i.e. quotients of dimerization degrees. Lysates within the same gel treated identically apart from the exposure of gefitinib (with/without FCS) were used as references. Data are presented as mean±S.E (n = 4).

*indicates treatments affecting dimerization, i.e. with a calculated effect significantly different from 1 ($p<0.1$). Gefitinib increases dimerization in A431 cells and in EGF treated SKOV3 cells, irrespective of FCS and pertuzumab.

doi:10.1371/journal.pone.0024739.t002

(Fig. 5E). Furthermore, the contribution of the less stable interaction D1 was reduced even further (E1). No equivavelent to the fast on–slow off interaction observed in A431 cells (B3/C3) appeared in gefitinib treated SKOV3 cells. The addition of pertuzumab resulted in an interaction pattern (Fig. 5F) resembling a mixture of the other two Interaction Maps (Fig. 5D and E), with the more stable interaction F2 somewhere in between the previous two positions D2 and E2 while as the weaker interaction F1 remained in position (Fig. 5F).

Discussion

The aim of this study was to further investigate the binding of ^{125}I-EGF to EGFR in order to explain previous results which indicated an impact of the tyrosine kinase inhibitor gefitinib on the interaction [22]. The study started with the quantification of EGFR and HER2 expression on the four previously studied cell lines. The total number of EGFR and HER2 receptors did not vary at different treatments and can thus not explain the effects of gefitinib on the EGF binding.

All EGF incubations described in this paper (i.e. in real-time interaction measurements using LigandTracer and prior to cell lysis for the cross-linking assay) were performed at room temperature. Measurements at 37°C would have been more comparable to the reality inside a body, but the heat triggers EGFR to internalize upon EGF binding, resulting in processing or recycling of EGFR. These intracellular processes are difficult to distinguish from the activities of the membrane bound receptors. Thus, to make the data analysis manageable, room temperature were chosen as an adequate alternative to 37°C. The pre-treatments of gefitinib or pertuzumab before LigandTracer measurements or cell lysis were all done at 37°C.

The antibody pertuzumab disrupts the dimerization ability of HER2, creating fewer EGFR–HER2 heterodimers and more

Table 3. The effect of pertuzumab on EGFR dimerization in A431 and SKOV3 cells.

A431						
	Without EGF			**With EGF**		
Effect of:	**Complete medium**	**Gefitinib+complete medium**	**Gefitinib +serum free medium**	**Complete medium**	**Gefitinib+complete medium**	**Gefitinib +serum free medium**
Pertuzumab	0.9±0.2	1.1±0.3	1.5±0.1	1.0±0.0	1.5±0.1	1.1±0.1
SKOV3						
	Without EGF			**With EGF**		
Effect of:	**Complete medium**	**Gefitinib+complete medium**	**Gefitinib +serum free medium**	**Complete medium**	**Gefitinib+complete medium**	**Gefitinib +serum free medium**
Pertuzumab	0.5±0.0*	0.5±0.1*	0.4±0.1*	0.5±0.0*	0.5±0.1*	0.6±0.1*

The table presents EffectValues, i.e. quotients of dimerization degrees. Lysates within the same gel treated identically apart from the exposure of pertuzumab were used as references. Data are presented as mean±S.E (n = 4).

*indicates treatments affecting dimerization, i.e. with a calculated effect significantly different from 1 ($p<0.1$). Pertuzumab disrupts approximately 50% of the dimerization in SKOV3 cells, regardless of treatment of EGF, FCS or gefitinib. No effects of pertuzumab on EGFR dimerization in A431 cells are observed.

doi:10.1371/journal.pone.0024739.t003

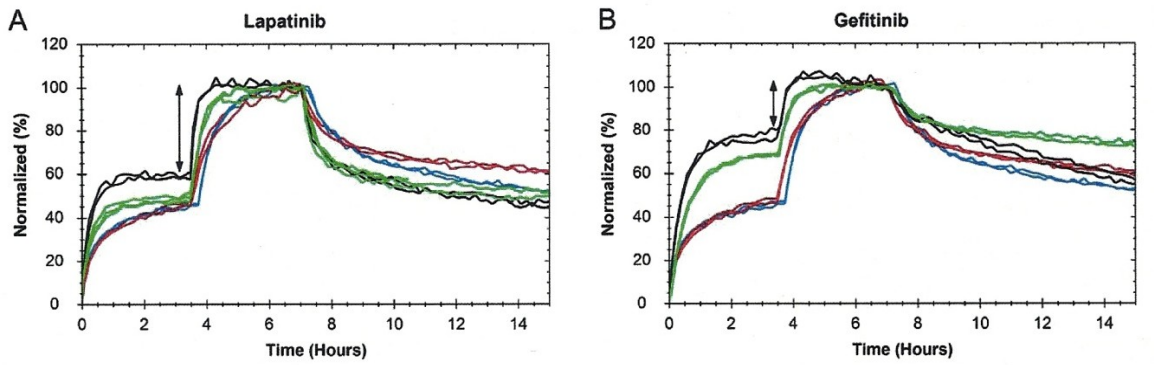

Figure 3. The effect of lapatinib on the ^{125}I-EGF–A431 interaction. The binding of ^{125}I-EGF to cultured A431 cells treated with complete medium (red), serum free medium (blue), 1 μM of lapatinib (A) or gefitinib (B) in complete medium (green) or 1 μM lapatinib (A) or gefitinib (B) in serum free medium (black) was measured in LigandTracer Grey. A) Lapatinib alters the kinetics of the interaction, as shown as a faster overall association rate and dissociation rate. In serum free medium, the difference between the first and second concentration (indicated by an arrow) is slightly less. B) Gefitinib increases the affinity, observed as a slower dissociation rate and small difference in signal height between the first and second concentration (arrow). The effect of gefitinib is larger in serum free medium.
doi:10.1371/journal.pone.0024739.g003

EGFR homodimers [26]. In this paper, real-time interaction data of the binding of ^{125}I-EGF to EGFR on A431 and SKOV3 depicts the impact of pertuzumab on association and dissociation rates, thus establishing a connection between dimer quantities and kinetic properties. In A431 and U343 cells, where the HER2 count is about 10% of the EGFR count, no obvious effect of pertuzumab was detected. Upon pertuzumab exposure in HER2 overexpressing SKOV3 cells, the overall affinity decreased in gefitinib treated

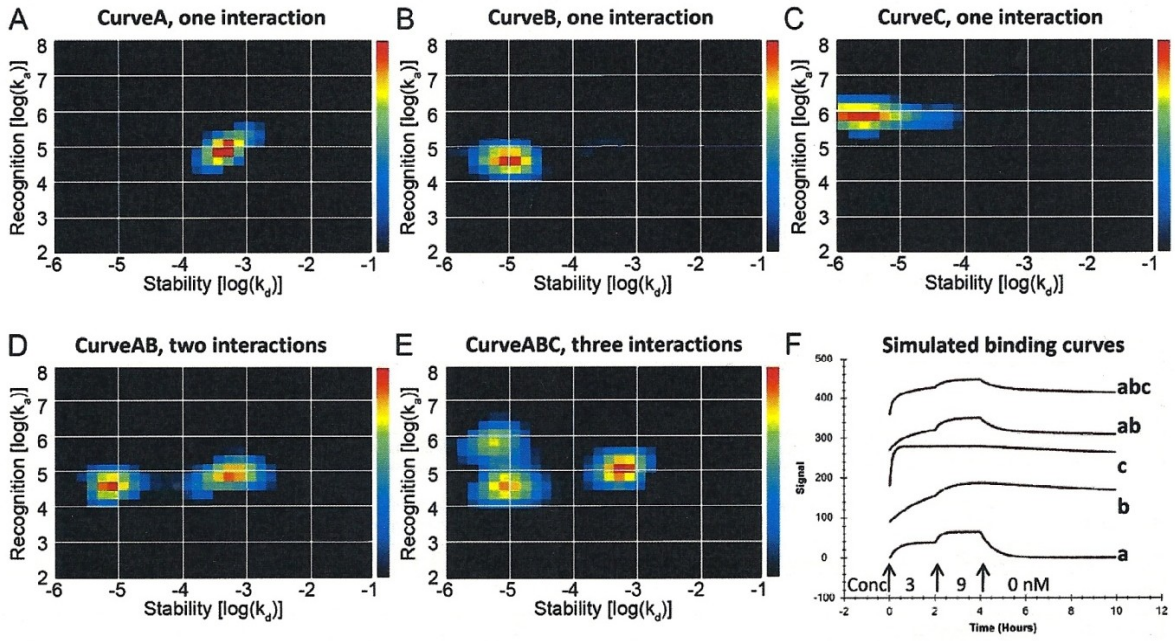

Figure 4. Heterogeneity and kinetic properties of simulated binding curves, presented as Interaction Maps. Interaction Maps were calculated from simulated binding measurements to illustrate the ability to decipher complex interactions. The Interaction Maps display every contributing interaction of the measured binding curve as a peak with specific recognition ($\log(k_a)$) and stability ($\log(k_d)$) coordinates using colors representing the relative degree of contribution (red: large contribution, blue: small contribution). Panels A, B, and C contains maps for monovalent interactions (CurveA, CurveB, CurveC). Panel D shows a map for the complex interaction CurveAB known to contain two independent interactions (CurveA+CurveB). Panel E shows a map for the complex interaction CurveABC known to contain three independent interactions (CurveA+CurveB+CurveC). The corresponding simulated binding curves are shown in Panel F. The binder was added first at 3 nM, then at 9 nM, followed by dissociation during several hours, as indicated by the arrows.
doi:10.1371/journal.pone.0024739.g004

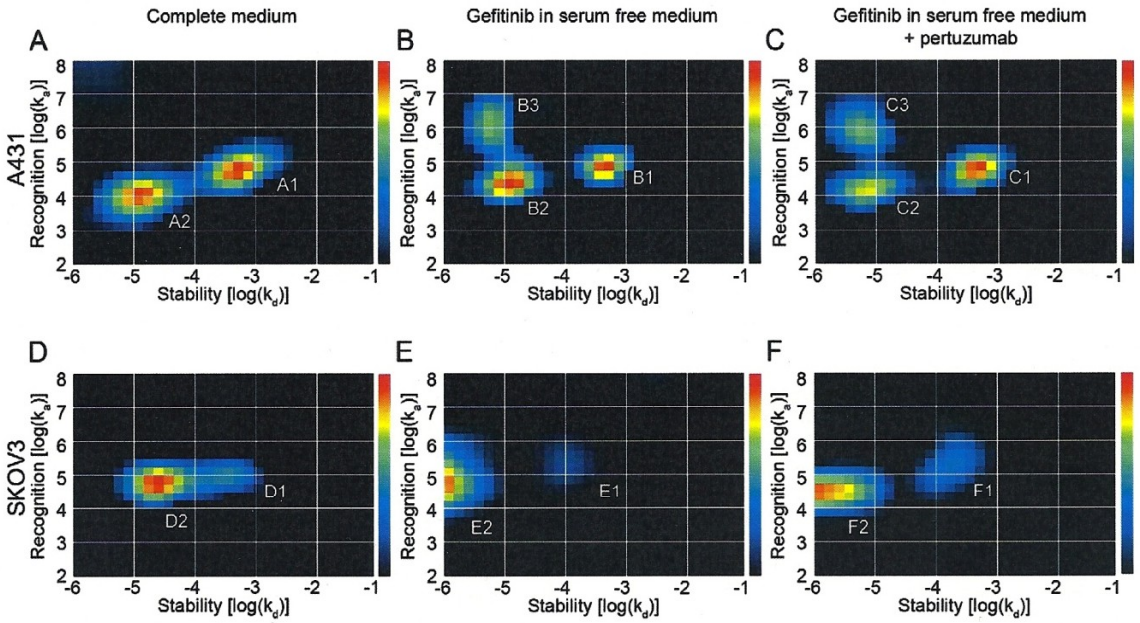

Figure 5. Heterogeneity and kinetic properties of the ^{125}I-EGF–EGFR interaction, presented as Interaction Maps. Interaction Maps were calculated from real-time binding measurements of the interaction between ^{125}I-EGF and A431 (A–C) or SKOV3 (D–F) cells, using complete medium (A and D), gefitinib in serum free medium (B and E) or gefitinib in serum free medium in the presence of pertuzumab (C and E). A) Under normal conditions in A431 cells, a fast on-fast off (A1: [4.79,−3.25]) and a slow on-slow off (A2: [3.98,−4.94]) interaction are observed. B) When treated with gefitinib in serum free medium, the more stable peak (A2) is slightly shifted to a higher recognition (B2: [4.37,−4.96]), but more importantly another peak at [6.11,−5.28] (B3) appears. C) The coordinates and the contributions of the different peaks are approximately the same with pertuzumab as without, indicating no effect of pertuzumab on the binding of ^{125}I-EGF in A431 cells. D) The binding of ^{125}I-EGF to SKOV3 cells at normal conditions consists of two interactions at [4.85,−4.59] (D2) and [5.07,−3.48] (D1), the latter less contributing. E) For gefitinib and serum free treated SKOV3 cells, the more stable interaction (D2) is shifted to even higher stability (E2: [4.89,−5.82]) while the contribution of the other interaction is reduced (E1). F) The Interaction Map of gefitinib and serum free treated SKOV3 cells in the presence of pertuzumab seems to be a mixture of Interaction Maps D and E.
doi:10.1371/journal.pone.0024739.g005

cells, observed as a higher dissociation rate and larger differences in signal height between the first and second concentration in the binding traces. In other words, pertuzumab seems to interrupt most of the affinity enhancing effect of gefitinib. This indicates that gefitinib may affect the ^{125}I-EGF–EGFR interaction in SKOV3 by a process involving dimerization.

A goal in this project was to disrupt EGFR homodimerization as well, in order to investigate its connection to the binding characteristics of the ^{125}I-EGF–EGFR interaction. However, no agent was found that accomplish this without simultaneously competing with EGF for the binding site (creating side effects impossible to distinguish from homodimerization disruption effects), thus this could not be established.

By the use of the cross-linking reagent BS^3, the dimers on the cell surface will remain together during cell lysis and immunoblot analysis [27]. In the cross-linking analysis presented in this paper, EGFR dimers are visible without EGF stimulation in both A431 and SKOV3 cells, however to a low extent in A431 cells. The increase of a factor 4 upon EGF stimulation in A431 cells affirms the hypothesis that EGF binding induces dimerization. On the other hand, no impact of EGF on the EGFR dimerization in SKOV3 cells was detected, providing strength in the hypothesis of existing dimers independent of EGF stimulation. The cell dependent matter of dimerization may be due to differences in EGFR and HER2 receptor quantities. HER2 is known to spontaneously form homodimers [28–29]. The findings in this paper indicate that this applies also to EGFR–HER2 heterodimers. EGFR homodimerization on the other hand, appears to require the presence of EGF, as observed in EGFR-rich A431 cells.

In this study, complete medium containing FCS was used in most assays. FCS is known to include some amount of growth stimulators such as EGF, although this is assumed to be low and is not expected to affect the outcome. Furthermore, FCS is often included in similar studies by other groups, making the results comparable.

The immunoblot results further highlight the impact of gefitinib on the dimerization. Gefitinib increased EGFR dimerization in A431 cells, more evidently in the absence of EGF where the overall dimerization was comparably low. In SKOV3 cells on the other hand, the impact of gefitinib was generally less. The induction of EGFR dimers by gefitinib have been studied previously. Yarden et al. proposed that the binding of gefitinib stabilizes an active conformation of the kinase domain of EGFR, creating "quasi-dimers" solely connected intracellularly [21]. Gefitinib is known to prevent growth in both A431 and SKOV3 cells [30], suggesting that the tyrosine kinase activity of the induced EGFR dimers are inhibited, but this does not specify whether they resemble the naturally formed dimers or not. The impact of gefitinib on the kinetics of the extracellular interaction with ^{125}I-EGF [22] indicates that the increased dimerization is more than an intracellular phenomenon although further conclusions about the nature of the dimers are difficult to draw.

Serum free medium did not affect the dimerization degree of gefitinib treated cells. This indicates that the effect of serum free medium to the kinetics of the interaction between ^{125}I-EGF and gefitinib treated A431 cells cannot be explained by dimerization variation or is too small to be detected by immunoblotting.

The HER2 dimerization inhibitor pertuzumab did not affect the overall EGFR dimerization in A431 cells to a detectable degree, regardless of EGF stimulation, indicating that the EGFR dimers on A431 cells are mostly homodimers. In SKOV3 cells on the other hand, EGFR dimerization drops to 50% upon pertuzumab treatment. The pertuzumab concentration used in the experiment (20 nM) will prevent approximately 75–85% of the HER2 population to form dimers [32], which explains that there are still visible amounts of EGFR dimers in SKOV3 cells. Other factors, like EGFR forming heterodimers with HER3 or HER4 as binding partners are possible but less likely because these receptors are believed to be expressed in much lower levels and are assumed not to affect the outcome much [31]. On the whole, pertuzumab clearly reduces EGFR dimerization.

The combination of pertuzumab and gefitinib is interesting. Looking at the numbers in Table 2 and 3, gefitinib doubles the amount of EGFR dimers in EGF stimulated SKOV3 cells, while pertuzumab simultaneously decreases the amount to 50%. The counteraction of pertuzumab on the gefitinib effect was visible in the real-time interaction data of ^{125}I-EGF–SKOV3 as well, yet again suggesting dimerization as a strong contributor to the mechanism of action of gefitinib on the extracellular binding of EGF. As pointed out earlier, it is unclear to what extent EGFR forms heterodimers and homodimers in the cells. Gefitinib may induce solely EGFR homodimers and pertuzumab disrupts EGFR–HER2 dimers but may increase EGFR homodimers. This way, the dimers observed for cells in normal conditions (Fig. 1A, black curve) and when exposed to a combination of gefitinib and pertuzumab (Fig. 1C and D, red curves) may be of different nature, possibly creating the small but visible difference in interaction kinetics observed in the real-time interaction data.

The measurement of the effect of lapatinib on the binding of ^{125}I-EGF to A431cells complements the gefitinib study. Lapatinib binds the inactive forms of EGFR and HER2 and does not induce EGFR dimers as opposed to gefitinib that stabilize the active conformation of EGFR [18,19,20,21]. In this paper, real-time interaction data shows that lapatinib affects the binding of ^{125}I-EGF, demonstrating that there are other examples of intracellular binders with the potential to influence extracellular interactions. However, the effect of lapatinib on the kinetic properties was unlike what was observed for gefitinib, indicating that the mechanism of action is different between the two tyrosine kinase inhibitors. This strengthens the hypothesis that the generation of EGFR dimers, not observed for lapatinib, is an important part of the effect of gefitinib on the ^{125}I-EGF binding. By binding and stabilizing the inactive conformation of EGFR, lapatinib may alternatively inhibit EGFR dimerization, as suggested from the clear, but different, shape of the real-time binding curve.

Interaction Map analysis opens up possibilities for speculation. The two to three visible peaks in each of the Interaction Maps in Figure 5 demonstrate a heterogeneous nature of the binding of EGF to EGFR and provide a detailed description of both the contribution and kinetic properties of the simultaneously occurring interactions. One peak at approximately [5, −3.5] is visible in all six Interaction Maps (A1, B1, C1, D1, E1, F1). A peak representing a more stable interaction is observed as well (A2, B2, C2, D2, E2, F2), but it changes in position and contribution between treatments and cell lines and may even be divided into two peaks in the gefitinib treated A431 cells (B3, C3). One hypothesis is that the right-most peaks (A1–F1) visible in all treatments correspond to the binding of ^{125}I-EGF to monomeric EGFR and that the more stable peaks (A2–F2, B3, C3) observed in the left parts of the Interaction Maps represent the interaction between ^{125}I-EGF and its two major dimeric forms. The comparably low amount of HER2 receptors in A431 cells makes HER2 an unlikely dimerization partner, leaving EGFR as monomers and homodimers. In SKOV3 cells on the other hand, the large HER2 count will likely "consume" most EGFR receptors, shifting the equilibrium to a more heterodimeric state (Fig. 6A). The differences in A2 and D2 may thus represent the two types of EGFR dimer types. This peak is altered in the presence of the dimerization altering factors gefitinib and pertuzumab, strengthening the idea of it representing the dimeric state. If this hypothesis is valid, Figures 5B and 5E shows that gefitinib induces a shift in contribution from a monomeric state towards a dimeric. It also alters the interaction of EGF with the dimeric form, observed as a new fast on–slow off peak (B3, C3) in A431 cells and a change towards higher stability (from D2 to E2) in SKOV3 cells. The effect of pertuzumab (Fig. 5C and F) indicates that the gefitinib induced dimers are still mostly homodimers in A431 cells (unaffected by pertuzumab) and heterodimers in SKOV3 cells (clearly affected by pertuzumab) (Fig 6B). One necessary experiment for verifying the accuracy of this hypothesis would be to distinguish between EGFR homodimers and EGFR–HER2 heterodimers, in normal conditions and upon gefitinib treatment. Gefitinib is directed towards EGFR [33], suggesting that the induced dimers are solely EGFR homodimers if presuming the need of gefitinib binding to both binding partners for a functioning dimerization. However, kinase inhibitors are notoriously promiscuous [34] and it is possible that gefitinib also binds to HER2 to some extent.

The question remains whether EGF can bind to pre-existing EGFR dimers or if the differences in interaction are merely the result of EGF dissociating from either EGFR monomers or dimers. The observed association rate of a ligand to its target will relate to the recognition and stability of the interaction and the concentration of the ligand, while the observed dissociation rate is dependent on the stability alone [35]. The differences in stability between the observed peaks can thus represent various forms of dissociation. In A431 cells there are differences in recognition as well, indicating that EGF is able to not only dissociate from, but also associate *to* at least two different structures. Our hypothesis is that these structures are EGFR monomers and EGFR dimers, i.e. ^{125}I-EGF binds independently and directly to both EGFR monomers and existing EGFR homo/hetero dimers on A431 cells.

One of the goals of this paper was to establish the biological processes behind the effect of the tyrosine kinase inhibitor gefitinib on the EGF–EGFR interaction. We propose that gefitinib induces dimers with higher affinity to ^{125}I-EGF than EGFR monomers or the EGFR dimers normally displayed on the cell surface. Furthermore, the heterogeneity of the ^{125}I-EGF–EGFR interaction proposes an explanation to the previously observed differences in affinity between cell lines. The epidermal growth factor receptors may be identical in both sequence and tertiary structure, but to what extent they form dimers may depend on e.g. the receptor expression of the hosting cell line. Each EGFR monomer/dimer form interacts with EGF with specific kinetics properties (recognition and stability), which results in differences in overall affinity depending on the prevalence of these interactions. Interaction Maps can decipher a measured interaction into its contributing components, thus opens up for a detailed understanding of the EGFR family puzzle.

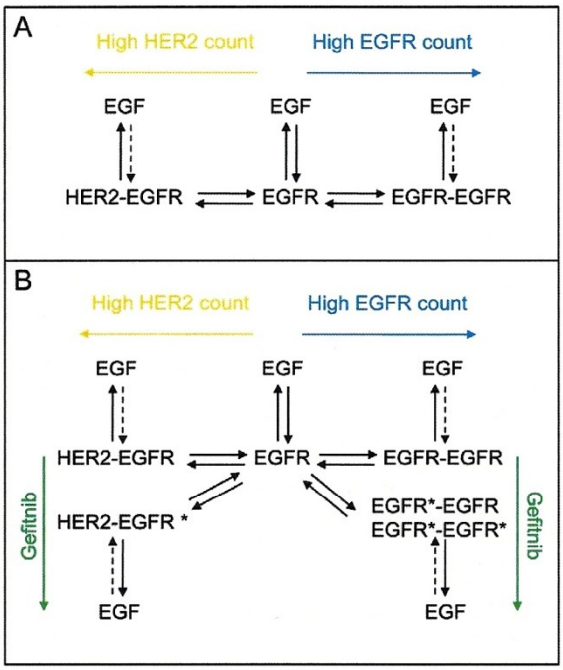

Figure 6. Proposed mechanism of EGF binding to EGFR in normal conditions and when treated with gefitinib. A) Real-time binding data of ^{125}I-EGF to A431 and SKOV3 cells, as presented in Interaction Maps, depicts a reality where EGF interacts with not only one receptor form, but several. The different receptor populations may be the monomeric, heterodimeric and homodimeric form of EGFR. The equilibration between the different monomer/dimer states will likely be dependent on the number of EGFR and HER2 receptors expressed on the cell surfaces, where a large HER2 count shifts the equilibrium to more EGFR–HER2 heterodimers and a high EGFR expression results in more EGFR homodimers. Differences in stability of the interaction imply that EGF can dissociate from all three forms. The ability of EGF to bind to ligand free dimers (dashed lines) remains unclear, as the existence of such dimers. B) When treated with gefitinib, the binding of EGF to the dimeric form is altered, suggesting that a new dimeric form is created, either as an addition (A431) or as a replacement (SKOV3).
doi:10.1371/journal.pone.0024739.g006

In conclusion, the results presented in this paper show that gefitinib induces formation of EGFR dimers which alters the apparent interaction characteristics with EGF. The prevalence of monomers, homodimers and heterodimers are different between cell lines and are likely dependent on EGFR and HER2 expression. EGF binds to the various monomeric/dimeric forms of EGFR with unique binding properties, thus the distribution of the different EGFR forms in a cell will affect the overall affinity.

Materials and Methods

Antibodies and reagents

The tyrosine kinase inhibitors gefitinib and lapatinib was from Biaffin GmbH (Kassel, Germany) and GlaxoSmithKline (London, UK) respectively. Cetuximab was purified from Erbitux® (Merck KGaA, Darmstadt, Germany) and trastuzumab was purified from Herceptin® (Roche AB, Stockholm, Sweden). The humanized monoclonal antibody pertuzumab, directed towards HER2 to prevent dimerization, was purified from Omnitarg™ from Genentech (San Fransisco, CA, USA). The cross-linking reagent bis(sulfosuccinimidyl)suberate (BS^3) was purchased from Thermo Scientific (Rockford, IL, USA). The polyclonal rabbit anti-EGFR antibody was from Santa Cruz (Santa Cruz, CA, USA) and the monoclonal mouse anti-β-actin antibody (clone AC-15) was from Sigma Aldrich (St Louis, MO, USA). Peroxidase-conjugated anti-rabbit antibody and peroxidase-conjugated anti-mouse antibody was purchased from GE Healthcare (Waukesha, WI, USA).

Cell culture

Four cell lines were used: the human squamous carcinoma cell line A431 (CLR 1555, ATCC, Rocksville, MD, USA), the human ovarian carcinoma cell line SKOV3 (HTB-77, ATCC, Rocksville, MD, USA) the human glioma cell line U343MGaCl2:6 (a subclone of U343MG [36]), denoted U343, and the human breast cancer cell line SKBR3 (HTB-30, ATCC, Rocksville, MD, USA). In all cellular experiments, the cells were grown in a humified incubator at 37°C, equilibrated with 5% $C0_2$ until experimental day. The cells were cultured in Ham's F10 cell culture medium (Biochrom Ag, Berlin, Germany) supplemented with 10% fetal calf serum (Sigma, St Louis, MO, USA), L-glutamine (2 mM) and PEST (penicillin 100 IU/ml and streptomycin 100 µg/ml, from Biochrom Ag, Berlin Germany) if not otherwise specified.

Radiolabeling

Human Epidermal growth factor (EGF, Chemicon International, USA) was labeled with ^{125}I (Perkin-Elmer, Wellesley, MA, USA) using the Chloramine-T protocol [37].

Treatment of cells with tyrosine kinase inhibitors

Cells were exposed to four different treatments, as described previously [22]. In brief, cells were incubated for 24−48 h in either complete or serum free Hams F10 culturing medium in the presence or absence of 1 µM of either gefitinib or lapatinib.

Estimating number of receptors

The expression levels of EGFR and HER2 were estimated using either the manual or the kinetic extrapolation (KEX) method, as described by Bárta et. al. [24]. For the manual protocol, cells were seeded in triplicates in 12-wells plates (NuclonTM, Roskilde, Denmark). ^{125}I-labeled cetuximab and trastuzumab were used for the quantification of EGFR and HER2 respectively. A single concentration of 100 nM antibody was estimated to be sufficient for saturating the receptors, as it corresponds to approximately $100\times K_D$. After 3–4 hours of incubation at 4 °C, the cells were washed repeatedly with serum free medium, followed by trypsination. The number of resuspended cells were counted and the radioactivity measured (automatic gamma counter 1480 WIZARD™ 3", PerkinElmer) to evaluate cell receptor levels [38]. For the KEX method, cells were incubated with increasing concentrations of either ^{125}I-labeled trastuzumab or cetuximab in LigandTracer Grey at room temperature. The binding traces were to a kinetic model describing a bivalent interaction, using TraceDrawer 1.2 (Ridgeview Instruments AB, Uppsala, Sweden). This resulted in an estimation of B_{max}, which was used to correct for non-saturation of receptors.

Real-time interaction measurements of ^{125}EGF in LigandTracer

Real-time measurements of the binding of ^{125}I-EGF to EGFR on the cells were performed at room temperature in LigandTracer Grey instruments, according to previously published protocol [39]. After a short baseline, the cells were incubated for 3.5 h twice using increasing concentrations of ^{125}I-EGF. The concentrations were chosen based on the affinity to EGF for the three cell lines

(2.8 and 9 nM for A431, 0.5 and 1.5 nM for U343, 0.7 and 2 nM for SKOV3). The ligand solution was replaced with fresh medium (containing 1 μM gefitinib or 1 μM lapatinib in the TKI treatment studies) and the dissociation rate was followed over night.

Dimerization perturbation

To prevent EGFR-HER2 dimerization, A431, SKOV3 and U343 cells were incubated with 20 nM of pertuzumab over night prior to the detection of the ^{125}I-EGF – EGFR interaction in LigandTracer Grey or the cross-linking experiments. The antibody remained in the ^{125}I-EGF solution during measurement (LigandTracer) or EGF incubation (cross-linking). Pertuzumab effects were studied in combination with four of the treatments described above (complete medium, serum free medium, 1 μM gefitinib and serum free medium+gefitinib).

Cross-linking of EGFR and HER2

Prior to cross-linking, the cells were treated with or without 1 μM gefitinib (48 h) and 20 nM pertuzumab (over-night) in 37°C as described previously, followed by incubation with or without EGF (9 nM) for 3.5 hours at room temperature. After three times washing with ice cold PBS, the cells were subjected to 1 mM of the cross-linking reagent BS^{3}at room temperature for 30 min. The reaction was terminated using 20 mM (final concentration) Tris-Cl, pH 8.5 for 15 min at room temperature. Subsequently, cells were washed with ice cold PBS and solubillized in lysis buffer containing 150 mM NaCl, 20 mM Tris(amino), 5 mM EDTA, 10% (v/v) glycerol and 1% (v/v) Triton X-100 and a cocktail of protease and phosphatase inhibitors.

Immunoblotting and image analysis

Cell lysates were separated by SDS-PAGE in a 3–8% tris-acetate gel (Invitrogen, Carlsbad, CA, USA) and transferred to PVDF membranes (Millipore Corporation, Billerica, MA, USA), which were blocked for 1 h with PBS-T with 5% BSA (w/v) before incubation with primary antibodies at 4°C over-nigh. The proteins were visualized using peroxidase-conjugated ImmobilionTM Western Chemiluminescent HRP Substrate (Millipore Corporation, Billerica, MA, USA) in a cooled charge-coupled device (CCD) camera (FujiFilm, Luminescent Image analyzer LAS-1000plus). The intensity of bands was quantified in ImageJ (Rasband, W.S., ImageJ, U. S. National Institutes of Health, Bethesda, Maryland, USA, http://imagej.nih.gov/ij/, 1997–2011) to study the consequences of treatments upon dimerization. Statistical analysis was performed in Minitab® 15 (Minitab Inc., State College, PA, USA) using Student's t-tests. Results with p-values less than 0.1 were deemed significant. The HiMark™ (Invitrogen, Carlsbad, CA, USA) molecular weight protein standards ranging from 31 kDa to 460 kDa was used to assess the molecular weight of identified bands.

Interaction Map analysis

The mathematical method Interaction Map [25] expresses the measured binding of a (homogeneous) ligand to a heterogeneous group of targets as a sum of interactions, each having a unique combination of the association rate constant k_a and dissociation rate constant k_d:

$$MeasuredCurve = \sum_{i=1}^{n}\sum_{j=1}^{m}\left[W_{ij} \times CurveComponent\left(conc, k_a^i, k_d^j\right)\right]$$

where conc is the concentration of protein in solution (the "ligand") and W_{ij} is the weighing factor describing the contribution to the measured real-time interaction curve. The calculated contributing curves are represented as colored (red = - large W_{ij}, dark blue = small W_{ij}) peaks in an on-off plot. In this paper, the Interaction Map method used 24 (k_a)×30 (k_d) different nodes with kinetic parameter values evenly distributed in log-space ($\log10(k_a)$ = {2.0000, 2.2609, 2.5217, …, 7.4783, 7.7391, 8.0000} , $\log10(k_d)$ = {-6.0000, −5.8276, −5.6552, …, −1.3448, −1.1724, −1.0000}). A Tichonov-type regularization algorithm was used to real-time binding curves measured in LigandTracer Grey, adding penalty to the sum-of-square residuals if there are many peaks in the Interaction Map. A similar algorithm has been presented previously [23] and has been applied to SPR-based real-time interaction analysis.

The non-linear fitting algorithm was implemented in Visual Basic/Visual Studio 2003 (Microsoft, Mountain View, CA). The ability of the Interaction Map algorithm to accurately decompose a complex binding data was validated on a series of binding curves simulated in MATLAB 6.5 (The Mathworks, Natic, MA, USA). The peak position was estimated as the center of gravity for the peak and is reported as [$\log10(k_a)$, $\log10(k_d)$]. The contribution of a peak was estimated as the percentage of the weight factors (W_{ij}) for the pixels of the peak in comparison to the sum of all weight factors.

The interaction map algorithm was tested using a range of different simulated binding curves with known interaction properties. In this paper, simulated curves with similar binding properties as what was found in the investigated ^{125}I-EGF - EGFR interaction were used: monovalent CurveA ($k_a = 10^5$ $M^{-1}s^{-1}$; $k_d = 5*10^{-4}$ s^{-1}), monovalent CurveB ($k_a = 5*10^4$ $M^{-1}s^{-1}$; $k_d = 10^{-5}$ s^{-1}), monovalent CurveC ($k_a = 8*10^5$ $M^{-1}s^{-1}$; $k_d = 8*10^{-6}$ s^{-1}), complex CurveAB (CurveA+CurveB) and complex CurveABC (CurveA+CurveB+CurveC). In all cases, an assay of first 2 h of 3 nM binder, then 2 h of 9 nM binder and finally 6 h of dissociation (i.e. 0 nM binder) was simulated. Noise corresponding to 1% of the signal was added to each curve. These five curves were subjected to Interaction Map analysis and were expected to produce single, double or triple peak maps.

Author Contributions

Conceived and designed the experiments: HB KA. Performed the experiments: HB PB. Analyzed the data: HB LG MM KA. Contributed reagents/materials/analysis tools: LG KA. Wrote the paper: HB KA. Designed the software used in Interaction Map analysis: KA. Read and approved the final version of the manuscript: HB LG PB MM KA.

References

1. Liu P, Sudhaharan T, Koh RM, Hwang LC, Ahmed S, et al. (2007) Investigation of the dimerization of proteins from the epidermal growth factor receptor family by single wavelength fluorescence cross-correlation spectroscopy. Biophys J 93: 684–698.
2. Tao RH, Maruyama IN (2008) All EGF(ErbB) receptors have preformed homo- and heterodimeric structures in living cells. J Cell Sci 121: 3207–3217.
3. Yarden Y, Schlessinger J (1987) Epidermal growth factor induces rapid, reversible aggregation of the purified epidermal growth factor receptor. Biochemistry 26: 1443–1451.
4. Sorkin A, Carpenter G (1991) Dimerization of internalized epidermal growth factor receptors. J Biol Chem 266: 23453–23460.
5. Bublil EM, Yarden Y (2007) The EGF receptor family: spearheading a merger of signaling and therapeutics. Curr Opin Cell Biol 19: 124–134.
6. Normanno N, De Luca A, Bianco C, Strizzi L, Mancino M, et al. (2006) Epidermal growth factor receptor (EGFR) signaling in cancer. Gene 366: 2–16.
7. Tzahar E, Waterman H, Chen X, Levkowitz G, Karunagaran D, et al. (1996) A hierarchical network of interreceptor interactions determines signal transduction

by Neu differentiation factor/neuregulin and epidermal growth factor. Mol Cell Biol 16: 5276–5287.
8. Yarden Y, Sliwkowski MX (2001) Untangling the ErbB signalling network. Nat Rev Mol Cell Biol 2: 127–137.
9. Hommelgaard AM, Lerdrup M, van Deurs B (2004) Association with membrane protrusions makes ErbB2 an internalization-resistant receptor. Mol Biol Cell 15: 1557–1567.
10. Ullrich A, Schlessinger J (1990) Signal transduction by receptors with tyrosine kinase activity. Cell 61: 203–212.
11. Lax I, Bellot F, Howk R, Ullrich A, Givol D, et al. (1989) Functional analysis of the ligand binding site of EGF-receptor utilizing chimeric chicken/human receptor molecules. EMBO J 8: 421–427.
12. Ozcan F, Klein P, Lemmon MA, Lax I, Schlessinger J (2006) On the nature of low- and high-affinity EGF receptors on living cells. Proc Natl Acad Sci U S A 103: 5735–5740.
13. Shechter Y, Hernaez L, Cuatrecasas P (1978) Epidermal growth factor: biological activity requires persistent occupation of high-affinity cell surface receptors. Proc Natl Acad Sci U S A 75: 5788–5791.
14. Baselga J (2006) Targeting tyrosine kinases in cancer: the second wave. Science 312: 1175–1178.
15. Wakeling AE, Guy SP, Woodburn JR, Ashton SE, Curry BJ, et al. (2002) ZD1839 (Iressa): an orally active inhibitor of epidermal growth factor signaling with potential for cancer therapy. Cancer Res 62: 5749–5754.
16. Kris MG, Natale RB, Herbst RS, Lynch TJ, Jr., Prager D, et al. (2003) Efficacy of gefitinib, an inhibitor of the epidermal growth factor receptor tyrosine kinase, in symptomatic patients with non-small cell lung cancer: a randomized trial. JAMA 290: 2149–2158.
17. Spector N (2008) Treatment of metastatic ErbB2-positive breast cancer: options after progression on trastuzumab. Clin Breast Cancer 8 Suppl 3: S94–99.
18. Stamos J, Sliwkowski MX, Eigenbrot C (2002) Structure of the epidermal growth factor receptor kinase domain alone and in complex with a 4-anilinoquinazoline inhibitor. J Biol Chem 277: 46265–46272.
19. Wood ER, Truesdale AT, McDonald OB, Yuan D, Hassell A, et al. (2004) A unique structure for epidermal growth factor receptor bound to GW572016 (Lapatinib): relationships among protein conformation, inhibitor off-rate, and receptor activity in tumor cells. Cancer Res 64: 6652–6659.
20. Yun CH, Boggon TJ, Li Y, Woo MS, Greulich H, et al. (2007) Structures of lung cancer-derived EGFR mutants and inhibitor complexes: mechanism of activation and insights into differential inhibitor sensitivity. Cancer Cell 11: 217–227.
21. Bublil EM, Pines G, Patel G, Fruhwirth G, Ng T, et al. (2010) Kinase-mediated quasi-dimers of EGFR. FASEB J 24: 4744–4755.
22. Björkelund H, Gedda L, Andersson K (2011) Comparing the epidermal growth factor interaction with four different cell lines: intriguing effects imply strong dependency of cellular context. PLoS One 6: e16536.
23. Svitel J, Balbo A, Mariuzza RA, Gonzales NR, Schuck P (2003) Combined affinity and rate constant distributions of ligand populations from experimental surface binding kinetics and equilibria. Biophys J 84: 4062–4077.
24. Bárta P, Björkelund H, Andersson K (2011) Circumventing the requirement of binding saturation for receptor quantification using interaction kinetic extrapolation. Nucl Med Commun In Press.
25. Andersson K, Malmqvist M (2008) Method for the analysis of solid biological objects. Patent application WO 2010033069.
26. Hughes JB, Berger C, Rodland MS, Hasmann M, Stang E, et al. (2009) Pertuzumab increases epidermal growth factor receptor down-regulation by counteracting epidermal growth factor receptor-ErbB2 heterodimerization. Mol Cancer Ther 8: 1885–1892.
27. Fanger BO, Stephens JE, Staros JV (1989) High-yield trapping of EGF-induced receptor dimers by chemical cross-linking. FASEB J 3: 71–75.
28. Stern DF (2008) ERBB3/HER3 and ERBB2/HER2 duet in mammary development and breast cancer. J Mammary Gland Biol Neoplasia 13: 215–223.
29. Brennan PJ, Kumagai T, Berezov A, Murali R, Greene MI (2000) HER2/neu: mechanisms of dimerization/oligomerization. Oncogene 19: 6093–6101.
30. Moasser MM, Basso A, Averbuch SD, Rosen N (2001) The tyrosine kinase inhibitor ZD1839 ("Iressa") inhibits HER2-driven signaling and suppresses the growth of HER2-overexpressing tumor cells. Cancer Res 61: 7184–7188.
31. Aguilar Z, Akita RW, Finn RS, Ramos BL, Pegram MD, et al. (1999) Biologic effects of heregulin/neu differentiation factor on normal and malignant human breast and ovarian epithelial cells. Oncogene 18: 6050–6062.
32. Björkelund H, Gedda L, Andersson K (2011) Avoiding false negative results in specificity analysis of protein-protein interactions. J Mol Recognit 24(1): 81–9.
33. Ciardiello F (2000) Epidermal growth factor receptor tyrosine kinase inhibitors as anticancer agents. Drugs 60 Suppl 1: 25–32; discussion 41-22.
34. Crespo A, Zhang X, Fernandez A (2008) Redesigning kinase inhibitors to enhance specificity. J Med Chem 51: 4890–4898.
35. Hulme EC, Trevethick MA (2010) Ligand binding assays at equilibrium: validation and interpretation. Br J Pharmacol 161: 1219–1237.
36. Westermark B, Magnusson A, Heldin CH (1982) Effect of epidermal growth factor on membrane motility and cell locomotion in cultures of human clonal glioma cells. J Neurosci Res 8: 491–507.
37. Hunter WM, Greenwood FC (1962) Preparation of iodine-131 labeled human growth hormone of high specific activity. Nature 194: 495–496.
38. Nestor M (2010) Effect of cetuximab treatment in squamous cell carcinomas. Tumour Biol 31: 141–147.
39. Bjorke H, Andersson K (2006) Automated, high-resolution cellular retention and uptake studies in vitro. Appl Radiat Isot 64: 901–905.

IV. PROTEIN INTERACTION WITH HER-FAMILY RECEPTORS CAN HAVE DIFFERENT CHARACTERISTICS DEPENDING ON THE HOSTING CELL LINE

Barta P, Malmberg J, Melicharova L, Strandgård J, Orlova A, Tolmachev V, Laznicek M, Andersson A: Protein interactions with HER-family receptors can have different characteristics depending on the hosting cell line. Int J Oncol. 2012 May; 40(5):1677-82.

Protein interactions with HER-family receptors can have different characteristics depending on the hosting cell line

PAVEL BARTA[1*], JENNIE MALMBERG[2*], LUDMILA MELICHAROVA[1], JOHN STRANDGÅRD[3], ANNA ORLOVA[2], VLADIMIR TOLMACHEV[4], MILAN LAZNICEK[1] and KARL ANDERSSON[3,4]

[1]Department of Pharmacology and Toxicology, Faculty of Pharmacy in Hradec Kralove, Charles University in Prague, Heyrovského 1203, 50005 Hradec Králové, Czech Republic; [2]Preclinical PET Platform, Uppsala University, Dag Hammarskjölds väg 14C, SE 75183 Uppsala; [3]Ridgeview Instruments AB, Ulleråkersv 62, SE 75643 Uppsala; [4]Department of Radiology, Oncology, and Radiation Sciences, Rudbeck Laboratory, Uppsala University, SE 75185 Uppsala, Sweden

Received October 14, 2011; Accepted November 29, 2011

DOI: 10.3892/ijo.2011.1307

Abstract. Cell lines are common model systems in the development of therapeutic proteins and in the research on cellular functions and dysfunctions. In this field, the protein interaction assay is a frequently used tool for assessing the adequacy of a protein for diagnostic and therapeutic purposes. In this study, we investigated the extent to which the interaction characteristics depend on the choice of cell line for HER-family receptors. The interaction characteristics of two therapeutic antibodies (trastuzumab and cetuximab) and one Affibody molecule ($Z_{HER2:342}$), interacting with the intended receptor were characterized with high precision using an automated real-time interaction method, in different cell lines (HaCaT, A431, HEP-G2, SKOV3, PC3, DU-145). Clear differences in binding affinity and kinetics, up to one order of magnitude, were found for the interaction of the same protein binding to the same receptor on different cells for all three proteins. For HER-family receptors, it is therefore important to refer to the measured affinity for a protein-receptor interaction together with the hosting cell line. The ability to accurately measure affinity and kinetics of a protein-receptor interaction on cell lines of different origins may increase the understanding of underlying receptor biology, and impact the selection of candidates in the development of therapeutic or diagnostic agents.

Correspondence to: Dr Karl Andersson, Ridgeview Instruments AB, Ulleråkersv 62, SE 75643 Uppsala, Sweden
E-mail: karl@ridgeviewinstruments.com

*Contributed equally

Key words: HER2, epidermal growth factor receptor, affinity, trastuzumab, cetuximab, affibody molecules

Introduction

Cell-based assays are commonly used in the development of therapeutic proteins and in the research on the underlying biology of cellular functions and dysfunctions. As the smallest element of living matter, cloned cells in culture represents an *in vitro* model system that reflects essential molecular function of tissues *in vivo*, such as signaling, metabolism and cell membrane transport. Protein interaction assays are one subclass of cell-based assays and they are particularly common in the development of diagnostic and therapeutic proteins, such as therapeutic antibodies or molecular imaging agents.

One important question is the validity of any particular cell line as a model for the disease under study. This question is very important in oncology, where the tumor cell is by definition altered into an immortal state. There is increasing evidence that the choice of model cell line can impact the estimation of the efficacy (1), or the pharmacokinetics (2), or the apparent affinity (3-5) of a compound by a factor 3-10. The validity of the cell line as a model has long-lasting impact on the development of therapeutic proteins and fundamental research, because it questions the scope of reported findings: Is the observed effect general for the disease under study or is the effect limited to the currently used model system?

The cell-based assays for protein-cell interactions have essentially remained the same during the last 40 years: Most assays rely on incubation of labeled protein with the cell culture, followed by a wash and finally a quantification of the amount of retained label on the cells after a wash. Even though the read-out modalities have been improved with increased sensitivity and throughput, the basic assay principle of incubate-wash-quantify has remained the same. Recent development in protein design and affinity maturation has however increased the binding strength of the proteins to K_D <1 nM, which leads to inherent problems with the assay principle of incubate-wash-quantify since the time required to reach equilibrium often exceeds 10 h (6). Therefore, we apply a novel type of assay capable of measuring how proteins interact with molecular targets on living cells in real-time, LigandTracer® (7). This assay is conducted

on an inclined, slowly rotating petri dish and was applied on protein-receptor interactions on different hosting cell lines.

This study is focused on interaction of targeting proteins with receptors belonging to HER (human epidermal growth factor receptor) tyrosine kinases family. Signaling and cross-interaction of HER family is described in a number of reviews (8-11). The HER family consists of four homologous receptors: EGFR (epidermal growth factor receptor, also called HER1), HER2, HER3 and HER4, and ten known ligands. One commonly accepted mechanistic model is that binding of a ligand to a HER receptor causes profound conformational changes, leading to homo- and heterodimerisation, even though other theories have been presented (12). Of note, HER2 has no known ligand, but is capable of dimerizing with other members of HER family without ligand binding (11). Cellular responses to HER receptor tyrosine kinase activation are numerous, and include cell division, differentiation and motility, as well as apoptosis suppression.

It is well documented that excessive HER signaling, arising from receptor overexpression, mutations or autocrine stimulation, is a hallmark of a wide variety of solid tumors (8,10). Currently, several monoclonal antibodies targeting different receptors of HER2 family are approved for clinical use and a number are under active development (13).

Our main hypothesis is that for targeting proteins binding to HER-family receptors, the interaction characteristics will be strongly dependent on the choice of cell line. To verify this hypothesis, we performed a detailed characterization of three different molecular interactions: ^{131}I-cetuximab - EGFR, ^{125}I-trastuzumab - HER2 and Affibody molecule ^{111}In-Z342 - HER2, each conducted on three different cell lines.

Materials and methods

Cell lines. The cell lines used in this study were human squamous carcinoma cell line A431 (Health Protection Agency, Salisbury, UK), the human ovarian carcinoma cell line SKOV3 (HTB-77, ATCC, Rocksville, MD, USA), the human prostate cancer bone metastasis cell line PC3 (CRL-1435, ATCC), the human prostate cancer brain metastasis cell line DU-145 (HTB-81, ATCC), the human keratinocyte cell line HaCaT (DKFZ, Heidelberg, Germany), and the human Caucasian hepatocyte carcinoma cell line HEP-G2 (Health Protection Agency). The cells were seeded on a small local area of a petri dish (Nuclon™, dish size 100x20, NUNC A/S, Roskilde, Denmark) as previously described (7). Cells were cultivated in RPMI cell culture medium (Biochrom AG, Berlin, Germany) for SKOV3, PC3 and DU-145 cells, Eagle's MEM cell culture medium (Sigma-Aldrich, Germany) for A431 and Hep-G2 cells and Dulbecco's MEM cell culture medium (Sigma-Aldrich) for HaCaT cells. Cell culture media were supplemented with 10% fetal calf serum (FCS, Sigma, St. Louis, MO, USA), L-glutamin (2 mM, Biochrom AG), PEST (penicillin 100 IU/ml and streptomycin 100 μg/ml for SKOV3, PC3 and DU-145 only, Biochrom AG). The cells were cultivated at 37°C in incubator with humidified atmosphere and 5% CO_2 until experimental day.

Radiolabeling. Monoclonal antibody cetuximab (80 μg) (purified from Erbitux, Merck KGaA, Darmstadt, Germany) were labeled with 10 MBq ^{131}I (Institute of Isotopes Co., Ltd. Budapest, Hungary) using Chloramine-T according to the protocol (14). Monoclonal antibody trastuzumab (80 μg) (purified from Herceptin, Roche AB, Stockholm, Sweden) was labeled with 5-10 MBq ^{125}I (Perkin-Elmer, Wellesley, MA, USA) using the same protocol (14). The labeling reactions were performed with chloramine-T (Sigma) and sodium metabisulfite (Aldrich, Stockholm, Sweden). The desired radiolabeled protein was purified on a NAP-5 column (GE Healthcare, Waukesha, WI, USA) equilibrated with PBS (10 mM, pH 7.4, 140 mM NaCl). Affibody molecule $Z_{HER2:342}$ was pre-conjugated with DOTA (1,4,7,10-tetraazacyclododecane-1,4,7-tris-acetic acid-10-maleimidoethylacetamide) and radiolabeling with ^{111}In (Covidien, Hazelwood, MO) through chelation was performed essentially as previously described (15).

Real-time interaction measurements in LigandTracer. Real-time measurements of the binding of labeled proteins to their respective receptors on the cells were performed at room temperature in LigandTracer® (Ridgeview Instruments AB, Uppsala, Sweden). LigandTracer Yellow was used for ^{131}I-cetuximab and Affibody molecule ^{111}In-Z342 measurements, and LigandTracer Grey for ^{125}I-trastuzumab measurements, all according to previously published protocol (3). After a short baseline measurement, the cells were incubated first at a lower concentration of protein, then at a higher concentration and finally the cells were put in fresh cell culture medium to monitor the release of bound material. The concentrations and incubation times used for the different proteins are shown in Table I. All measurements were repeated at least twice. Affinity estimations were made using non-linear fits to the 'OneToOne', 'OneToOneDepletionCorrected' or the 'OneToTwo' interaction model in TraceDrawer 1.3 (Ridgeview Instruments AB).

Interaction Map analysis. The mathematical method Interaction Map (12,16) expresses the measured binding of a (homogeneous) ligand to a heterogeneous group of targets as a sum of interactions, each having a unique combination of the association rate constant k_a and dissociation rate constant k_d:

$$MeasuredCurve = \sum_{i=1}^{n} \sum_{j=1}^{m} \left[W_{ij} \text{ x } CurveComponent\left(conc, k_a^i, k_d^j\right) \right]$$

where *conc* is the concentration of protein in solution (the 'ligand') and W_{ij} is the weighing factor describing the contribution to the measured real-time interaction curve. The calculated contributing curves are represented as grayscale (black = large W_{ij}, white = small W_{ij}) peaks in an on-off plot. In this study, the Interaction Map method used 24 (k_a) x 30 (k_d) different nodes with kinetic parameter values evenly distributed in log-space ($\log10(k_a)$ = {2.00, 2.25, 2.50, ... , 7.25, 7.50, 7.75}, $\log10(k_d)$={-6.60, -6.40, -6.20, ... , -1.20, -1.00, -0.80}). A Tichonov-type regularization algorithm was employed, adding penalty to the sum-of-square residuals if there are many peaks in the Interaction Map. A similar algorithm has been presented previously (17) and has been applied to SPR-based real-time interaction analysis.

Table I. Concentrations and incubation times used in LigandTracer assays.

Protein	Label	First incubation	Second incubation	Third incubation	Retention measurement
Cetuximab	^{131}I	3 nM, 4-5 h	15 nM, 5-6 h	-	0 nM, ~5 h
Trastuzumab	^{125}I	1 nM, 2-3 h	4 nM, 2-3 h	7 nM, 2-3 h[a]	0 nM, ~5 h
$Z_{HER2:342}$	^{111}In	1 nM, 2-3 h	4 nM, 2-3 h	-	0 nM, ~5 h

In most assays, the binding protein was incubated at two different concentrations. [a]For ^{125}I-trastuzumab measurements on DU-145 and PC3 cells, a third concentration was applied as well.

Table II. Affinity values for the investigated protein-receptor interactions.

Targeting protein	Molecular target	Cell line	K_{D1} (pM)	Prevalence (%)	K_{D2} (nM)	Prevalence (%)
^{131}I-cetuximab	EGFR	A431	135±40	100	-	
^{131}I-cetuximab	EGFR	HaCaT	119±21	100	-	
^{131}I-cetuximab	EGFR	HEP-G2	≈10	100	-	
^{125}I-trastuzumab	HER2	SKOV3	100±50	100	-	
^{125}I-trastuzumab	HER2	PC3	90±50	~10	80±11	~90
^{125}I-trastuzumab	HER2	DU-145	120±100	~50	29±17	~50
^{111}In-$Z_{HER2:342}$	HER2	SKOV3	50±30	100		
^{111}In-$Z_{HER2:342}$	HER2	PC3	13±4	~15	10^{-8}	~85
^{111}In-$Z_{HER2:342}$	HER2	DU-145	46±5	~40	10^{-8}	~60

In cases where two affinities were derived for an interaction, the estimated relative prevalence is reported.

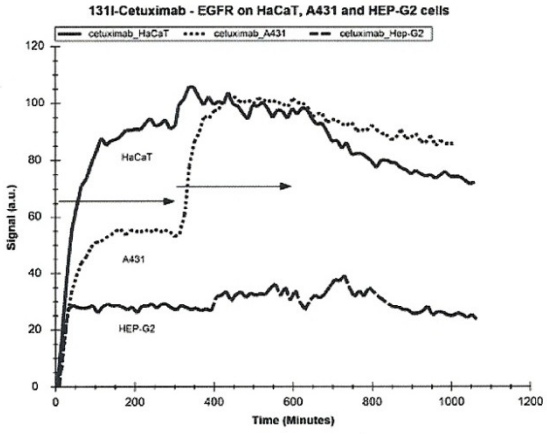

Figure 1. Binding curves representing ^{131}I-cetuximab interacting with EGFR on three different cell lines. ^{131}I-cetuximab was used at two different concentrations (indicated with two arrows); 3 nM for the initial 4-5 h, followed by 15 nM for another 5-6 h, followed by a wash-out measurement in pure cell culture medium (i.e. 0 nM ^{131}I-cetuximab). The signal levels from HaCaT and A431 were comparable, and HEP-G2 measurements resulted in significantly lower signal level. Curves have been scaled to enhance visibility.

Results

^{131}I-cetuximab - EGFR. Binding curves from ^{131}I-cetuximab interacting with A431, HaCaT and HEP-G2 cell lines are shown in Fig. 1. There were clear differences in how the ^{131}I-cetuximab binding progress in time. The results for the cell lines A431 and HaCaT may look different, but this difference is related to assay conditions. The large number of EGFR receptors per A431 cell ($2x10^6$/cell) (18) depletes the antibody-containing medium of unbound antibody, resulting in lower effective antibody concentration at equilibrium during the incubation of the lower concentration. Thus an interaction model that accounts for depletion of antibody is required for accurate analysis of data for A431. The interaction to HEP-G2 is very rapid (i.e. short time to reach equilibrium) and shows minor increase in signal when the concentration is elevated during the second incubation step. The HEP-G2 binding curves do not contain sufficient curvature for a detailed kinetics and affinity analysis. The estimated affinities for the interactions are provided in Table II.

^{125}I-trastuzumab - HER2. Binding curves from ^{125}I-trastuzumab interacting with HER2 on SKOV3, PC3, and DU-145 cell lines are shown in Fig. 2. The binding of ^{125}I-trastuzumab to HER2 on SKOV3 is slower than to HER2 on the other cell lines. When comparing signal magnitude, SKOV3 cells have approximately 2 orders of magnitude more HER2 receptors per cell than the others. The binding profiles of the three interactions are very different: ^{125}I-trastuzumab interacting with SKOV3 produced a monophasic binding profile, while as ^{125}I-trastuzumab interacting with HER2 on PC3 cells produced a biphasic profile. For DU-145, a weak biphasic profile was found. Therefore, SKOV3 results were analyzed using the OneToOne model

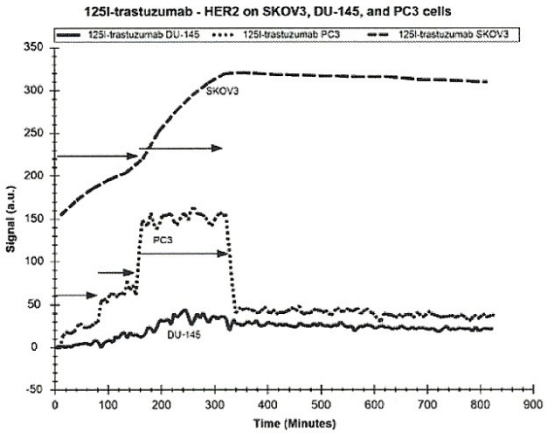

Figure 2. Binding curves representing ^{125}I-trastuzumab interacting with HER2 on three different cell lines. ^{125}I-trastuzumab was used at two different concentrations on SKOV3 (indicated with two arrows); first 1 nM for the initial 3 h, followed by 4 nM for another 3-4 h, followed by a wash-out measurement in pure cell culture medium. For PC3 and DU-145, three concentrations were used (indicated with three arrows); first two shorter incubations at 1 nM and 4 nM, followed by a 3 h incubation at 7 nM. Since the signal level from SKOV3 was 30-100 times higher than the signal levels from PC3 and DU-145, the curves have been scaled and moved to enhance visibility.

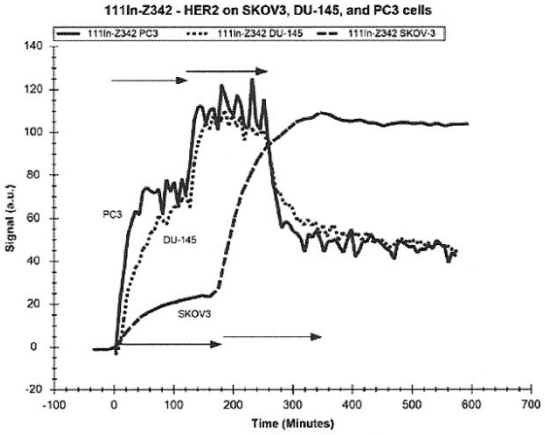

Figure 3. Binding curves representing ^{111}In-$Z_{HER2:342}$ interacting with HER2 on three different cell lines. ^{111}In-$Z_{HER2:342}$ was used at two different concentrations (indicated with two arrows); first 1 nM for the initial 2-3 h, followed by 4 nM for another 2-3 h, followed by a wash-out measurement in pure cell culture medium. For SKOV3 cells, longer incubation times were required as indicated with a separate set of arrows. The signal level from SKOV3 was ~10 times higher than the signal levels from PC3 and DU-145. The curves have been scaled to enhance visibility.

and the other two cell lines were analyzed using the biphasic OneToTwo model. The affinity values are presented in Table II. The binding properties of the single interaction to SKOV3 and the stronger interactions of PC3 and DU-145 are all similar.

^{111}In-DOTA-$Z_{HER2:342}$ - HER2. Binding curves from Affibody molecule ^{111}In- DOTA-$Z_{HER2:342}$ interacting with HER2 on PC3, DU-145, and SKOV3 cell lines are shown in Fig. 3. There are clear differences in how the ^{111}In-DOTA-$Z_{HER2:342}$ binding progress in time. The binding curves on PC3 and DU-145 are biphasic. The association rate of ^{111}In-DOTA-$Z_{HER2:342}$ to PC3 is higher than that to DU-145, but the affinity is approximately the same. For SKOV-3, the association rate is ~10 times slower as compared to PC3 and DU-145, and only one interaction seems to occur. The large number of HER2 receptors per SKOV-3 cell causes depletion (as described for the cetuximab measurements above) and thus a depletion-corrected analysis model was used. All estimated affinities are shown in Table II. The weaker interaction of PC3 and DU-145 was difficult to quantify, indicating that it is a weak interaction available but it is difficult to accurately estimate its properties.

Also in this case, the affinity of the ^{111}In-DOTA-$Z_{HER2:342}$ interaction with HER2 on SKOV-3 was close to the higher affinity of binding to PC3 and DU-145 cells. Of note, for both prostate cancer cell lines, the approximate prevalence of binding sites with lower affinity for ^{111}In-DOTA-$Z_{HER2:342}$ was similar to the prevalence for ^{125}I-trastuzumab.

To further illustrate the biphasic behavior of ^{111}In-Z342 interacting with HER2 on PC3 and DU-145, Interaction Maps were calculated (Fig. 4). Both interactions result in Maps with two distinct peaks, one representing a high-affinity event (the leftmost peaks A1 and B1) and another representing a weaker event (A2, B2). The affinities corresponding to the peaks are A1: 45 pM, A2: 3.2 nM, B1: 10 pM, B2: 3.1 nM.

Discussion

This study confirms the hypothesis that the binding strength (affinity) and binding kinetics of targeting proteins to a cell-surface HER-family receptor can be strongly dependent on the hosting cell line. This finding is corroborated by the observation by Björkelund *et al* (3) that binding of a natural ligand, EGR, is different to different EGFR-expressing cell lines. Furthermore, our findings are in agreement with data (obtained by classical Scatchard analysis) that affinities of HER2- and EGFR- targeting antibodies is dependent on the cell line (4,5). Thus, we issue a warning for transferring an affinity value measured on one cell line to other cell lines. We suggest that an affinity, which has been determined in a cell-based assay, should always be referred to together with the identity of the hosting cell line; otherwise the results may be misinterpreted and used in situations where they are not valid. The risk of the transferred affinity value being about one order of magnitude different is large, clearly for HER family receptors and potentially also for other receptor families.

To be more specific, for ^{131}I-cetuximab interacting with EGFR, there is a factor 10 in affinity difference across three cell lines. For ^{125}I-trastuzumab interacting with HER2, all three cell lines result in a strong interaction of approximately the same affinity (~100 pM), but two prostate cancer cell lines have clear biphasic behavior which is missing in the ovarian cancer cell line. Similarly, binding of ^{111}In- DOTA-$Z_{HER2:342}$ to HER2 shows clear difference in terms of interaction kinetics and in the degree of biphasic behavior. In any of these three cases, reporting the interaction characteristics from one of the

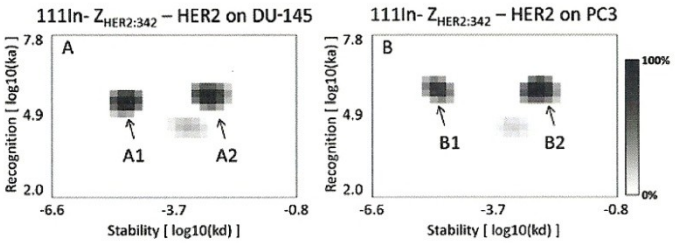

Figure 4. Interaction Maps illustrating the heterogeneity of the interactions of ^{111}In-$Z_{HER2:342}$ - HER2 on the cell lines DU-145 and PC3. For DU-145, two different interactions are visible, one stronger (A1) with an apparent affinity of 45 pM and one weaker (A2) with an apparent affinity of 3.2 nM. The two interactions A1 and A2 have a similar contribution to the total binding. For PC3, two interactions are visible, one stronger (B1) with an apparent affinity of 10 pM and one weaker (B2) with an apparent affinity of 3.1 nM. The weaker interaction B2 contributes more to the total interaction than the stronger interaction.

cell lines would typically not be representative for the other cell lines.

One potential origin of the observed differences is that the protein-receptor interactions on cells may be heterogeneous in a cell-dependent manner. Heterogeneity can have many underlying causes: The receptor on the cell may exist with different glycosylation patterns or as different isoforms, they may dimerize with themselves or with other receptors, or may be mutated to mention only a few possibilities. It is therefore understandable that the protein-receptor interaction in a cellular context may be very complex. This is illustrated in the Interaction Maps (Fig. 4) where ^{111}In- DOTA-$Z_{HER2:342}$ binding to HER2 on DU-145 and PC3 are depicted as two different events of very different affinities. What these two peaks represent is not known. It is previously shown that the EGF-EGFR interaction (12) is strongly dependent on the balance between receptor dimers and monomers, and this is a potential explanation also in this case.

The observed differences in binding profile open up for speculation on the biological origin of the heterogeneity. For ^{131}I-cetuximab-EGFR, the deviating cell line HEP-G2 is derived from liver and may have not only EGFR but also other less specific receptors for the capture and subsequent catabolism of circulating proteins. The observed interaction of ^{131}I-cetuximab with EGFR on HEP-G2 is however very strong, which is an argument against less specific receptors being part of the picture. In the case of HER2 expressing cells, there is a clear difference between the prostate cancer cell lines and SKOV3, both in terms of binding characteristics, and of the relative response to the two different proteins used in this study. As assessed using ^{125}I-trastuzumab, PC3 and DU-145 have a small amount of HER2 receptors with different binding characteristics compared to SKOV3. However, the binding of ^{111}In- DOTA-$Z_{HER2:342}$ to HER2 does not result in such large differences of receptor quantity, as evident from smaller difference in signal level across the three cell lines. PC3 and DU-145 both have signs of heterogeneity (similar for trastuzumab and $Z_{HER2:342}$), which is not seen on SKOV3. The origin of the differences is currently unknown, but trastuzumab and $Z_{HER2:342}$ are known to bind different receptor epitopes meaning that the Z342 epitope is more abundantly exposed. It is further known that SKOV3 expresses one order of magnitude more HER2 receptors than EGF receptors (18), while as PC3 and DU-145 have similar expression levels of the two receptors (15,19). Formation of HER2-EGFR dimers is a probable factor influencing the observed heterogeneity in this case.

In the development of therapeutic or diagnostic agents, protein interaction assays provide important decisive information during the initial phases. During protein selection in selection or screening processes, candidate proteins are chosen on their ability to bind the receptor in a variety of biophysical assays. These assays may produce perfectly accurate results for the environmental conditions they represent, but do the values reflect the interaction properties in the target environment, i.e. the living cell? Since this study indicates that interaction properties can vary one order of magnitude between different hosting cell lines, it would be advisable not to discard any strong binders when moving from biophysical assays to cell-based assays. It may be that strongest binders in the biophysical assays turn out to perform moderately on cells, and that the best binder in cells is found among those performing good, but not the best, in biophysical assays. We strongly believe that a poor binder in biophysical assays will also be poor in cell-based assays.

It is well known that there is a large variation in the efficacy of therapeutic and diagnostic agents in a population of patients. The ultimate goal would be personalized medicine, wherein the patient is first characterized with respect to probable response to a variety of treatments, and then provided the treatment most likely to be effective. Understanding the underlying cause of differences in the interaction of a therapeutic or diagnostic agent with the target protein in different cell lines is one of the first important steps. This study shows that the detection technology of today can accurately map the variation across cell lines in a far more detailed manner than manual incubate-wash-quantify assays, and potentially pave the way for more detailed characterization of patients prior to selecting treatment.

In conclusion, we confirm that the binding affinity of the same protein binding to HER-family receptors can vary one order of magnitude due to cellular context. Care is advised in transferring an affinity value measured on one cell line to other cell lines, and we suggest that an affinity should always be referred to together with the identity of the hosting cell line.

Acknowledgements

The authors thank Affibody AB, Stockholm, for providing ABY-025, and Apoteket Farmaci AB (Cytostatikaberedningen,

Sjukhusapoteket, Uppsala) for assistance in obtaining trastuzumab. The study was supported by the Grant Agency of the Czech Republic - grant No. P304/10/1738. We thank Dr Magnus Malmqvist for valuable comments on the manuscript. Ridgeview Instruments AB develops and manufactures the device LigandTracer. K.A. and J.S. are employed by Ridgeview Instruments AB, and K.A. is a shareholder of Ridgeview Instruments AB. The other authors have no conflict of interest.

References

1. Chinn DC, Holland WS, Yoon JM, Zwerdling T and Mack PC: Anti-tumor activity of the HSP90 inhibitor SNX-2112 in pediatric cancer cell-lines. Pediatr Blood Cancer: July 27, 2011 (Epub ahead of print).
2. Milenic DE, Wong KJ, Baidoo KE, Ray GL, Garmestani K, Williams M and Brechbiel MW: Cetuximab: Cetuximab: preclinical evaluation of a monoclonal antibody targeting EGFR for radioimmunodiagnostic and radioimmunotherapeutic applications. Cancer Biother Radiopharm 23: 619-631, 2008.
3. Björkelund H, Gedda L and Andersson K: Comparing the epidermal growth factor interaction with four different cell lines: intriguing effects imply strong dependency of cellular context. PLoS One 6: e16536, 2011.
4. Nestor M: Effect of cetuximab treatment in squamous cell carcinomas. Tumor Biol 31: 141-147, 2010.
5. Xu FJ, Yu YH, Bae DS, Zhao XG, Slade SK, Boyer CM, Bast RC Jr and Zalutsky MR: Radioiodinated antibody targeting of the HER-2/neu oncoprotein. Nucl Med Biol 24: 451-459, 1997.
6. Andersson K, Björkelund H and Malmqvist M: Antibody-antigen interactions: What is the required time to equilibrium? Available from Nature Precedings <http://hdl.handle.net/10101/npre.2010.5218.1>, 2010.
7. Björke H and Andersson K: Automated, high-resolution cellular retention and uptake studies in vitro. Appl Radiat Isot 64: 901-905, 2006.
8. Hynes NE and Lane HA: ERBB receptors and cancer: the complexity of targeted inhibitors. Nat Rev Cancer 5: 341-354, 2005.
9. Yarden Y and Sliwkowski MX: Untangling the ErbB signalling network. Nat Rev Mol Cell Biol 2: 127-137, 2001.
10. Marmor MD, Skaria KB and Yarden Y: Signal transduction and oncogenesis by ErbB/HER receptors. Int J Radiat Oncol Biol Phys 58: 903-913, 2004.
11. Citri A and Yarden Y: EGF-ERBB signalling: towards the systems level. Nat Rev Mol Cell Biol 7: 505-516, 2006.
12. Björkelund H, Gedda L, Barta P, Malmqvist M and Andersson K: Gefitinib induces epidermal growth factor receptor dimers which alters the interaction characteristics with ^{125}I-EGF. PLoS One 6: e24739, 2011.
13. Press MF and Lenz HJ: EGFR, HER2 and VEGF pathways: validated targets for cancer treatment. Drugs 67: 2045-2075, 2007.
14. Greenwood FC, Hunter WM and Glover JS: The preparation of ^{131}I-labelled human growth hormone of high specific radioactivity. Biochem J 89: 114-123, 1963.
15. Malmberg J, Tolmachev V and Orlova A: Imaging agents for *in vivo* molecular profiling of disseminated prostate cancer: Cellular processing of [^{111}In]-labeled CHX-A"DTPA-trastuzumab and anti-HER2 ABY-025 Affibody in prostate cancer cell lines. Exp Ther Med 2: 523-528, 2011.
16. Andersson K and Malmqvist M: Method for the analysis of solid biological objects. Patent application WO 2,010,033,069, 2008.
17. Svitel J, Balbo A, Mariuzza RA, Gonzales NR and Schuck P: Combined affinity and rate constant distributions of ligand populations from experimental surface binding kinetics and equilibria. Biophys J 84: 4062-4077, 2003.
18. Barta P, Björkelund H and Andersson K: Circumventing the requirement of binding saturation for receptor quantification using interaction kinetic extrapolation. Nucl Med Commun 32: 863-867, 2011.
19. Malmberg J, Tolmachev V and Orlova A: Imaging agents for *in vivo* molecular profiling of disseminated prostate cancer - targeting EGFR receptors in prostate cancer: comparison of cellular processing of [^{111}In]-labeled affibody molecule $Z_{EGFR:2377}$ and cetuximab. Int J Oncol 38: 1137-1143, 2011.

V. A COMPARISON OF IN VITRO METHODS FOR DETERMINING THE MEMBRANE RECEPTOR EXPRESSION IN CELL LINES

Novy Z, **Barta P**, Mandikova J, Laznicek M, Trejtnar F: A comparison of in vitro methods for determining the membrane receptor expression in cell lines. Nucl Med Biol. 2012 Apr; [Epub ahead of print].

Elsevier Editorial System(tm) for Nuclear Medicine and Biology
Manuscript Draft

Manuscript Number: NUCMEDBIO-D-11-00272R2

Title: A comparison of in vitro methods for determining the membrane receptor expression in cell lines

Article Type: Research Paper

Corresponding Author: Assoc. Prof. Frantisek Trejtnar,

Corresponding Author's Institution:

First Author: Zbynek Novy, M.D.

Order of Authors: Zbynek Novy, M.D.; Pavel Barta, M.D.; Jana Mandikova, M.D.; Milan Laznicek, Prof.; Frantisek Trejtnar, Assoc.Prof.

Abstract: Introduction: Determining the number of expressed receptors per cell (NRPC) in cell lines is an important prerequisite for many experimental procedures in biomedical research. This paper focuses on the comparison of a newly developed method of determining NRPC - the Kinetic extrapolation method (KEX) - with the standard saturation method. These two methods, both based on radiolabeled ligand-receptor binding, were compared with the data on receptor expression found using quantified western blotting.
Methods: Four cell lines with different expressions of epidermal growth factor receptor (EGFR) were chosen for the experiment: A431, HaCaT, HCT116 and HepG2. Two radiolabeled monoclonal antibodies specific for EGFRs were used as ligands: [131I]-cetuximab and [131I]-panitumumab. The classic manual technique based on the saturation of cell receptors was performed on cells seeded in 24-well plates. The KEX method uses the LigandTracer, a special instrument which detects ligand retention in real time from seeded cells onto a rotating Petri dish. The western blot analysis was performed according to the routinelly used procedure.
Results: A very close accordance between the manual saturation technique and the KEX method was found in all four cell lines used. The NRPC in the cell lines follows the same order using both ligands: A431>HaCaT>HCT116~HepG2. Similarly, consistent data on EGFR expression in the studied cell lines were obtained using western blot analysis and the radiolabeled ligand binding assays.
Conclusions: The KEX method could be as similarly useful for determining receptor expression as is the classic saturation method and western blotting.

1. Introduction

Cell lines are used extensively in biomedical research and drug development as in vitro models for normal or cancerous tissues. The validity of the data obtained in such experiments depends on the quality of the cell line, particularly when it is being used as a surrogate for the tissue of origin [1]. However, the typical parameters of cell lines may change due to range of factors and the authentic characteristics may be lost. Until recently, this issue has received little attention. Several methods are available for the characterization of cell lines, such as isoenzyme analysis, karyotyping, HLA-typing, DNA fingerprinting and immunological approaches. However, the data produced by these methods have not been sufficiently reproducible among laboratories [1]. A common type of measurement in biology and biochemistry, pharmacology, cancer research and drug discovery is the assessment of ligand-receptor interactions. For such type of experimental studies, one crucial cellular parameter which must be defined is the expression of intended receptors in the cell lines. As the number of receptors may change due to a variety of factors, the continuous inspection of the receptor expression in the used cells during passage is necessary. The increasing study of new biological drugs such as peptides, monoclonal antibodies and antibody fragments is likely to increase interest in quick and inexpensive in vitro methods of describing receptor expression in cell lines. Thus, determining the number of expressed receptors per cell (NRPC) has become a relatively important technique for biomedical research in general and especially in oncology.

To evaluate membrane receptor expression, researchers frequently use the methods based on the interaction between specific radiolabeled receptor ligands and the cells expressing the receptor being studied. To determine NRPC, the standard saturation method known as the classic manual technique is commonly utilized. This method uses a ligand

which interacts with the target receptors at concentrations sufficiently high to saturate the receptor population on the cells [2; 3]. Recently, an alternative method for obtaining NRPC called the Kinetic extrapolation method (KEX) has been published [4]. KEX uses real-time detection by an instrument called the LigandTracer® (Ridgeview Instruments AB, Uppsala, Sweden). Of course, several other methods based on different procedures, may be used to characterize the expression of the receptor of interest on the cellular membrane. Alternatively, the amount of the receptors may be determined using methods such as immunoblotting or flow cytometry [5, 6]. A comparison of the results obtained by the above mentioned methods in one laboratory using the same cellular models may be useful to evaluate the reliability and validity of these techniques. In addition, possible advantages and disadvantages may be more closely observed under such conditions.

Our work focused on a comparison of three techniques used to evaluate the amount of selected receptors on the cellular membrane. In the first step, we compared two methods based on radiolabeled ligand-receptor binding, the standard saturation method and the Kinetic extrapolation method. As radioactive ligands ^{131}I-labeled monoclonal antibodies were used. The results obtained using these procedures were compared with quantified western blotting analysis in the second step. As a model receptor, the epidermal growth factor receptor (EGFR) was chosen. This receptor is overexpressed in various types of tumors and is also a target structure for antitumor monoclonal antibodies [7]. The study was performed *in vitro* on four cell lines (A431, HaCaT, HCT116, HepG2) expressing various amount of EGRF receptors, with two monoclonal antibodies ([^{131}I]-cetuximab and [^{131}I]-panitumumab) being used as EGFR ligands.

2. Materials and methods

2.1. Cell cultures

Four different cell lines expressing EGFR were chosen for the experiment – A431, HaCaT, HCT116 and HepG2. The human squamous carcinoma cell line A431 (CLR 1555, ATCC, Rocksville, MD, USA) was cultured in Dulbecco's Modified Eagle's Medium (Sigma-Aldrich) supplemented with 10% fetal bovine serum (Sigma-Aldrich). The human keratinocyte cell line HaCaT (DKFZ, Heidelberg, Germany) was cultured in Dulbecco's Modified Eagle's Medium supplemented with 10% fetal calf serum (Sigma-Aldrich) and 2 nM L-glutamine (Sigma-Aldrich). The human colorectal carcinoma cell line HCT116 (CCL-247, ATCC, Rocksville, USA) was cultured in McCoy's 5a Medium Modified (Sigma-Aldrich) with 10 % fetal bovine serum (Sigma-Aldrich) and 5 % L-glutamin (Sigma-Aldrich). The hepatocellular carcinoma cell line HepG2 (HB-8065, ATCC, Rocksville, USA) was cultured in Eagle's Minimum Essential Medium (Sigma-Aldrich) with 10% fetal bovine serum (Sigma-Aldrich). The cultivation for the purposes of the KEX method was performed in Petri dishes (NuclonTM, dish size 100x20, NUNC A/S, Roskilde, Denmark). The cells were seeded on the entire surface of petri dish, with one third of the cells removed by special scraper (Corning) just before the experiment. In the case of the manual saturation technique the cells were seeded in 24-well plates (NuclonTM, 24-wells plate, NUNC A/S, Roskilde, Denmark). The cells were grown in 37 °C, in a humidified atmosphere of 5% CO2.

2.2. Ligands and radiolabeling

Two monoclonal antibodies were chosen as EGFR ligands – cetuximab and panitumumab. Cetuximab (IMC-C225, Erbitux®, Merck) is a chimeric mouse-human monoclonal antibody targeted against EGFR. As an inhibitor of EGFR cetuximab is already used to treat colorectal

cancer as well as cancer of the head and neck [8]. Panitumumab (Vectibix®, Amgen) is a fully human monoclonal antibody used in the treatment of patients with colorectal cancer [9]. These two antibodies were labeled with iodine-131 (Perkin-Elmer, USA) via the chloramite-T protocol [10]. In brief, 20 MBq of a iodine sodium solution was mixed with 200 μg of monoclonal antibody and 20 μl of chloramine T (4 mg/ml, Sigma-Aldrich). The mixture was then incubated on ice for 10 minutes, then the reaction was stopped by the addition of 40 μL of $Na_2S_2O_5$ (4 mg/l, Sigma-Aldrich). Four radioiodinations were done for each antibody. Antibodies were labeled with specific activity of 100 MBq/mg of protein. Average radiochemical yield for cetuximab was 90.3 ± 4.2% and 52.0% ± 3.0% for panitumumab, respectively. The labeled antibody was separated on a Sephadex column PD-10 (GE Healthcare). Radiochemical purity was verified by instant thin layer chromatography (ITLC-SG, Varian, USA). Average radiochemical purity was 97.1 ± 1.5% for cetuximab and 98.3% ± 1.2 for panitumumab, respectively. Saline was used as the mobile phase for ITLC-SG. The quality of the final product was verified also by HPLC using 0.05M NaCl as mobile phase (flow rate 0.8 ml/min), BioRad Gel column BIO-Sil Sec 250, 300x7.8 mm and radiometric detection. The retention times were 9.7 min for both labeled antibodies while free iodine peak had the retention time of 13.2 min. The stability of radiolabeled cetuximab and panitumab in appropriate cell culture media at 37 °C was tested with following results (mean ± S.D.): radiochemical purity was 95.1 ± 1.6% in case of cetuximab and 96.5% ± 2.0% in case of panitumumab, respectively, after 24 hours of incubation.

2.3. Western blot analysis

The cells were lysed using a lysis buffer containing 0.5% SDS and 10 mmol/L Tris/HCl, pH 7.4; the mixture was supplemented with 0.5 μg/mL leupeptin (SERVA, Germany), 2 μg/mL aprotinin (SERVA, Germany), 50 μg/mL benzamidine (SERVA, Germany), and 40 μg/mL

PMSF (SERVA, Germany). The homogenate was centrifuged at 6,000*g* for 10 minutes at 4°C. The protein content of the supernatants was determined by the BCA method using the Thermo Scientific Pierce BCA Protein Assay Kit (Thermo Scientific, USA). Protein extracts were separated by sodium dodecyl sulfate-polyacrylamide gel electrophoresis (SDS-PAGE) for EGFR and for the protein loading control β-actin on a 10% gel (5 μg protein/lane) on a Power Pac HC apparatus (Bio Rad, UK). Proteins were electrotransferred onto a polyvinilidene (PVDF) membrane (Sigma - Aldrich, USA). Transfers of proteins were checked routinely by staining the membrane with Ponceau S solution (SERVA, Germany). The proteins were blocked for one hour at room temperature with 5% low-fat dried milk (Bio-Rad, UK) in a Tris-buffered saline solution containing 0.05% Tween 20 (TBST). For immunoblotting, the antibodies were dissolved in a TBST buffer with 5% low-fat dried milk. The membrane was immunoblotted overnight with a monoclonal anti epidermal-growth factor receptor antibody produced in mouse clone F4 (Sigma - Aldrich, USA) at dilution 1:100 or monoclonal anti-β-actin antibody produced in mice at dilution 1:2000, then washed four times with a TBST buffer. Detection was performed for 1 hour with anti-mouse IgG (Fab specific) – a peroxidase conjugated antibody at 1:8000 dilution for EGFR and β-Actin (Sigma - Aldrich, USA). After washing the membrane four times with a TBST buffer, chemiluminiscence was developed using the reagent SuperSignal West Femto Chemiluminescent Substrate (Thermo Scientific, USA) for EGFR, and SuperSignal West Pico Chemiluminescent Substrate (Thermo Scientific, USA) for β-Actin. The immunoreactive bands on the X-ray films (FOMA Bohemia, Czech Republic) were scanned with calibrated the CCD Image Quant 400 camera (GE Healthcare, Sweden), then evaluated using NIS elements software, version 3.22 (Laboratory Imaging Prague, Czech Republic). [11]

2.4. The manual saturation technique

For this method the cells were seeded in triplicates in 24-well plates. The experiment was performed after reaching a confluence of about 80%. The media was removed, the cells washed with PBS and the media in six various concentrations of ^{131}I-labeled ligand (0.5, 1.5, 5, 15, 50 and 150 nM; 0.5 ml/well) was added to the cells. An incubation at 4 °C for 4 hours proceeded, followed by six washes of the cells in a serum-free culture medium. Then the cells were trypsinised, counted and radioactivity was measured with an automatic gamma counter (1480 Wizard™, Perkin Elmer, USA) to determine the receptor number.

2.5. The kinetic extrapolation method (KEX)

The ligand retention on each appropriate receptor was measured in real-time by a LigandTracer Yellow (Ridgeviews Instruments AB, Uppsala, Sweden) at room temperature. The cells were seeded into Petri dishes and cultured until the confluence reached cca 80%. Then one third of the cells were removed by a cell scraper to provide a reference point for the measurement. The cells were washed with PBS, and 5ml of full media was added to the dish for the experiment. During the first 10 minutes of measurement without the added ligand the baseline of background was set; this was followed by the three-step addition of a labeled ligand to reach concentrations of 3, 15 and 30 nM. The incubation times for each step were chosen individually according to the point of saturation shown by the accumulation curve. When the assay was finished, the cells were washed once in bovine serum albumin solution in PBS (1% w/v) and once with PBS. Then they were trypsinized, counted and radioactivity was measured (Automatic gamma counter 1480 Wizard™, Perkin Elmer, USA). Each cell line and ligand combination was tested five times. The binding curves measured by the Ligand Tracer Yellow were fitted to a bivalent kinetic model in TraceDrawer 1.2 (Ridgeviews Instruments AB, Uppsala, Sweden) [12].

3. Results

An overview of the results in A431, HaCaT, HCT116 and HepG2 cells for the manual method is shown in Fig. 1 and for the KEX method in Fig. 2.

The found average NPRC for each cell line using manual saturation technique and [^{131}I]-cetuximab was as follows: A431 – 1.65*10^6 EGFR/cell, HaCaT – 0.87*10^6 EGFR/cell, HCT116 – 0.22*10^6 EGFR/cell and HepG2 – 0.08*10^6 EGFR/cell. The following average NPRC for each cell line using manual saturation technique and [^{131}I]-panitumumab was obtained: A431 – 1.99*10^6 EGFR/cell, HaCaT – 0.67*10^6 EGFR/cell, HCT116 – 0.14*10^6 EGFR/cell and HepG2 – 0.16*10^6 EGFR/cell.

The found average NPRC for each cell line using the KEX method and [^{131}I]-cetuximab was as follows: A431 – 1.84*10^6 EGFR/cell, HaCaT – 0.91*10^6 EGFR/cell, HCT116 – 0.13*10^6 EGFR/cell and HepG2 – 0.07*10^6 EGFR/cell. The following average NPRC for each cell line using the KEX method and [^{131}I]-panitumumab was obtained: A431 – 1.93*10^6 EGFR/cell, HaCaT – 1.06*10^6 EGFR/cell, HCT116 – 0.20*10^6 EGFR/cell, and HepG2 – 0.19*10^6 EGFR/cell.

The quantified data on EGFR protein expression in A431, HaCaT, HCT116, and HepG2 cells obtained by western blot analysis are presented in Fig. 3. The data obtained by KEX method and manual saturation technique were analyzed using one-way ANOVA test combined with Bonferonni post-hoc test. The analysis showed that the differences in mean values of NRPC between four tested cells lines are significant with exception of HCT116 and HepG2 for both ligands.

4. Discussion

The amount of receptors of interest expressed in the biological membranes is a very significant parameter, one which has been evaluated in various types of biological and pharmacological studies. The cell lines commonly used as in vitro models in biomedical experimental studies can be unintentionally swapped, contaminated or mutated. Any of these occurrences may result in variations in different cellular parameters including the number of intended receptors. Thus, verification of receptor expression in the cells under study should be a routine procedure during experimental procedures to eliminate possible errors and limit incorrect conclusions. Such examination, however, should be as effective, time-consuming and reliable as possible. With these goals we sought to compare selected, potentially useful methods to determine the expression of a model receptor in cell lines.

The expression of receptors may be determined by several methods. We compared a new automatized procedure with the classic manual method of assessing receptor expression as well as with a method based on immunoblotting. Whereas the standard saturation method and western blotting are considered well-known and well-described methods, the Kinetic extrapolation method using the LigandTracer has been developed relatively recently [13, 14]. With its special rotating dish, this apparatus has been successfully applied in the measurement of the affinity of radioligands to the cell-surface receptors of intact cancer cells [14]. When using an appropriate radioligand the instrument can be also successfully used to determine in vitro cellular retention and uptake [13], especially in case of radiolabeled monoclonal antibodies [3]. Results have recently been published describing semi-automated real-time

measurement using LigandTracer technology to analyze membrane-protein expression in tissue sections [15].

Our results showed a very close accordance between the manual saturation technique and the KEX method in all four cell lines used. In addition, western blot analysis confirms that the measured values of NPRC for EGFR are correct. To exclude possible bias in the evaluation of the results of western blot analysis, a quantification of the blots was performed. The differences in the quantity of receptor protein found by immunoblotting may be considered, therefore, to be relatively objective and reliable. However, western blot showed accordance with other techniques only in the sense of relative order of studied cell lines. Blotting techniques are principally semi-quantitative and full objectification may be difficult to be reached. Western immunoblotting has rarely been used as a quantitative gold standard in targeted probe design. The gold standard in determining NRPC is still the manual technique that is used for a very long time.

KEX measurements contained time resolved measurement of the binding during incubation at three different concentrations (3 nM, 15 nM and 30 nM). We denote the measurement during incubation "association phase". It is in certain cases possible to continue measuring after incubation by replacing the incubation liquid with plain cell culture medium, such a measurement we denote "dissociation phase". As shown by Nakajima and coauthors [16], the shape of the bivalent binding curve during association phase is determined by four different kinetic constants: kon1, koff1, kon2, koff2. This means that it is possible to extract all kinetic and affinity parameters and the Bmax from only an association measurement, provided that the data contains sufficient curvature. The precision would be better if a dissociation measurement is also conducted, but in the KEX assay that is impossible. The analytical program TraceDrawer 1.2 uses a numerical integrator to calculate theoretical bivalent binding curves and a non-linear fitting algorithm to fit the kinetic constants kon1,

koff1, kon2, koff2 and Bmax to match the measured data. In this way, all kinetic constants and the Bmax can be estimated through use of only one association phase, provided it contains different concentrations and results in clear curvature in the binding trace. For KEX method we use only estimated Bmax value.

We can conclude that the KEX method is an equivalent method for determining NPRC as compared to the classic saturation technique, thus may be an effective tool in biological research. A drawback seems to be a relative high initial investment to purchase the LigandTracer apparatus. On the other hand, as Barta et al. [4] has showed that the time of lab-work needed and the demand of disposable cell culture dishes and media by the KEX method was reduced by approximately 60% and 90%, respectively, compared to the classical saturation technique. The method requires only a fraction of the reagents, cells and working time in comparison to a manual protocol. The KEX method is versatile, and may be used to determine NRPC for other types of receptors besides EGFRs, e.g. somatostatin (SST) and cholecystokinin/gastrin (CCK), and in general all receptors expressed onto a cell membrane with a known ligand that can be radiolabeled.

According to the results obtained, the use of the novel KEX methods seems to be beneficial. Beside the previously mentioned advantages, the KEX method limits radiation exposure to the laboratory staff to a minimum in comparison with the manual technique [13]. However, the KEX method has several limits. The rotating technique is designed only for adherent cells not for suspensions. The potentially useful cells need to be sufficiently adherent to withstand the rotation of the cell dish [13]. This could preclude the use in some cases, since some cell lines are only available as suspension culture. The possible evaporation of cell culture medium during the course of the experiment may also be a problem in long-term studies. In our experiments the incubation interval was a maximum of four hours. Since

proper functionality has been proved for an operational interval of up to 48 h [13], this issue was not relevant for our study.

In our experiments we used the type of the LigandTracer Yellow constructed not only for detection of iodine-131. This apparatus is able to measure radioactivity of other gamma emmitors, so various ligands labeled with technecium-99m, indium-111, or other convenient radiolabels are acceptable for these types of studies. In addition, other types of LigandTracer instrument with different type of detectors are available. Thus labeling is not limited only to gamma emmitors -- beta-emmitors or fluorescently labeled ligands could be also used to evaluate receptor expression.

5. Conclusions

The KEX method could be just as useful in the determination of receptor expression as the classic saturation method and western blotting. The comparison of the two methods based on receptor-ligand interaction demonstrated a very close similarity regarding the data obtained on the expression of EGFR in the selected cell lines. However, the ligand consumption and work load was substantially lower in case of the KEX method. The reliability of the methods used was confirmed by the general agreement found between both the KEX and saturation methods as well as western blotting. Because of its reliability and effectiveness, the KEX method may be useful in the evaluation of the expression of other types of membrane receptors in the future. And also the described methods could be important in studies on the change in receptor density within culturing time and the different number of passage in a single laboratory.

Acknowledgements

The project was supported by the Grant Agency of Charles University in Prague grant No. 124409/C, by project SVV No. 263 003, and by Grant Agency of the Czech Republic grant No. P304/10/1738. The authors would like to thank Karl Andersson from Uppsala University, Sweden for valuable comments on the manuscript.

References

[1] Masters JRW. Cell line misidentification: the beginning of the end. Nat Rev Cancer 2010;10(6):441-8

[2] Hulme EC, Trevethick MA. Ligand binding assays at equilibrium: validation and interpretation. Br J Pharmacol 2010;161:1219-37

[3] Nestor M, Andersson K, Lundqvist H. Characterization of 111In and 177Lu-labeled antibodies binding to CD44v6 using a novel automated radioimmunoassay. J Mol Recognit 2008;21(3):179-83

[4] Barta P, Björkelund H, Andresson K. Circumventing the requirement of binding saturation for receptor quantification using interaction kinetic extrapolation. Nucl Med Commun 2011;32:863-7

[5] Brotherick I, Lennard TW, Wilkinson SE, Cook S, Angus B, Shenton BK. Flow cytometric method for the measurement of epidermal growth factor receptor and comparison with the radio-ligand binding assay. Cytometry 1994;16(3):262-9

[6] Hanna W. Testing for HER2 status. Oncology 2001; 61 Suppl, 22-30

[7] Lurje G, Lenz HJ. EGFR Signaling and Drug Discovery. Oncology 2009;77:400-410

[8] Delbaldo C, Pierge JY, Dieras V, Faivre S, Laurence V, Vedovato JC. Pharmacokinetic profile of cetuximab (Erbitux™) alone and in combination with irinotecan in patiens with advanced EGFR-positive adenocarcinoma. Eur J Cancer 2005;41:1739-1745

[9] Bernardi R, Onofri A, Pistelli M, Maccaroni E, Scartozzi M, Pierantoni C. Panitumumab: the evidence for its use in the treatment of metastatic colorectal cancer. Core Evidence 2010;5:61-76

[10] Greenwood FC, Hunter WM, Glover JS. The preparation of ^{131}I-labelled human growth hormone of high specific radioactivity. Biochem J 1963;89:114

[11] Song JY, Lee SW, Hong JP, Chang SE, Choe H, Choi J. Epidermal growth factor competes with EGF receptor inhibitors to induce cell death in EGFR-overexpressing tumor cells. Cancer Lett 2009;283: 135-142

[12] Björkelund H, Gedda L, Andersson K. Avoiding false negative results in specificity analysis of protein-protein interactions. J Mol Recognit 2011;24(1):81-9

[13] Björke H, Andersson K. Automated, high-resolution cellular retention and uptake studies in vitro. Appl Radiat Isot 2006;64(8):901-5

[14] Björke H, Andersson K. Measuring the affinity of a radioligand with its receptor using a rotating cell dish with in situ reference area. Appl Radiat Isot 2006;64(1):32-7

[15] Gedda L, Björkelund H, Andersson K. Real-time immunohistochemistry analysis of embedded tissue. Appl Radiat Isot 2010;68(12):2372-6

[16] Nakajima H, Kiyokawa N, Katagiri YU, Taguchi T, Suzuki T, Sekino T. Kinetic Analysis of Binding between Shiga Toxin and Receptor Glycolipid Gb3Cer by Surface Plasmon Resonance. J Biol Chem 2001;276(46):42915–42922

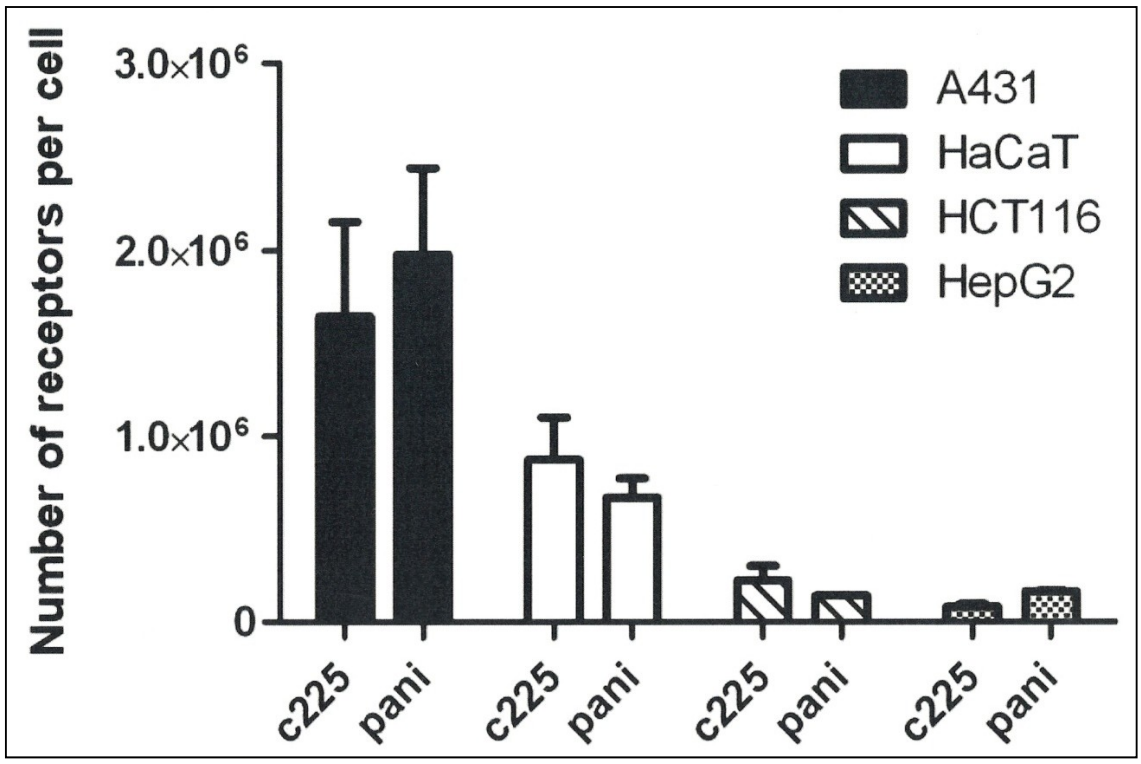

Fig. 1 The NRPC (EGFR) obtained by manual saturation technique, expressed in number of EGFR per cell for each cell line (c225 ´cetuximab, pani = panitumumab), x ± S.D., n=5

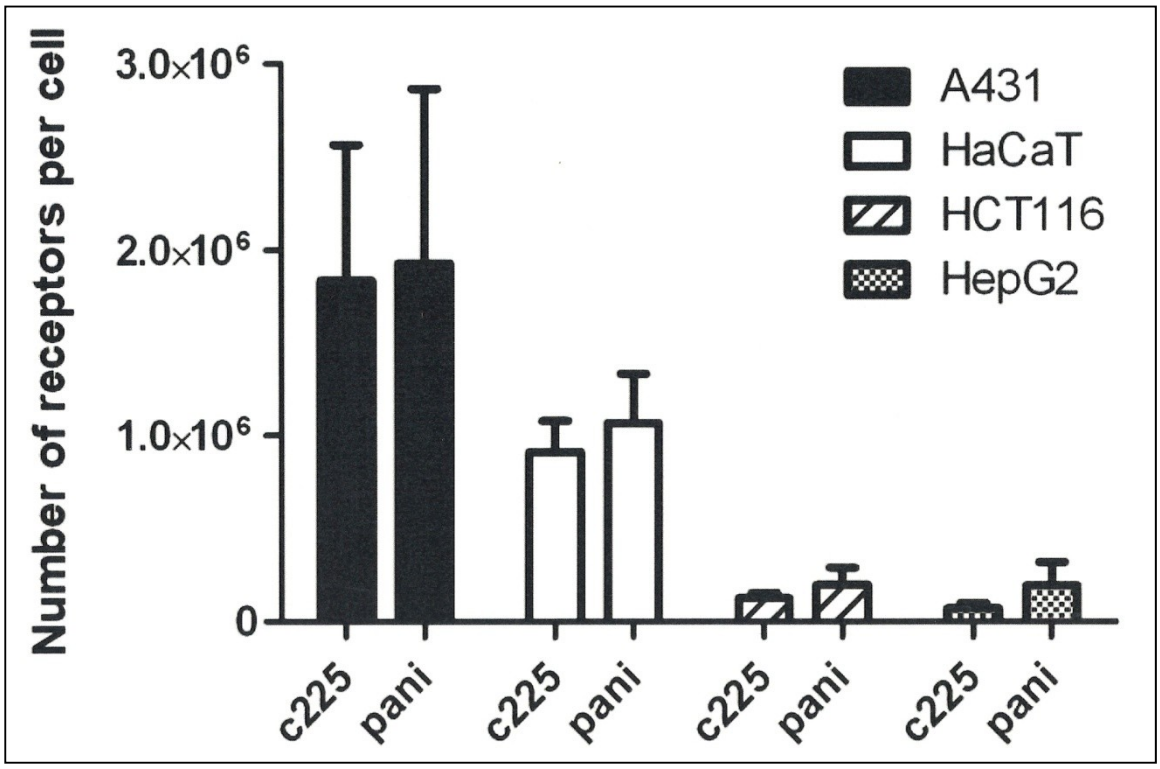

Fig. 2 The NRPC (EGFR) obtained by KEX method, expressed in number of EGFR per cell for each cell line (c225 = cetuximab, pani = panitumumab), x ± S.D., n=5

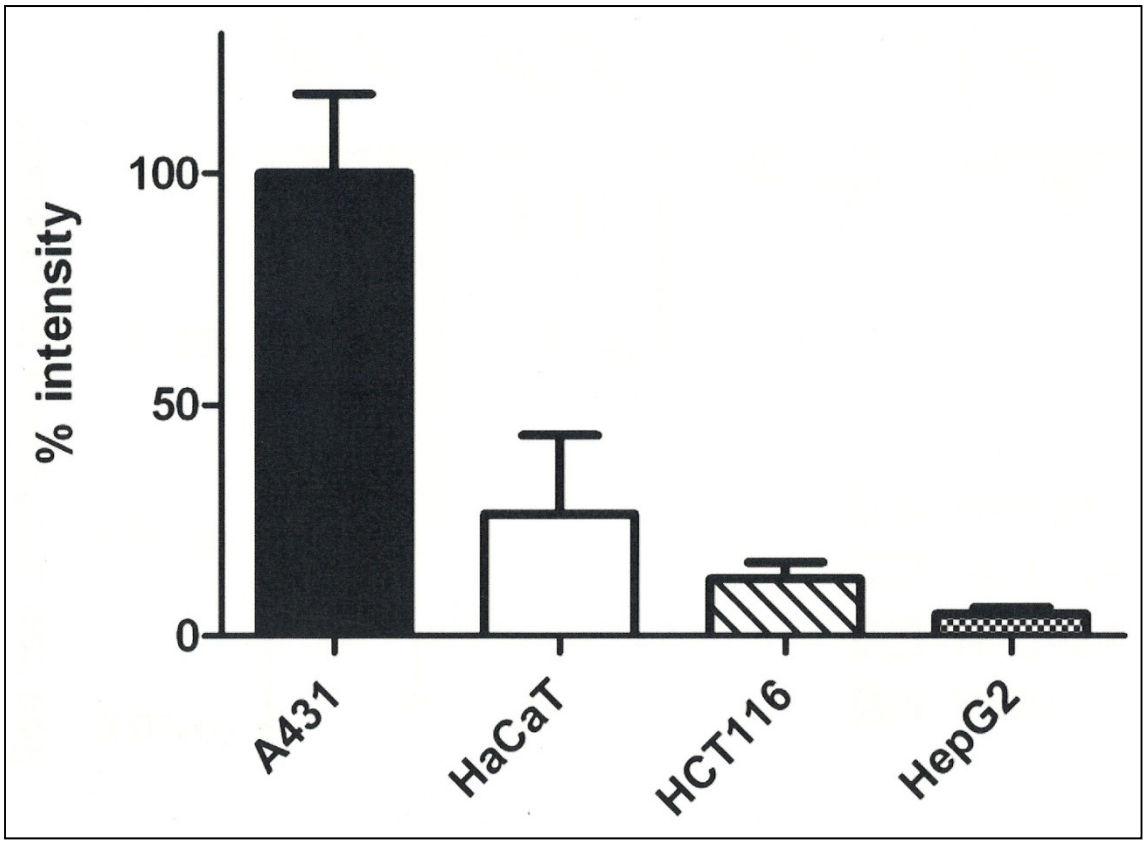

Fig. 3 Quantification of EGFR in four cell lines, obtained by NIS elements software, version 3.22

VI. THE PRECLINICAL EVALUATION OF RADIOLABELLED NIMOTUZUMAB, THE PROMISING MONOCLONAL ANTIBODY TARGETING THE EPIDERMAL GROWTH FACTOR RECEPTOR

Barta P, Laznickova A, Laznicek M, Beckford Vera DR, Beran M: The preclinical evaluation of radiolabelled nimotuzumab, the promising monoclonal antibody targeting the epidermal growth factor receptor. J Labelled Comp Radiopharm; [Under review].

The preclinical evaluation of radiolabelled nimotuzumab, the promising monoclonal antibody targeting the epidermal growth factor receptor

Authors:

Pavel Barta [1,*], Alice Laznickova[2], Milan Laznicek[1], Denis Rolando Beckford Vera[3] and Milos Beran[3]

[1] Department of Pharmacology and Toxicology, Faculty of Pharmacy in Hradec Kralove, Charles University in Prague, Czech Republic
[2] Department of Biophysics and Physical Chemistry, Faculty of Pharmacy in Hradec Kralove, Charles University in Prague, Czech Republic
[3] Department of Radiopharmacy, Nuclear Physics Institute of the Academy of Sciences, Husinec – Rez, Czech Republic
[*] Corresponding author: email address: Pavel.Barta@faf.cuni.cz; Institution: Faculty of Pharmacy in Hradec Kralove, Department of Pharmacology and Toxicology; Postal address: Heyrovskeho street 1203, Hradec Kralove, ZIP code: 50005; Phone: 00420-495-067-450; Fax: 00420-495-518-002

Keywords: EGFR, Iodine, Lutetium, Nimotuzumab, Radioimmunotherapy

Abstract

Background: Radiolabelled monoclonal antibodies with affinity towards tumour-associated antigens may enhance the effectiveness of cancer treatment in targeted radiotherapy. The humanised monoclonal antibody nimotuzumab represents a promising vector to deliver radioactivity to tumours that are overexpressing epidermal growth factor receptor type 1 (ErbB1). This paper analyses the effect of radiolabelling nimotuzumab on the uptake of the antibody to cancer cells that have a high density of ErbB1 and on the biodistribution profile of the labelled antibody in preclinical experiments.

Methods: Nimotuzumab was labelled with ^{131}I by oxidative iodination and with ^{177}Lu using nimotuzumab conjugates with two different chelators (DTPA and DOTA) and two different spacers. For the receptor studies, two cell lines (HaCaT and A431) were used. Biodistribution studies were performed on male Wistar rats.

Results: The choice of radiolabel and the manner of its attachment to nimotuzumab had little effect on the antibody internalization ability to the ErbB1-expressing cell lines. However, the selection of radiolabel, the way in which it was attached to nimotuzumab and the radiolabelling procedure significantly affected blood clearance, liver uptake and liver persistence of radiolabelled nimotuzumab.

Introduction

Radiolabelled monoclonal antibodies (MAb) and their fragments that have an affinity towards tumour-associated antigens can be used as a delivery system to target radiotracers to tumour cells for diagnostic and therapeutic purposes. This approach is particularly effective in targeting tumours present at distant sites or that are inoperable, i.e., where surgical resection is limited or impossible. The use of radiolabelled MAbs may enhance the effectiveness of cancer treatment, and the selective delivery of radioactivity to tumour sites could improve its efficacy and reduce toxic side effects in healthy organs. One of the most promising targets in cancer-specific radioimmunotherapy is the family of epidermal growth factor receptors (EGFRs).

Solid tumours expressing receptors for the epidermal growth factor are linked to poor patient survival and/or a more advanced disease stage [14; 23]. For these reasons, tumours expressing EGFRs have been a focal point in the development of anticancer therapies since 1980 [13; 14].

The epidermal growth factor receptor is a tyrosine kinase receptor, which regulates cell growth, lineage determination, cell repair and functional differentiation in normal cells [20]. The family of EGFRs are grouped into four types, including: ErbB1 (also known as EGFR), ErbB2, ErbB3 and ErbB4. EGF receptor function is activated by several ligands naturally produced in the body, such as EGF, TGFα, HB-EGF, amphiregulin, betacellulin and epiregulin [15; 18; 22; 24].

The interaction of the ligand with the extracellular binding domain of the receptor triggers a cascade of kinase activity (TK) leading to gene transcription and cell proliferation or differentiation [3; 24; 25]. These physiological processes also occur in tumour cells in solid tumours, for example in non-small cell lung cancer (NSCLC) and bladder, pancreatic, gastric, colorectal, prostate, breast, ovarian, head and neck cancers. Solid tumour cells over-expressing EGFRs, mainly of the ErbB1 subtype, are characterised by increased proliferation, angiogenesis and tumour cell invasion and decreased apoptosis [14; 17; 21; 23].

The EGFR tumour anticancer strategy is focussed on the generation of tyrosine kinase inhibitors (TKIs) or monoclonal antibodies (MAbs). These anti-EGFR agents can be used either in monotherapy or, preferably, in combination with standard chemotherapy or radiation treatment [13; 14].

Anti-EGFR monoclonal antibodies either inhibit EGFR-ligand interactions or hinder receptor dimerisation. In both cases, EGFR receptor activation is prevented, and programmed cell death is activated [13; 14]. Another use of MAbs is in the delivery of a toxin or radioisotope to tumour cells. This latter strategy is used to target MAbs specifically to tumour cells in radiotherapy and thus reduce the radiotoxicity burden on patients [2].

In this study, we analysed the *in vivo* biodistribution profiles of radiolabelled nimotuzumab (hR3) in rats and the uptake of radiolabelled nimotuzumab to tumour cells. The hR3 antibody is a humanised anti-EGFR monoclonal antibody, subtype IgG1. This novel antibody lacks some of the common side effects observed with other monoclonal antibodies, such as the development of an acneiform rash. Due to the good tolerance of hR3, which has already been approved in Phase I, II and III trials for some tumour-types, such as brain malignancies and squamous cell carcinoma of the head and neck (SCCHN), it has been approved for marketing in 27 countries [5; 9; 19; 26]. *In vitro* studies were performed on the immortalised human cancer cell line, A431 (human squamous carcinoma cells) and the HaCaT cell line (human keratinocyte), both of which express a high amount of the ErbB1 receptor

The hR3antibody was labelled with two isotopes: ^{131}I or ^{177}Lu. The isotope ^{131}I was either directly bound to the antibody or in case of ^{177}Lu bound through one of two different chelators and one of two different spacers attached to the ligand. These two isotopes were chosen due to their different applications in nuclear medicine. The ^{131}I isotope emits both beta and gamma ray radiations, which can be used either for imaging or for therapy. In contrast, ^{177}Lu is mostly used for radiotherapy due to its preferable beta decay, which damages the targeted tissue.

Methods

Cell cultures

In this study, two cancer cell cultures were used, namely the human squamous carcinoma cell line A431 (Health Protection Agency Culture Collection, Salisbury, United Kingdom) and the human keratinocyte cell line HaCaT (DKFZ, Heidelberg, Germany). For the *in vitro* experiments, cells were seeded onto a Petri dish (dimension 60 x 16 mm, TPP AG, Trasadingen, Switzerland) and allowed to grow to confluence. A431 cells were grown in Eagle´s MEM cell culture medium (EMEM, Sigma-Aldrich), and HaCaT cells were grown in Dulbecco´s MEM cell culture medium (DMEM, Sigma-Aldrich). Both media types were supplemented with 10 % foetal bovine serum (FBS, PAA, Pasching, Austria), L-glutamine (L-glu, Sigma-Aldrich, 1 % for EMEM or 0.1 % for DMEM) and 1 % non-essential amino acids (NEAA, Sigma-Aldrich). The cells were grown at 37°C and 5 % CO_2 atmosphere in a humidified incubator until the experimental day.

Radiolabelling with ^{131}I

The antibody nimotuzumab (hR3, Theraloc, Oncoscience AG, Wedel, Germany) was labelled using oxidative iodination, according to the Chloramin-T protocol [12]. The carrier-free isotope ^{131}I was directly bound to the antibody nimotuzumab molecule (covalent binding to benzene ring of tyrosine). Because the chemical amount of antibody exceeded concentration of 131-I by several orders, only some molecules of antibody were radioactively labeled.
The monoclonal antibody (80 µg) in isotonic phosphate buffer solution (PBS 10 mM, pH 7.4) was labelled with ^{131}I (10 MBq, 8 – 10 µl of ^{131}I sodium iodide solution) (Institute of Isotopes Co., Ltd. Budapest, Hungary). Twenty microlitres of chloramin-T (Sigma-Aldrich) solution (concentration 4 mg/ml), corresponding to 80 µg of the agent, was added to the same buffer as an oxidation agent. The reaction was stopped with 40 µl of sodium metabisulphite solution (Sigma-Aldrich; concentration 4 mg/ml). After stopping the reaction, labelled protein was purified from non-labelled ^{131}I on a NAP-5 column (GE Healthcare, Uppsala, Sweden) using PBS (10 mM, pH 7.4) as the elution buffer.
Isocratic HPLC analysis was performed on Agilent System 1100 with UV-VIS and radiometric detection, equipped with a Bio-Sil Sec-250 column (Bio-Rad Laboratories, Hercules CA, USA). For the mobile phase, 0.05 M sodium chloride solution with 0.01 M NaN_3 was used with a flow rate of 0.8 ml/min.

Radiolabelling with ^{177}Lu

Radiolabelling of nimotuzumab with ^{177}Lu was performed after the modification of the antibody with different chelators: *p*-SCN-Bn-DOTA (*p*-isothiocyanatobenzyl-1,4,7,10-tetraazacyclododecane-1,4,7,10-tetraacetic acid), *p*-SCN-Bn-DTPA (2-(4-

Isothiocyanatobenzyl)diethylenetriaminepentaacetic acid) or DOTA-NHS-ester (N-hydroxysuccinimidyl-DOTA). The average number of chelates linked to the antibody molecule was determined using ^{90}Y by a radioactive method previously described by Meares CF et al. [16]. The average degree of substitution was 4-5 chelator groups per 1 antibody molecule.
Radiolabelling was performed as described previously by Beckford Vera DR et al. [6]. Briefly, aliquots of $^{177}LuCl_3$ (15–185 MBq, in 1–25 µl 0.05 mol/l HCl, PerkinElmer) were added to 25–50 µl of 0.5 mol/l NH_4OAc buffer at pH 7.0, followed by 50–100 µl (0.200–0.540 mg) of the conjugate. The reaction mixture was incubated at 42°C for 1.5 hours. To scavenge any free radiometals for further quality control, a solution of DTPA or EDTA (7–17 µl, 0.01 mol/l, pH 6.0) was added to the reaction vial and the mixture was incubated for 15 min at room temperature. Purification of the radiolabelled product was performed by gel filtration on a Sephadex G-50 in physiological solution (0.9 % NaCl).
HPLC analysis was performed on the Agilent System (see above). For the mobile phase, ammonium acetate (0.1 M) with EDTA (1 mM) and NaN_3 (0.01 M) pH 7 was used with a flow rate of 0.8 ml/min.
For fast analysis, thin-layer chromatography on ITLC-SG (Pall Corporation, USA) was performed in sodium citrate solution (0.1 M).

In vitro experiments

Cells seeded on a Petri dish were washed with PBS (2 x 5 ml, 10 mM, pH 7.4, 37°C, sterile). Krebs Ringer solution (3 ml, pH 7.4, 37°C, sterile) containing either ^{177}Lu-hR3 or ^{131}I-hR3 was added to the cells. The incubation was performed at 37°C in a humidified atmosphere supplied with 5% CO_2. Incubation times were 0 (to detect non-specific binding), 30, 60, 90, 120, 150 and 180 minutes for ^{177}Lu-DOTA(NHS)-nimotuzumab (without the 90 and 150 minutes time-points), ^{177}Lu-DOTA(p-SCN-Bn)-nimotuzumab, ^{177}Lu-DTPA(p-SCN-Bn)-nimotuzumab and ^{131}I-nimotuzumab.
At the end of the incubation period, the cells were washed with PBS (3 x 5 ml, 1 to 3 minutes per washing, 10 mM, pH 7.4, cold), followed by glycine-HCl buffer (2 x 3 ml, 5 minutes per washing, pH 2.2, cold). The cells were lysed with NaOH solution (3 ml, 1 M). The radioactivity in the lysates was measured using the automatic gamma counter 1480 WIZARD^{TM} 3" (PerkinElmer), and the counts were normalised against the amount of cell protein, as measured by a BCA Protein Assay (Thermo Fisher Scientific).

In vivo experiments - animals

For the biodistribution studies, male Wistar rats weighing 190-260 g were used. The animals were starved overnight before the experiment (to empty the bowels), but had free access to water. All the animal experiments were approved by the Ethics Committee of the Faculty of Pharmacy in Hradec Kralove, Charles University in Prague.

In vivo experiments - biodistribution in rats

Radiolabelled nimotuzumab was administered to the animals intravenously in a volume of 0.2 ml. The mass and activity of the individual antibodies were as follows: ^{177}Lu-DOTA-(p-SCN-Bn)-nimotuzumab (0.01 mg and 3.6 MBq per animal), ^{177}Lu-DOTA-(NHS)-nimotuzumab (0.01 mg and 3.6 MBq per animal) and ^{177}Lu-DTPA-(p-SCN-Bn)-nimotuzumab (0.01 mg and 3.0 MBq per animal). During the experiments, the rats were housed singly. At various time points after injection, the carotid artery was exposed under

ether anaesthesia and a blood sample was collected in a glass tube containing dry heparin. The rats were then sacrificed and dissected. The organs of interest were weighed, and the radioactivity was measured in the automatic gamma counter 1480 WIZARD 3. The results were expressed as the mean ± standard deviation of at least four animals.

Statistical analysis

The data are shown as the mean ± standard deviation. The GraphPad Prism program, version 5.02, was used for the blood radioactivity-time course fitting and calculation of the elimination half-life.

Results

Stability testing of ^{131}I-nimotuzumab

Stability testing of ^{131}I-nimotuzumab was performed in both a physiological solution or in rat plasma. The samples were analysed at specific time points after the radiolabelling procedure. The analysis was performed on a HPLC system. The results are summarised in Figure 1 and 2.

^{131}I-nimotuzumab stability in a physiological solution was measured at 0, 1, 3, 5.5 and 24 hours after labelling. The radiochemical purity of labelled nimotuzumab slightly decreased after 5.5 hours, when a small peak of a low molecular weight impurity appeared (eluted after the main peak of the labelled antibody). The most significant impurity was detected at 24 hours after labelling.

The stability of ^{131}I-nimotuzumab was also tested in rat plasma at 0, 1, 2, 3, 24 and 48 hours after radiolabelling. The very small impurity from decaying radiolabelled nimotuzumab was detected from the third hour after the labelling procedure and increased over time.

The found impurities in the stability testing of the agents under study possibly originated either from auto-radiolysis or instability of the antibody molecule.

In vitro binding of nimotuzumab

The antibody nimotuzumab was labelled with two isotopes: ^{177}Lu and ^{131}I. The binding characteristics of the labelled ligand were tested on living cells. A431 and HaCaT cells express a large amount of ErbB1 on their surface [3; 14]. Therefore, these cell lines provide a very good model to test the receptor-antibody interaction.

Four differently labelled MAbs were tested: ^{177}Lu-DOTA-(p-SCN-Bn)-nimotuzumab, ^{177}Lu-DOTA-(NHS)-nimotuzumab, ^{177}Lu-DTPA-(p-SCN-Bn)-nimotuzumab and ^{131}I-nimotuzumab. One nanomolar solution of the labelled monoclonal antibody in the internalisation medium (Krebs Ringer solution) was incubated with the cells for the indicated lengths of time: 0 (to detect non-specific binding), 30, 60, 90, 120, 150 and 180 minutes (0, 30, 60, 120 and 180 minutes for ^{177}Lu-DOTA-(NHS)-nimotuzumab only). Triplicates were prepared for each time point. The unbound ligand was washed out after the incubation. Labelled antibody, which was still bound to the receptor, was washed out with a glycine buffer solution. The cells were lysed, the radioactivity in the protein lysate was counted, and the amount of protein was measured. The final result for each time point was formulated as the internalised activity (CPS) per mg of cellular protein.

The *in vitro* uptake efficiency of each labelled antibody is summarised in Figures 3-6. The uptake of all four differently labelled antibodies was not particularly effective, as

demonstrated by low values for the internalised activities.
Figure 4 shows the *in vitro* internalisation activity of ^{177}Lu-DOTA-(NHS)-nimotuzumab, which has the highest value of internalised activity of all four of the tested antibodies. At equilibrium, internalized activity represented 1.4% (±0.02) and 1.1% (±0.09) of the total activity in the system for the A431 and HaCaT cells, respectively.
The kinetic interaction plateaus for ^{177}Lu-DOTA-(p-SCN-Bn)-nimotuzumab, ^{177}Lu-DTPA-(p-SCN-Bn)-nimotuzumab and ^{131}I-nimotuzumab occurred at the following percentages of internalised activity: 1.2% (±0.01) and 1.1 (±0.09); 0.8% (±0.14) and 0.6% (±0.08); and 0.9% (±0.21) and 1.0% (±0.39), respectively, for the A431 and HaCaT cells.

Biodistribution studies

The distribution profiles of intravenously administered nimotuzumab radiolabelled with ^{177}Lu in selected rat organs and systems are summarised in Tables 1-3 and the profiles for ^{131}I-labelled nimotuzumab are summarised in Table 4. Calculated elimination half-lives of radiolabelled nimotuzumabs are summarized in Table 5.
The distribution of radioactivity in the whole blood was calculated by assuming that blood represents 6.5% of total body weight. The radioactivity disappeared from the blood very slowly, the main distribution organ being the liver. The slowest blood radioactivity time decrease was for ^{131}I-nimotuzumab. When nimotuzumabs differentially labelled with ^{177}Lu are compared, the rate of blood radioactivity clearance increased in the order ^{177}Lu-DTPA-(p-SCN-Bn)-nimotuzumab < ^{177}Lu-DOTA-(p-SCN-Bn)-nimotuzumab < ^{177}Lu-DOTA-(NHS)-nimotuzumab, the same order in which radioactivity uptake in the liver increased. Contrary to ^{177}Lu-labelled agents, radioactivity uptake in the thyroid after ^{131}I-labelled nimotuzumab administration increased with time, suggesting a partial deiodination of the agent. Radioactivity found in the kidney and gastrointestinal tract was most likely connected with a slow elimination of the degradation products of radiolabelled nimotuzumab from the body. Radioactivity in other organs was below 1% of the administered dose.

Discussion

The antibody nimotuzumab belongs to the group of monoclonal antibodies (like cetuximab) with the significant influence on the tumour cell biology. Even if nimotuzumab binds to the ErbB1 receptors with moderate affinity ($K_D \sim 1 \times 10^{-9}$) as proved in prior *in vitro* studies (A431 cells), it has still ability to decrease tumour cell proliferation, which was confirmed in clinical trials [4; 11; 13; 21]. Nimotuzumab affinity to ErbB1 receptors opens also fascinating possibility to utilize this agent as a vehicle for the delivery of radioactivity to ErbB1- rich tumour cells. The successful targeting of radiolabelled antibody to tumour cells requires not only carrier specificity towards tumour-associated antigens, but also the use of an appropriate radionuclide and a suitable method for radionuclide attachment to the agent. A radiolabelled antibody is thus composed of several parts, the most important being a receptor-specific antibody, which may be coupled to a spacer and a chelator for binding the radionuclide. Both the spacer and the chelator may alter the pharmacological properties of the antibody (its binding affinity, distribution profile in the body, etc). This approach is usually used for labelling with radiometals. Another option is the direct labelling of the antibody with an appropriate radionuclide, such as radioiodine. For therapeutic use, the choice of a suitable radionuclide is relatively limited. Besides ^{90}Y (a pure beta-emitter with a relatively short half life of 2.7 days), ^{177}Lu (beta- and gamma-emitter with a half life 6.7 days and a shorter penetration range) is also a suitable candidate, especially in smaller lesions [10]. In this paper,

we have studied the effect of different chelators (DOTA, DTPA) and different spacers (p-SCN-Bn and NHS) on the accumulation of ^{177}Lu-nimotuzumab radioactivity in two tumour cell lines and on its distribution characteristics in rats. The results were compared with those of ^{131}I-nimotuzumab.

The *in vitro* experiments were performed on two well-characterised cell lines, both of which express the ErbB1 receptor at a high level. The A431 cell line is a gold standard for experiments targeting epidermal growth factor receptor. However, useful attributes, such as stable ErbB1 expression and good growth characteristics, also increase the utility of the HaCaT cell line for these experiments. A recent study has quantified the number of ErbB1 receptors per cell [5]. The number of receptors was found to be approximately 2.0 million ErbB1 receptors per cell for A431 and 1.0 million per cell for HaCaT.
When we compare the results of our *in vitro* experiments, no significant difference in ligand uptake was found between the differently labelled antibodies. Cellular uptake of the radiolabelled antibodies reached the equilibrium for both cell lines after 1-2 hours of incubation (Figure 3-6); at this time, the complete saturation of the receptors could be assumed.
The highest value of internalised activity was found for the A431 cell line for the ^{177}Lu-DOTA-(NHS)-nimotuzumab and ^{177}Lu-DTPA-(p-SCN-Bn)-nimotuzumab antibodies. However, the difference between the maximal internalised activity dose in A431 and HaCaT cells was small. In most cases, antibody internalisation was similar between both cell lines. However, we would expect to obtain a higher internalised dose of activity for all the radiolabelled antibodies tested in A431 cells. The reason we do not see this difference may be due to the affinity of receptors to labelled antibodies. The process of radiolabelling can modify the targeted structure (the antibody in this case) and thus change the conformation of the antibody-binding site. The alteration of antibody structure may cause a lower affinity of antibodies to receptors and thus reduce antibody internalisation.
On the other hand, if the structure of the radiolabelled antibody was changed, then the internalisation dose should still be lower in HaCaT cells than in A431 cells. Therefore, the similar internalisation doses we observed for both cell lines may be the result of either an excessive cell surface receptor density, the interaction between receptors on A431 cells or receptor expression changes emerging as a result of long cultivation times, which is a known risk when using immortalised cell lines. An excessively high density of receptors can lead to the protection of receptor binding sites from the ligand-receptor interaction. Similar protective interactions can occur between the ErbB1 receptor and other members of the EGF receptor family.
Study of interactions of receptor-specific ligands with cell receptors is the first step in the development of new radiopharmaceuticals, which have the potential to become new therapeutic substances. Nimotuzumab was designed as a new anticancer drug due to its antiproliferative, antiangiogenic and proapoptotic activity [11]. The present paper deals with its possible employment for targeted radioimmunotherapy. The labelled antibodies were internalized into the carcinoma cells bearing ErbB1 and thus can deliver the radioactivity to tumours.

With respect to the biodistribution profile of radioactivity in rats, all agents under study remained in the circulating blood for relatively long periods of time. This behaviour is a general characteristic of antibodies. The blood radioactivity half-lives decreased in the following order: ^{131}I-nimotuzumab > ^{177}Lu-DTPA-(p-SCN-Bn)-nimotuzumab > ^{177}Lu-DOTA-(p-SCN-Bn)-nimotuzumab > ^{177}Lu-DOTA-(NHS)-nimotuzumab. The uptake of radioactivity in the liver increased in the same order.

In the case of nimotuzumab labelled with ^{177}Lu-DOTA and DTPA, a large percentage of ^{177}Lu-radioactivity was localised in the liver, and the uptake of radioactivity in this organ increased over time. The persistence of liver radioactivity may result from the normal metabolic turnover of the agents under study and/or from partial damage of the structure of nimotuzumab caused by chelator attachment and the radiolabelling procedure. The transchelation of ^{177}Lu from the chelator to the metal-avid proteins of the liver may also contribute to a high and long-term liver radioactivity uptake. Whereas the change of the spacer (p-SCN-Bn or NHS) attaching ^{177}Lu-DOTA-chelate to the nimotuzumab molecule had only a limited effect on the blood radioactivity half-life and on liver radioactivity uptake, the antibody bearing the DOTA-chelator exhibited a more rapid blood clearance and higher liver radioactivity accumulation in comparison with that of DTPA. Because DOTA forms thermodynamically and kinetically more stable complexes with trivalent metals than DTPA, this difference may result from different alterations of the native antibody structure during the course of the chelator (DOTA or DTPA) attachment to the parent macromolecule and/or the radiolabelling procedure.
^{131}I-nimotuzumab was cleared from the blood more slowly, radioactivity uptake in the liver was lower and ^{131}I was cleared from the liver faster when compared to ^{177}Lu-labelled nimotuzumabs. At longer time intervals, ^{131}I-radioactivity was partly accumulated in the thyroid and stomach. The reason for this is that iodinated macromolecules frequently suffer from *in vivo* deiodination to form free iodide and/or iodinated thyrosine. Iodinated thyrosine is structurally similar to the thyroid hormones that are known to be rapidly deiodinated by enzymes found in the liver, kidney and thyroid. The thyroid (and partly also the stomach) is also a target organ of free iodine. Therefore, the radiolabelled degradation products of ^{131}I-nimotuzumab were probably externalised from the liver to the bloodstream, accumulated in the thyroid for some time and finally eliminated from the body via the urine. The radiolabelled degradation products of ^{131}I-nimotuzumab in the blood may also increase the value of total blood radioactivity, prolonging its elimination half-life. Alternatively, breakdown products of ^{177}Lu-labelled nimotuzumab antibodies containing a radiometal-chelator may partly persist in the liver (due to high hydrophilicity) for a substantially longer time.
Radioactivity found in the kidney and bowels was most likely due to urinary and biliary excretion of radiolabeled antibody fragments. Long term radioactivity accumulation in the kidney suggests that a partial tubular reabsorption of these fragments by receptor-mediated endocytosis could be involved in the renal handling of the antibody break-down products (this process is well documented for peptides and antibody fragments in literature [1; 8]).
The highest radioactivity concentrations in the kidney and liver were determined after administration of the agents under study to rats. These organs are likely to be dose-limiting ones in possible radio-immunotherapy using radiolabeled hR3.

In summary, neither the selection of the radiolabel (^{131}I or ^{177}Lu) nor the method of ^{177}Lu attachment to the nimotuzumab significantly affected the internalisation characteristics of radiolabelled nimotuzumab in A431 and HaCaT cells. On the other hand, the radioactivity distribution profiles in rats were different depending on the radiolabelling procedure employed. Nimotuzumab labelled with ^{131}I exhibited the longest elimination half-life and the lowest radioactivity uptake in the liver. Attachment of the chelator (DTPA and DOTA) to the nimotuzumab molecule and radiolabelling of the conjugate with ^{177}Lu resulted in a reduction in the elimination half-lives and a several-fold increase of radioactivity retention in the liver. This effect was most pronounced for DOTA-immunoconjugates that were radiolabelled at a higher temperature. With ^{131}I-nimotuzumab, the liver radioactivity uptake decreased with

time, probably due to a partial deiodination of the parent radioimmunoconjugate. However, ^{177}Lu persisted in the liver for substantially longer periods of time (liver radioactivity increased over time, even up to 72 hours after administration).

Acknowledgement:

This study was supported by the Grant Agency of the Czech Republic – Grant No. P304/10/1738. The authors wish to thank Mrs. J. Hoderova and Mrs. E. Teichmanova for excellent technical assistance.

References

[1]. Akizawa H, Uehara T, Arano Y. Advanced Drug Delivery Rew. 2008; 60, 1319-28 [PubMed: 18508156].
[2]. Argyriou AA, Kalofonos HP. Mol. Med. 2009; 15(5-6), 183-91. [PubMed: 19305491]
[3]. Arteaga, CL. Oncologist. 2002; 4, 31-9. [PubMed: 12202786]
[4]. Arteaga, ME. Cancer Biol Ther. 2007, 6(9), 1390-5. [PubMed: 17827980]
[5]. Barta P, Bjorkelund H, Andersson K. Nucl. Med. Commun. 2011; 32(9), 863-7. [PubMed: 21760560]
[6]. Beckford VDR, Eignes S, Beran M, Eigner HK, Laznickova A, Laznicek M, Melichar F, Chinol M. Canc. Biother. Radiopharm. 2011; 26(3), 287-97. [PubMed: 21711096]
[7]. Crombet-Ramos T, Rak J, Pérez R, Viloria-Petit A. 2002; 101(6), 567-75. [Pubmed: 12237899]
[8]. Behr TM, Goldenberg DM, Becker W. Eur. J. Nucl. Med. 1998; 25, 201-12. [Pubmed: 9473271]
[9]. Boland W, Bebb G. Biologics. 2010; 4, 289-98. [PubMed: 21116327]
[10]. De Jong M, Valkema R, Jamar F, Kvols LK, Kwekkeboom DJ, Breeman WA, Bakker WH, Smith C, Pauwels S, Krenning EP. Semin. Nucl. Med. 2002; 32(2), 133-140. [PubMed: 11965608]
[11]. Diay Miqueli A, Blanco R, Garcia B, Badia T, Batista AE, Alonso R, Montero E. Hybridoma (Larchmt) 2007, 26(6), 423-31. [Pubmed: 18158788]
[12]. Greenwood FC, Hunter WM, Glover JS. Biochem. J. 1963; 89, 114-23. [PubMed: 14097352]
[13]. Huang SM, Harari PM. Invest. New Drugs 1999; 17(3), 259-69. [PubMed: 10665478]
[14]. Laskin JJ, Sandler AB. Cancer. Treat. Rev. 2004; 30(1), 1-17. [PubMed: 14766123]
[15]. Marqués MM, Martínez N, Rodríguez-García I, Alonso A. Exp. Cell. Res. 1999; 252(2), 432-8. [PubMed: 10527633]
[16]. Meares CF, McCall MJ, Reardan DT, Goodwin DA, Diamangti CI, McTigue. Anal Biochem. 1984, 142 (1), 68-78. [Pubmed: 6440451]
[17]. Moscatello DK, Holgado-Madruga M, Godwin AK, Ramirez G, Gunn G, Zoltick PW, Biegel JA, Hayes RL, Wong AJ. Cancer. Res. 1995; 55(23), 5536-9. [PubMed: 7585629]
[18]. Pastore S, Mascia F, Mariani V, Girolomoni G. J. Invest. Dermatol. 2008; 128(6), 1365-74. [PubMed: 18049451]
[19]. Ramakrishnan MS, Eswaraiah A, Crombet T, Piedra P, Saurez G, Iyer H, Arvind AS. MAbs. 2009; MAbs. 1(1): 41-8. [PubMed: 20046573]
[20]. Rowinsky E. Drugs 60 Suppl 2000; 1, 1-14. [PubMed: 11129167]
[21]. Salamon DS, Brandth R, Ciardiello F, Normanno N. Crit. Rev. Oncol. Hematol. 1995; 19(3), 183-232. [PubMed: 7612182]

[22]. Sorkin A. Front. Biosci. 1998; 3, 729-738. [PubMed: 9671598]
[23]. Umekita Y, Ohi Y, Sagara Y, Yoshida H. Int. J. Cancer 2000; 89, 484-7. [PubMed: 11102891]
[24]. Yarden Y. Eur. J. Cancer 2001; 37, S3-8. [PubMed: 11597398]
[25]. Yarden Y, Sliwkowski MX. Nat. Rev. Mol. Cell Biol. 2001; 2, 127-37. [PubMed: 11252954]
[26]. YM_BioSciences website. Nimotuzumab: Clinical Trials. Available from: http://www.ymbiosciences.com/products/nimotuzumab/clinical_trials.php. [24th September 2011].

Tables

	5 min	60 min	24 h	72 h
Organs				
Blood(total)	82.15 ± 6.94	69.26 ± 8.81	19.58 ± 2.53	1.92 ± 2.50
Pancreas	0.09 ± 0.01	0.13 ± 0.03	0.12 ± 0.04	0.16 ± 0.16
Liver	12.51 ± 2.05	18.17 ± 2.19	20.77 ± 2.32	26.48 ± 4.04
Adrenals	0.05 ± 0.00	0.05 ± 0.01	0.04 ± 0.01	0.02 ± 0.00
Kidney	1.41 ± 0.24	1.67 ± 0.26	2.10 ± 0.14	2.04 ± 0.17
Lung	2.52 ± 0.45	2.23 ± 0.37	0.81 ± 0.10	0.39 ± 0.24
Heart	0.94 ± 0.23	0.74 ± 0.07	0.34 ± 0.05	0.10 ± 0.06
Spleen	0.73 ± 0.05	1.19 ± 0.16	1.41 ± 0.15	1.42 ± 0.08
Stomach	0.27 ± 0.03	0.33 ± 0.02	0.71 ± 0.38	0.14 ± 0.06
Intestine	1.28 ± 0.23	3.03 ± 0.37	3.04 ± 1.04	1.95 ± 0.45
Colon	0.43 ± 0.04	0.66 ± 0.16	3.71 ± 1.38	3.83 ± 0.75
Testes	0.26 ± 0.05	0.61 ± 0.09	0.83 ± 0.21	0.26 ± 0.11
Thyroid	0.03 ± 0.01	0.07 ± 0.01	0.04 ± 0.01	0.01 ± 0.01
Brain	0.56 ± 0.13	0.33 ± 0.11	0.10 ± 0.03	0.02 ± 0.01
Femur	0.22 ± 0.04	0.26 ± 0.04	0.42 ± 0.05	0.36 ± 0.09

Table 1 Distribution of radioactivity in selected organs and systems of rats after intravenous administration of ^{177}Lu-DOTA-(p-SCN-Bn)-nimotuzumab to rats (data expressed in %D/organ).

	5 min	60 min	24 h	72 h
Organs				
Blood(total)	70.94 ± 4.72	56.16 ± 6.17	8.69 ± 4.18	0.24 ± 0.15
Pancreas	0.08 ± 0.01	0.09 ± 0.01	0.11 ± 0.06	0.21 ± 0.24
Liver	12.58 ± 0.75	19.80 ± 1.95	34.98 ± 3.22	39.68 ± 8.64
Adrenals	0.05 ± 0.00	0.04 ± 0.00	0.03 ± 0.01	0.03 ± 0.01
Kidney	1.16 ± 0.27	1.31 ± 0.10	1.81 ± 0.16	1.69 ± 0.20
Lung	2.70 ± 1.43	1.79 ± 0.82	0.43 ± 0.16	0.18 ± 0.03
Heart	0.76 ± 0.17	0.70 ± 0.27	0.22 ± 0.07	0.09 ± 0.03
Spleen	0.76 ± 0.05	1.35 ± 0.23	1.64 ± 0.16	1.41 ± 0.22
Stomach	0.27 ± 0.03	0.39 ± 0.09	0.23 ± 0.08	0.13 ± 0.06
Intestine	1.48 ± 0.22	3.13 ± 0.60	2.39 ± 0.61	1.26 ± 0.44
Colon	0.40 ± 0.04	0.53 ± 0.09	12.69 ± 6.38	2.87 ± 0.49
Testes	0.26 ± 0.04	0.50 ± 0.07	0.58 ± 0.22	0.27 ± 0.07
Thyroid	0.03 ± 0.01	0.05 ± 0.03	0.03 ± 0.01	0.01 ± 0.00
Brain	0.40 ± 0.08	0.31 ± 0.06	0.06 ± 0.03	0.01 ± 0.00
Femur	0.24 ± 0.01	0.26 ± 0.02	0.23 ± 0.05	0.20 ± 0.02

Table 2 Distribution of radioactivity in selected organs and systems of rats after intravenous administration of ^{177}Lu-DOTA-(NHS)-nimotuzumab to rats (data expressed in %D/organ).

	5 min	60 min	24 h	72 h
Organs				
Blood(total)	69.65 ± 12.09	58.55 ± 13.31	22.88 ± 1.16	11.18 ± 0.83
Pancreas	0.07 ± 0.01	0.09 ± 0.02	0.11 ± 0.02	0.07 ± 0.04
Liver	11.66 ± 2.39	12.48 ± 2.40	14.68 ± 0.66	17.22 ± 0.97
Adrenals	0.04 ± 0.01	0.04 ± 0.01	0.03 ± 0.00	0.03 ± 0.00
Kidney	2.34 ± 1.31	2.15 ± 0.08	4.30 ± 0.28	4.54 ± 0.20
Lung	3.20 ± 1.02	2.16 ± 0.37	1.34 ± 1.08	0.71 ± 0.24
Heart	0.54 ± 0.07	0.57 ± 0.14	0.40 ± 0.03	0.21 ± 0.02
Spleen	0.53 ± 0.11	0.59 ± 0.07	0.82 ± 0.08	0.93 ± 0.10
Stomach	0.25 ± 0.03	0.28 ± 0.08	0.48 ± 0.16	0.22 ± 0.00
Intestine	1.08 ± 0.09	2.09 ± 0.31	2.04 ± 0.15	1.33 ± 0.15
Colon	0.37 ± 0.02	0.39 ± 0.06	4.80 ± 0.22	2.12 ± 0.41
Testes	0.25 ± 0.04	0.59 ± 0.08	0.80 ± 0.07	0.61 ± 0.12
Thyroid	0.03 ± 0.01	0.06 ± 0.03	0.04 ± 0.01	0.03 ± 0.00
Brain	0.43 ± 0.09	0.31 ± 0.03	0.13 ± 0.02	0.06 ± 0.01
Femur	0.23 ± 0.07	0.22 ± 0.04	0.19 ± 0.04	0.19 ± 0.01

Table 3 Distribution of radioactivity in selected organs and systems of rats after intravenous administration of ^{177}Lu-DTPA-(p-SCN-Bn)-nimotuzumab to rats (data expressed in %D/organ).

	5 min	60 min	24 h	72 h
Organs				
Blood(total)	88.84 ± 4.80	79.78 ± 1.49	38.83 ± 1.81	25.66 ± 1.04
Pancreas	0.15 ± 0.09	0.11 ± 0.02	0.16 ± 0.02	0.14 ± 0.02
Liver	7.57 ± 0.64	6.68 ± 0.51	3.56 ± 0.40	2.30 ± 0.13
Adrenals	0.07 ± 0.01	0.07 ± 0.00	0.04 ± 0.00	0.03 ± 0.00
Kidney	1.39 ± 0.27	1.51 ± 0.30	0.92 ± 0.14	0.54 ± 0.03
Lung	2.19 ± 0.42	1.90 ± 0.55	1.57 ± 0.72	0.98 ± 0.18
Heart	0.90 ± 0.13	0.84 ± 0.13	0.60 ± 0.14	0.39 ± 0.05
Spleen	0.59 ± 0.05	0.62 ± 0.05	0.31 ± 0.02	0.21 ± 0.04
Stomach	0.31 ± 0.05	0.53 ± 0.15	1.01 ± 0.28	0.69 ± 0.08
Intestine	1.12 ± 0.17	2.23 ± 0.18	2.11 ± 0.10	1.42 ± 0.02
Colon	0.37 ± 0.07	0.52 ± 0.10	1.29 ± 0.04	0.91 ± 0.08
Testes	0.26 ± 0.04	0.68 ± 0.13	1.61 ± 0.10	1.12 ± 0.09
Thyroid	0.03 ± 0.00	0.06 ± 0.02	0.53 ± 0.50	1.13 ± 0.86
Brain	0.49 ± 0.05	0.34 ± 0.06	0.19 ± 0.07	0.12 ± 0.02
Femur	0.24 ± 0.02	0.29 ± 0.01	0.16 ± 0.02	0.11 ± 0.01

Table 4 Distribution of radioactivity in selected organs and systems of rats after intravenous administration of ^{131}I-nimotuzumab to rats (data expressed in %D/organ).

Antibody	Half-life (hours)	Correlation coefficient R^2
^{177}Lu-DOTA-(p-SCN-Bn)-nimotuzumab	11.8	0.99
^{177}Lu-DOTA-(NHS)-nimotuzumab	7.4	0.99
^{177}Lu-DTPA-(p-SCN-Bn)-nimotuzumab	18.0	0.96
^{131}I-nimotuzumab	30.4	0.93

Table 5 Elimination half-lives of radiolabelled nimotuzumabs under study. Blood radioactivity-time decreases were fitted using one-compartment open pharmacokinetic model

according to equation $A_t = A_0 e^{-kt}$.

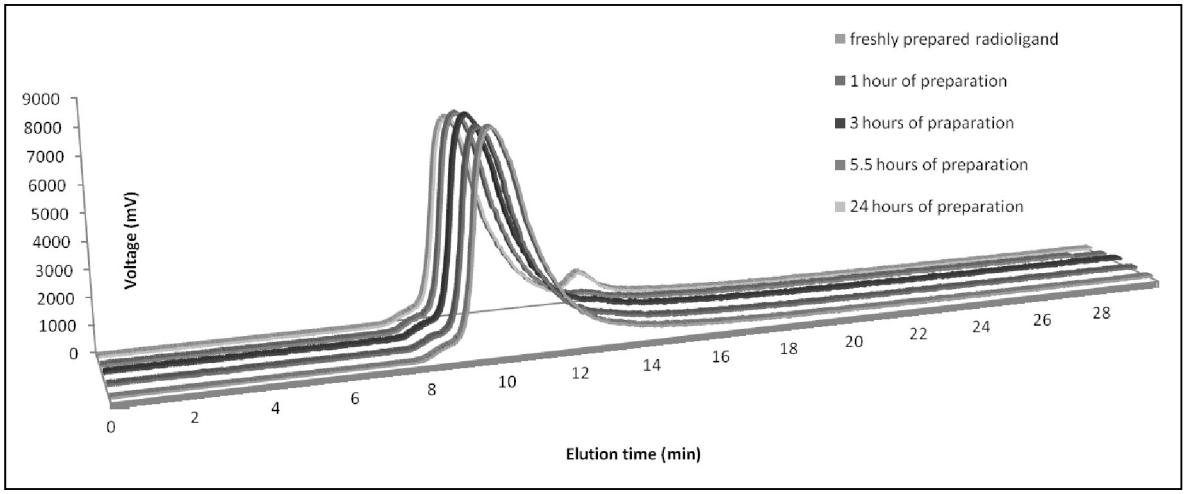

Figure 1 The stability testing of [131I]nimotuzumab incubated in a physiological solution (0.9 % NaCl, stored at 4°C) for indicated time performed on HPLC system. The chromatography records are depicted in order from front to back as described in the label on right. The voltage measured by a radiometric detector corresponds to a volume activity of the eluate.

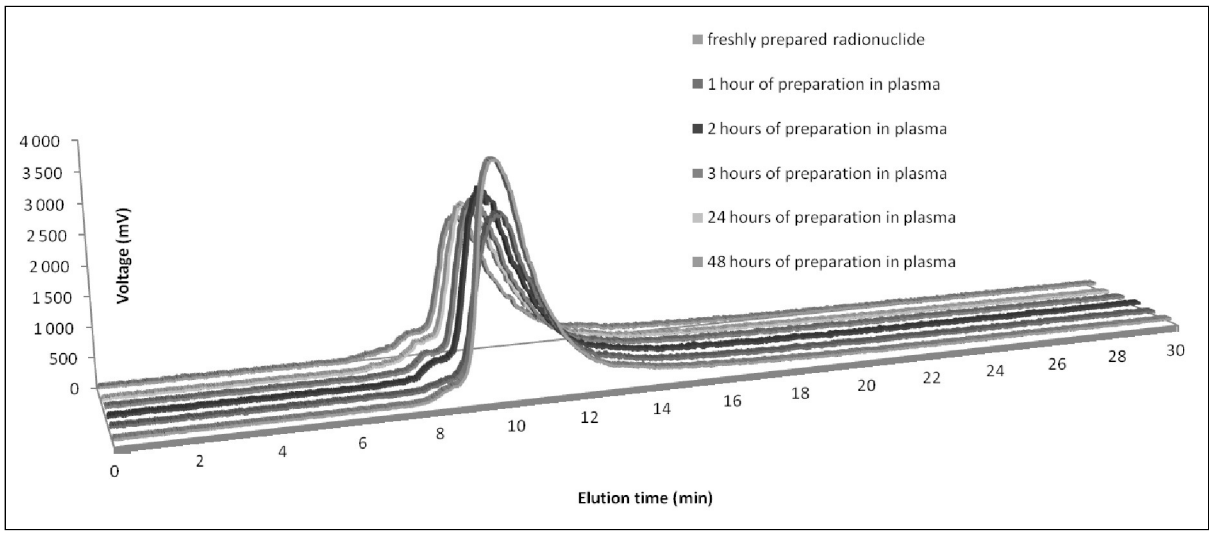

Figure 2 The stability testing of [131I]nimotuzumab incubated in plasma (stored at 37°C) for indicated time performed on HPLC system. The chromatography records are depicted in order from front to back as described in the label on right. The voltage measured by a radiometric detector corresponds to a volume activity of the eluate.

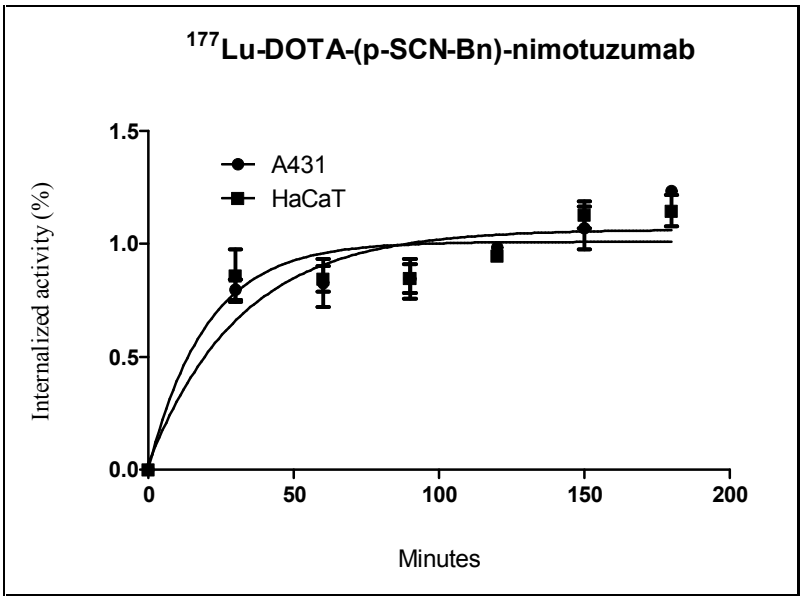

Figure 3 The time depending internalization of [177Lu]DOTA-(p-SCN-Bn)-nimotuzumab assayed on cancer cells A431 and HaCaT. Data expressed as mean±SD.

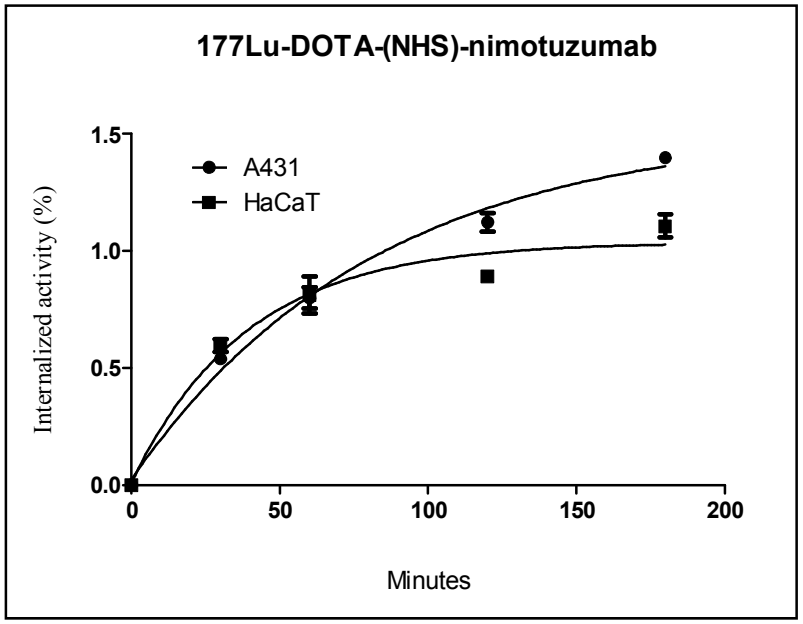

Figure 4 The time depending internalization of [177Lu]DOTA-(NHS)-nimotuzumab assayed on cancer cells A431 and HaCaT. Data expressed as mean±SD.

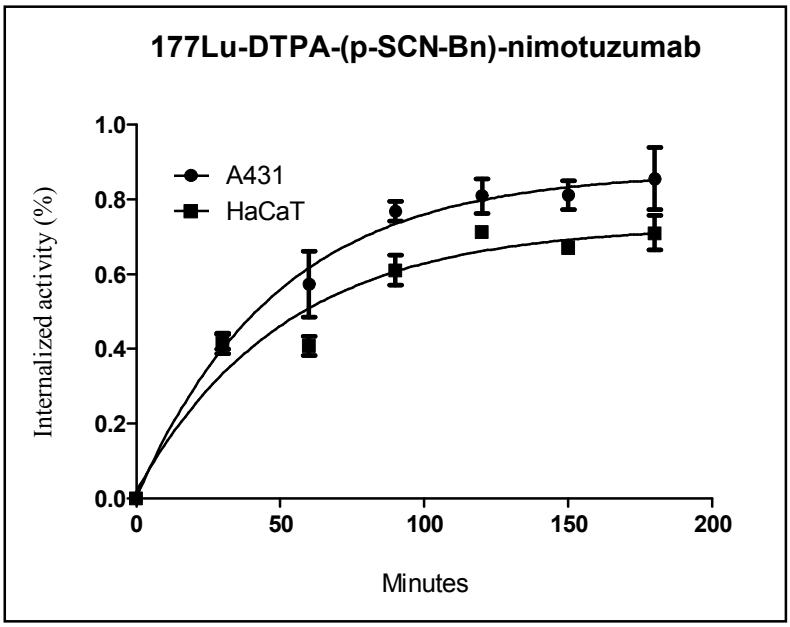

Figure 5 The time depending internalization process of [177Lu]DTPA-(p-SCN-Bn)-nimotuzumab on cancer cells A431 and HaCaT. Data expressed as mean±SD.

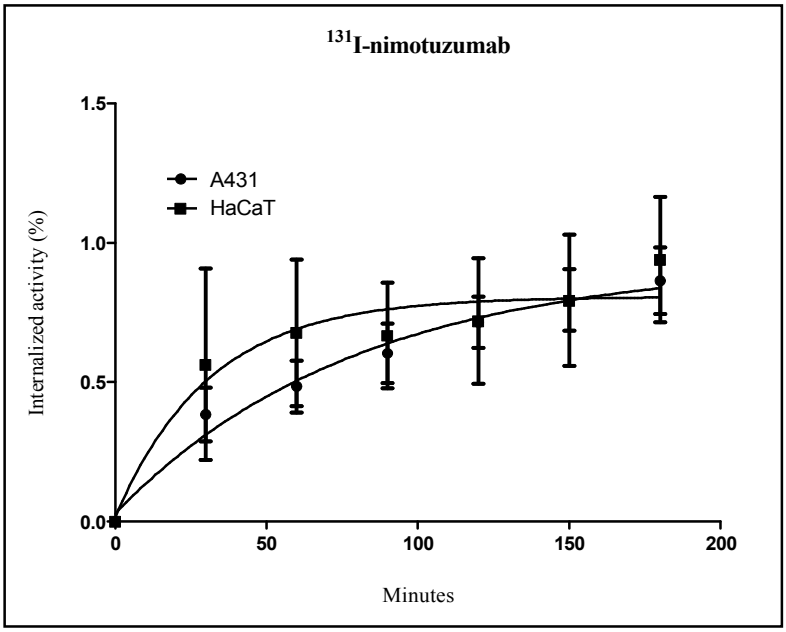

Figure 6 The time depending internalization process of [131I]nimotuzumab on cancer cells A431 and HaCaT. Data expressed as mean±SD.

7. Abstrakt

Univerzita Karlova v Praze, Farmaceutická fakulta v Hradci Králové

Katedra: Farmakologie a toxikologie

Kandidát: Mgr. Pavel Bárta

Školitel: Prof. PharmDr. Ing Milan Lázníček, CSc.

Název disertační práce: Studium interakce receptorově specifických radiofarmak s biologickým systémem na buněčné úrovni

Cílení nádorových buněk receptorově specifickými peptidy nebo protilátkami patří k významnému diagnostickému a někdy i terapeutickému nástroji v boji proti nádorovým onemocněním.

Receptorově specifické peptidy jsou především odvozené od tělu vlastních peptidových hormonů, proto o nich mluvíme jako o peptidových analozích. Analogy peptidů obsahují ve svém peptidovém řetězci vazebné místo shodné s přirozeným peptidem umožňující jejich specifické navázání na cílový receptor. Peptidové analogy se používají místo přirozených peptidů zejména z důvodu jejich lepších biologických vlastností usnadňujících jejich distribuci v organismu do místa jejich působení nebo z důvodu jejich ochrany před biologickou degradací. Vazba a internalizace peptidového ligandu do buňky většinou sama o sobě nenavozuje terapeutický efekt, proto peptidový analog nese aktivní látku jako je cytotoxin nebo radioizotop, která má terapeutický účinek anebo i diagnostický v případě radioaktivního izotopu. Terapeutický efekt radioizotopu pak zahrnuje poškození DNA nádorové buňky vedoucí ke ztrátě jejich proliferačních schopností a k zániku buňky. Vedle terapeutického efektu je častější použití radioaktivně značených peptidů pro zobrazovací účely. Zobrazovací schopnost gama záření emitujících izotopů usnadňuje nalezení ložiska nádoru.

Terapeuticky využívané receptorově specifické monoklonální protilátky jsou schopné bránit přenosu signálu vzniklého z interakce přirozeného ligandu na cílovém receptoru tím, že blokují vazebná místa na receptorech. Terapeutický účinek také spočívá v zabránění přenosu signálu z receptoru na efektorové proteiny uvnitř buňky a tím vzniku buněčné odpovědi. Monoklonální protilátky nemusejí mít sami o sobě dostatečný terapeutický účinek, proto se častěji používají ve formě transportních látek pro cytotoxická léčiva nebo radionuklidy, které působí zánik cílených buněk. Radioaktivní značení monoklonálních protilátek má stejně jako u peptidových analogů i diagnostický účel. Nevýhodou protilátek bývá velikost jejich molekuly. Zatímco peptidy o krátkém peptidovém řetězci snadněji

pronikají do místa působení, protilátky se jen pomalu distribuují a rychleji podléhají biodegradaci v játrech. Řešení této komplikace z posledních let spočívá ve vytvoření fragmentů protilátek, které se postupně „poskládají“ na cílové struktuře receptoru, mluví se o tzv. pre-targeting metodě. Vedle snadné distribuce v organismu se navíc snižuje riziko cytotoxické nebo radiologické zátěže pacienta.

Cíl publikované práce v kapitole I byl zaměřen na případné ovlivnění biologických vlastností peptidu minigastrin11 (MG11) radioaktivním značením, kdy se testovala jeho schopnost interakce na specifickém cholecystokininovém receptoru typu 2 (CCK2r) a míra jeho internalizace do pankreatických nádorových buněk AR42J. Minigastrinový analog byl značen radionuklidy ^{177}Lu a ^{111}In, kdy prvně uvedený má v onkologii terapeutické využití a druhý diagnostické. Vazba komplexu ^{111}In-DOTA-MG11 na receptor byla pomalá a nedosáhla rovnováhy mezi asociací a disociací reakce ligandu na receptoru ani po třech hodinách inkubace. Na druhou stranu, interakce komplexu ^{177}Lu-DOTA-MG11 na CCK2r dosáhla rovnováhy po jedné hodině inkubace včetně vyššího internalizovaného podílu radiopeptidu z celkového přidaného množství, než tomu bylo v případě ^{111}In-DOTA-MG11. Radiofarmakum ^{177}Lu-DOTA-MG11 je tedy schopno se efektivně vázat na cílový CCK2r a má tak slibné předpoklady pro své uplatnění v terapii radionuklidem značenými receptorově specifickými peptidy (PRRT). Výše zmíněná radiofarmaka se použila i pro zjištění případné radionefrotoxicity, která bývá častou doprovodnou komplikací aplikace radioaktivně značených peptidových analogů. Komplikace s poškozováním ledvin v případě radioaktivně značených peptidů je zapříčiněna zpětnou tubulární resorpcí, která kumuluje radioaktivní izotopy v ledvinných buňkách proximálního tubulu. Pro otestování případné kumulace ^{111}In- a ^{177}Lu-ligandu se použila buněčná linie izolovaná z proximálního tubulu ledvin vačice oposum (OK buňky). Výsledky experimentu byly příznivé, neboť neprokázaly významnou kumulaci radioligandů v ledvinných buňkách. Internalizace radiopeptidů vykazovala maximálních hodnot kolem 0.1 % z celkově přidaného množství aktivního ligandu k buňkám.

Publikace v kapitole II se zaměřila na zlepšení způsobu kvantifikace receptorů na buňkách (NRPC). Studie porovnala možnosti nabízené klasickou manuální technikou pro NRPC s novým způsobem kvantifikace receptorů na automatickém zařízení nesoucí název LigandTracer® určeného pro real-time měření interakce radioligandu s cílovým receptorem na buněčném povrchu. Nový způsob stanovení počtu receptorů dostal označení KEX metoda. Název je odvozen od základního principu metody, který spočívá v extrapolaci dat kinetické reakce vazby ligandu na receptor, tedy ve výpočtu teoretické hodnoty B_{max}, která odpovídá signálu kompletně saturovaného množství cílených receptorů na povrchu buňky. Manuální

metoda se řadí mezi techniky kvantifikace receptorů na povrchu buněk osvědčené mnohaletým užíváním a je tak zlatým standardem NRPC technik. Naměřené hodnoty kvantifikovaných receptorů manuální metodou a technikou KEX vykázaly shodu, pouze KEX technika v některých případech vykazovala mírné nadhodnocení počtu receptorů oproti klasické metodě. KEX technika se i přesto dá zařadit mezi metody umožňující kvantifikaci cílených buněčných receptorů s využitím v biologických vědách a s následným uplatněním v nukleární medicíně. Rychlé ověření množství receptorů a schopnosti radioligandu se vázat na zamýšlenou strukturu na povrchu nádorové buňky zefektivní výzkum nových terapeutických nebo diagnostických molekul pro onkologickou léčbu. Možný význam plynoucí z KEX techniky byl opakovaně ověřen i v další experimentální studii uvedené v kapitole V. Zde se porovnávaly hodnoty počtu receptorů na testovaných buněčných liniích měřených technikou KEX, klasickou manuální technikou a metodou western blottingu. Výsledek studie opětovně potvrdil uvedení KEX techniky mezi spolehlivé metody stanovení NRPC.

Možnost ovlivnění afinity receptoru epidermálního růstového faktoru (EGFR) pro ligand ^{125}I-EGF prostřednictvím tyrozin kinázového (TK) inhibitoru gefitinibu byla prozkoumána a popsána v odborné publikaci v kapitole III. Výsledkem práce je zjištění indukujícího vlivu gefitinibu na tvorbu EGFR dimerů. Tvorba receptorového dimeru ovlivňuje charakteristiku interakce EGFR s jeho přirozeným ligandem epidermálním růstovým faktorem (EGF). Prevalence receptorových monomerů, homodimerů a heterodimerů je odlišná mezi buněčnými liniemi a závisí především na míře exprese EGFR a HER2 receptoru na povrchu buněk. EGF se váže na monomerní a dimerní formy EGFR s rozdílnými vazebnými vlastnostmi. Výsledek studie poukazuje na kladný vliv gefitinibu na tvorbu EGFR dimerů, které pak mají vyšší afinitu k ^{125}I-EGF.

Publikovaná studie uvedená v kapitole IV se zaměřila na prokázání hypotézy, že afinita receptoru a kinetika reakce mezi ligandem a jeho receptorem se liší napříč buněčnými liniemi. Například přirozený ligand EGF se tak váže s rozdílnou vazebnou silou na ten samý receptor (EGFR) exprimovaný na rozdílných buněčných liniích. Tato zjištění byla ověřena pro protilátku ^{131}I-cetuximab, která se vázala na EGFR s rozdílnou afinitou pro tři buněčné linie. Faktor rozdílu v afinitě protilátky k ligandu měl napříč buněčnými liniemi hodnotu až 10. Možnou příčinou rozdílu v afinitě receptoru k ligandu je jeho různý stupeň glykosylace, nebo tvorba homodimerů či heterodimerů a v neposlední řadě možná mutace receptoru. Uvedené možnosti ovlivnění afinity receptoru pak vedou k případům, kdy velmi dobrý vazebný partner receptoru testovaný *in vitro* vykazuje velmi nízkou afinitu vazby na cílový

receptor v biologickém testování. Podobného zjištění se dosahuje i v aplikaci terapeutických a diagnostických činidel v populaci pacientů, kdy část pacientů neodpovídá na léčbu. Výsledky prací charakterizující úspěšnost *in vitro* aplikací zkoumaného receptorového ligandu by neměly být generalizovány pro všechny buňky nesoucí zkoumaný receptor, ale měl by být brán zřetel na možné diference mezi buněčnými liniemi. Podobně by měla být vedena i léčba pacientů, která by měla mít individuální přístup.

Poslední publikovaná studie zařazená do kapitoly VI si kladla za cíl ověřit, jaký je vliv zvoleného radioizotopu a způsobu radioaktivního značení na chování radioligandu v *in vivo* a *iv vitro* podmínkách. Výsledek práce uvádí, že zvolené izotopy ^{131}I a ^{177}Lu a stejně tak metody jejich vazby na transportní protilátku nimotuzumab cílenou proti EGFR nevedly k ovlivnění internalizační charakteristiky radioligandu u buněčných kultur. Opak prokázaly výsledky experimentů provedených *in vivo*, které poukázaly na některé odlišnosti v distribučních profilech v závislosti na použitých metodách radioaktivního značení. ^{131}I-nimotuzumab vykazoval nejnižší míru vychytávání v játrech a nejdelší čas krevní eliminace ze všech zkoumaných radioligandů. Protilátka nimotuzumab s izotopem ^{177}Lu navázaným prostřednictvím chelatačních činidel (DOTA, DTPA) byla charakterizována poklesem eliminačního času a mnohonásobně zvýšenou retencí v játrech. Uvedené *in vivo* výsledky potvrdily vliv typu použitého izotopu a způsobu jeho vazby na biologické vlastnosti značené protilátky nimotuzumab v případě testových faktorů, jako byla krevní clearance, vychytávání játry a následná kumulace v játrech.

8. Abstract

Charles University in Prague, Faculty of Pharmacy in Hradec Kralove
Department of Pharmacology and Toxicology
Candidate: Mgr. Pavel Bárta
Supervisor: Prof. PharmDr. Ing Milan Lázníček, CSc.
Title of Doctoral Thesis: The study of receptor-specific radiopharmaceuticals interactions with biological systems at the cellular level

The targeting of receptor specific peptides or antibodies is one important diagnostic and therapeutic tool in the fight against cancer diseases.

Receptor specific peptides often have their origin from the human natural peptide hormones; hence they are commonly marked as peptide analogues. The peptide analogues contain in their amino acids sequence the binding site identical with the site of natural peptides, which they are originated from. This binding site is responsible for the interaction with the targeted receptor. The peptide analogues are employed instead of the natural peptides because their biological properties can be improved, for example facilitating distribution in the organism to their place of action, or protection from biological degradation. The peptide ligand binding itself on targeted receptors and its internalization into cells typically does not trigger a therapeutic effect. From this reason, peptide analogues carry active substances like cytotoxine or radioisotope; this has the therapeutic or diagnostic effect. The therapeutic effect of radioisotope includes cancer cell DNA damage that leads to the loss of ability to proliferate, which in turn causes cell death. The diagnostic purpose of radioisotopes is more common. The gamma radiation is used in imaging techniques to localize tumours.

Therapeutic monoclonal antibodies are able to prevent receptor specific signal transmission coming from the interaction of natural ligand with the targeted receptor. The mechanism of this protection typically comes from the blocking of the receptor binding sites. Commonly, the monoclonal antibody effect lies in the blockage of signal transmission from a receptor to effectors proteins situated inside a cell. In fact, monoclonal antibodies themselves often have a low therapeutic effect; hence it is beneficial to use them as transport ligands for cytotoxic substances and radionuclide, which are responsible for the cell death. The radiolabelling of monoclonal antibodies has the diagnostic effect too. The disadvantage of antibody is the size of its molecule. Whereas peptides of short peptide chain are easily distributed to the place of action, antibodies are distributed slowly and undergo faster biodegradation in the liver. The

solution of this problem has its origin in the development of antibody fragments in the last years. The antibody fragments are gradually assembled on the targeted receptor protein structure. This method is termed the pre-targeting. The pre-targeting allows easy distribution in the body and decrease the risk of cytotoxic or radiological burden for patients.

The aim of the publication in chapter I was to study the potential influence of radiolabelling on the biological properties of minigastrin11 (MG11). This was performed with testing of its ability to interact with cholecystokinin receptor type 2 (CCK2r) and to internalize into pancreatic cancer cells AR42J. Minigastrin analogue was labelled with either ^{177}Lu or ^{111}In. The first mentioned isotope is used in therapeutic oncology and the second one for diagnostic purposes. The complex ^{111}In-DOTA-MG11 binding on the receptor was slow and did not reach ligand – receptor association and dissociation equilibrium even after three hours of incubation. However, the complex ^{177}Lu-DOTA-MG11 interaction on CCK2r reached the equilibrium after one hour incubation and the higher proportion of complex from the whole quantity added to cells was internalized than in the case of ^{111}In-DOTA-MG11. The radiolabelled ligand ^{177}Lu-DOTA-MG11 is able to effectively bind to the targeted CCK2r and has strong assumption to assert itself in Peptide receptor radionuclide therapy (PRRT). The radioligands ^{177}Lu-DOTA-MG11 and ^{111}In-DOTA-MG11 were investigated for their possible radionefrotoxicity, which often accompanies PRRT. The complication of damaged kidneys by radiolabelled peptides is caused with the rear tubular reabsorption, which cumulates radioactive isotopes in the proximal tubular cells. The cell line isolated from opossum kidney proximal tubular cells (OK cells) was employed to test the possible accumulation of ^{111}In- and ^{177}Lu- labelled ligands. The results of the testing were satisfying, because they demonstrated no important accumulation of radioligands into kidney cells. The internalization of radiolabelled peptides reached the maximal values about 0.1 % of the total added amount.

Improving the method for the number of receptor per cell (NRPC) quantification was the target in the publication given in chapter II. The study compared the possibilities of NRPC calculation offered by the classical manual method with the possibility of NRPC quantification based on the employment of the automatic instrument LigandTracer®. This instrument allows real-time measurement of the interaction of radiolabelled ligand with targeted receptor on cell surface. The new kind of NRPC quantification was denoted as KEX method. The name comes from the basic principle of the method, which lies in kinetic extrapolation of the ligand – receptor interaction, which means the calculation of the theoretical value B_{max}. The theoretical B_{max} corresponds to the signal of completely saturated

receptors on cell surface. The manual method belongs to the techniques of receptor quantification verified with many years of use and thus it is the golden standard of NRPC techniques. The measured values with the classical manual method and KEX technique demonstrated the compliance. The KEX technique sometimes showed slight overestimation of the calculated receptor number against the classical method. However, the KEX technique can be included among methods allowing cell receptor quantification and can be used in biological sciences or in nuclear medicine in the future. The rapid quantification of receptors and the ability binding of radiolabelled ligand to targeted cell surface protein structures can make the progress in the research of new potential therapeutic or diagnostic molecules for cancer treatment. The importance and validity of the KEX technique was repeatedly verified in another experimental study, which is summarized in the chapter V. The values of quantified number of receptors measured by the assays like the KEX technique, the classical manual method and western blotting on employed cell lines were compared in this study. The obtained results confirmed the accuracy of the KEX technique, so it can be counted in methods for NRPC quantification.

The scientific publication introduced in the chapter III was focused on the study of epidermal growth factor receptor (EGFR) affinity, which can be influenced in the present of gefitinib, the tyrosine kinase (TH) inhibitor. The finding of this study was that gefitinib could influence the formation of EGFR dimers. The formation of EGFR dimers can alter the interaction between EGFRr and its natural ligand epidermal growth factor (EGF). The prevalence of receptor monomers, homodimers and heterodimers differs among cell lines and depends on EGFR and HER2 receptor expression rate on a cell surface. EGF binds with different binding properties on monomer or dimer forms of EGFR. The conclusion of the study refers to the positive influence of gefitinib on EGFR dimers formation, which increases the receptor affinity to ^{125}I-EGF.

The publication in the chapter IV attempted to prove the hypothesis that the receptor affinity and the kinetic reaction between ligand and its receptor differed across the cell lines. For example, the natural ligand EGF binds with different binding strength on the same receptor (EGFR) expressed in various cell lines. This finding was proved with the employment of the monoclonal antibody ^{131}I-cetuximab attached to EGFR with different binding affinity on three used cell lines. The affinity difference factor among cell lines was about 10. The reason of the different receptor affinity to the ligand may lie in the various level of the receptor glycosylation, formation of homodimers or heterodimers and possible receptor mutation. The above mentioned options influencing the receptor affinity lead to the

cases, when very good receptor binding ligand tested *in vitro* have very low affinity *in vivo*. The same findings can be in the use of therapeutic or diagnostic substances in a patient population. Some patients do not respond to a treatment. The results of successfully *in vitro* tested receptor ligands should not be generalized for every cell line carrying the same receptor. It should be taken into account the differentiation among cell lines. The same should be reconsidered for patient treatment, which ought to have an individual approach.

The last publication included in this thesis is in the chapter VI. It was aimed at the characterisation of radioligand properties in *in vitro* and *in vivo* conditions after its radiolabelling. The two factors influencing the radioligand character were studied like the choice of isotope and the manner of radiolabelling. The findings made for *in vitro* studies concluded that the chosen isotopes ^{131}I and ^{177}Lu and the methods of their labelling on the transportation monoclonal antibody nimotuzumab did not alter antibody internalization characteristics into employed cell lines. However, the opposite was found for *in vivo* experiments which demonstrated the differences in distribution profiles depending on the methods for radiolabelling. ^{131}I-nimotuzumab showed the lowest rate of accumulation in the liver and the longest time of blood elimination of all examined radiolabelled ligands. The antibody labelled with ^{177}Lu via chelating compounds (DOTA, DTPA) was characterized with decreased elimination time and much more increased retention in the liver. The introduced *in vivo* results confirmed the influence of employed isotope and manner of its labelling on the radiolabelled antibody biological properties in the case of tested factors like blood clearance, the liver biodegradation and accumulation.

9. Seznam publikovaných prací

9.1 Původní práce publikované v odborných časopisech

Barta P, Björkelund H, Andersson K: Circumventing the requirement of binding saturation for receptor quantification using interaction kinetic extrapolation. Nucl Med Commun. 2011 Sep; 32(9):863-867. **IF** = 1,367

Bárta P, Melicharová L, Lázníčková A, Lázníček M: Cellular uptake of ^{111}In- and ^{177}Lu-radiolabelled DOTA-minigastrin11 on proximal kidney cells and tumor CCK2 receptor bearing cell line. Folia Pharm. Univ. Carol. 2011 XXXIX, ISBN 978-80-246-1912-5:7-16.

Björkelund H, Gedda L, **Barta P**, Malmqvist M, Andersson K: Gefitinib induces epidermal growth factor receptor dimmers which alters the interaction characteristics with ^{125}I-EGF. PLoS One. 2011 Sep; 6(9):e24739. **IF** = 4,411

Barta P, Malmberg J, Melicharova L, Strandgård J, Orlova A, Tolmachev V, Laznicek M, Andersson A: Protein interactions with HER-family receptors can have different characteristics depending on the hosting cell line. Int J Oncol. 2012 May; 40(5):1677-82.
IF = 2,571

Novy Z, **Barta P**, Mandikova J, Laznicek M, Trejtnar F: A comparison of in vitro methods for determining the membrane receptor expression in cell lines. Nucl Med Biol. 2012 Apr, [Epub ahead of print]. **IF** = 2,620

Barta P, Laznickova A, Laznicek M, Beckford Vera DR, Beran M: The preclinical evaluation of radiolabelled nimotuzumab, the promising monoclonal antibody targeting the epidermal growth factor receptor. J Labelled Comp Radiopharm; [Under review]. **IF** = 1,096

9.2 Abstrakta z mezinárodních konferencí

Annual Congress of the EANM 2009 (Barcelona, Spain)

Beckford D, Malkova M, Beran M, Kopracek M, Tomes M, Laznickova A, Laznicek M, **Barta P**, Leyva R, Melichar F: Lutetium-177 radiolabeling of the humanized ,omoclonal antibody h-R3 using macrocyclic and acyclic ligands. Eur J Nucl Med Mol Imaging 2009; 36 (Suppl 2):S281-S496.

Laznickova A, Laznicek M, **Barta P**, Beran M, Beckford D, Melichar F: Preclinical comparison of two hR3-DOTA derivatives labelled with ^{177}Lu. Eur J Nucl Med Mol Imaging 2009; 36 (Suppl 2):S281-S496.

9.3 Abstrakta publikovaná ve sbornících

58. Farmakologické dny (Praha září 2008)

Barta P, Cihlo J, Laznickova A, Laznicek M: Determination of transport kinetics of somatostatin receptor–specific peptide to opossum kidney cells. Sborník abstrakt

59. Farmakologické dny (Bratislava září 2009)

Barta P, Laznickova A, Laznicek M: Internalization of ^{177}Lu-labeled antibody Nimotuzumab in human cancer cell cultures. Farmakológia 2009, Zborník prác 59. Farmakologické dni, Univerzita Komenského Bratislava.

60. Farmakologické dny (Hradec Králové 2010)

Barta P, Laznickova A, Laznicek M: Internalization of 111In-labeled minigastrin in human gastric adenocarcinoma and kidney cell culture. Sborník abstrakt.

1. postgraduální vědecká konference (Farmaceutická fakulta v Hradci Králové 2011)

Barta P, Björkelund H, Andersson K, Laznicek M: *In vitro* receptor number quantification employing smart and labor-saving kinetic evaluation by real time automatic technique. Folia Pharmaceutica Universitatis Carolinae.

61. Farmakologické dny a EPHAR symposium (Brno 2011)

Barta P, Novy Z, Björkelund H, Andersson K, Laznicek M: A Novel Rapid and Simple Automatic Strategy for EGFR Quantification in A431 Cells. Sborník abstrakt.

9.4 Ústní presentace

1. postgraduální vědecká konference (Farmaceutická fakulta v Hradci Králové 2011)

Barta P, Björkelund H, Andersson K, Laznicek M: Receptor number quantification by the employment of the automatic technique.